IAEA
International Atomic Energy Agency

INDC(CCP)-0416

INDC International Nuclear Data Committee

Translation of Selected Papers published in
Jadernye Konstanty (Nuclear Constants) 3-4, 1997 and 1, 1998

Translated by the IAEA

October 1998

IAEA Nuclear Data Section, Vienna International Centre, A-1400 Vienna, Austria

Selected INDC documents may be downloaded in electronic form from
http://www-nds.iaea.org/reports-new/indc-reports/
or sent as an e-mail attachment.
Requests for hardcopy or e-mail transmittal should be directed to *services@iaeand.iaea.org*
or to:
Nuclear Data Section
International Atomic Energy Agency
Vienna International Centre
PO Box 100
A-1400 Vienna
Austria

Printed by the IAEA in Austria

October 1998

CONTENTS

98-10986 (76)
Translated from Russian

SERIYA: YADERNYE KONSTANTY, Vypusk 3-4, 1997, s. 41
(Series: Nuclear Constants, Issue No. 3-4 1997, p. 41)

UDC 539.172

STATUS OF NUCLEAR DATA FOR THE THORIUM FUEL CYCLE

B.D. Kuz'minov, V.N. Manokhin
Russian Federation State Science Centre
Institute of Physics and Power Engineering, Obninsk

STATUS OF NUCLEAR DATA FOR THE THORIUM CYCLE. Analysis was made of the evaluated data from the libraries ENDF/B-VI, JENDL-3.2, BROND-2 and JEF-2 and the available experimental data for the isotopes of interest for the thorium fuel cycle. The conclusion was made that the nuclear data are very inconsistent and in need of considerable improvement drawn by means of new measurements, theoretical model calculations and empirical systematics.

Much attention is currently being devoted to ways of using thorium in various schemes and scenarios for developing nuclear power.

In the early days of nuclear power the main reason for choosing the uranium-plutonium fuel cycle was the presence in natural uranium of the isotope ^{235}U, capable of sustaining a chain reaction in reactors with different neutron spectra and various degrees of enrichment of the fuel with this isotope.

Large stocks of ^{239}Pu (both civil and military) and uranium highly enriched in ^{235}U have now been accumulated, and the use of thorium in conjunction with these materials, opens up prospects for producing ^{233}U, an excellent fuel for different types of reactors.

Adoption of the thorium fuel cycle would offer the following advantages:

- Increased nuclear fuel resources thanks to the production of ^{233}U from ^{232}Th;
- Significant reduction in demand for the enriched isotope ^{235}U;

- Very low (compared with the uranium-plutonium fuel cycle) production of long-lived radiotoxic wastes, including transuraniums, plutonium and transplutoniums;

- Possibility of accelerating the burnup of plutonium without the need for recycling, i.e. rapid reduction of existing plutonium stocks;

- Higher fuel burnup than in the uranium-plutonium cycle;

- Low excess reactivity of the core with thorium-based fuel, and more favourable temperature and void reactivity coefficients;

- High radiation and corrosion resistance of thorium-based fuel;

- Considerably higher melting point and the better thermal conductivity of thorium-based fuel;

- Good conditions for ensuring the non-proliferation of nuclear materials.

All these observations are based on evaluations, physical calculations and comparisons of the established characteristics of the two fuel cycles.

As considerable financial investment is required for the thorium fuel cycle to attain the same large-scale industrial status as the uranium-plutonium cycle, the conceptual neutron physics calculations must be based on sufficiently reliable nuclear data. When comparing the characteristics of the different fuel cycles and scenarios for the development of nuclear power, it is necessary to evaluate the reliability of the basic nuclear data used in the calculations, in order to be able to assess the confidence limits of comparable parameters.

Evaluation of the required accuracy of nuclear data for the thorium fuel cycle

Figure 1 shows the scheme of the nuclear transformations in the thorium fuel cycle. Let us consider the role of the various isotopes and neutron reactions in reactors.

The isotope composition and quantity of thorium, protactinium and uranium in reactors depend on the reactor type, the reactor spectrum hardness, the cycle length, the neutron flux density, and the fuel cycle type (open, closed), and so on.

Table 1 contains the calculated values of the equilibrium density of transactinides for fast and thermal reactors. The quantity of secondary transactinide nuclei amounts to per cents (except for ^{234}U) with respect to the number of ^{233}U nuclei in both types of reactors, and the content of the same isotope differs for systems with a spectrum of thermal and fast neutrons by a maximum of a few times (but not by orders).

Table 1.

Relative atomic density of actinides in fast and thermal reactors (W = 3 GW(th), rate of fuel replacement 0.35 1/year)

Isotope	Relative number of nuclei n = N(x)/N(^{233}U)	
	Fast reactor	Thermal reactor
Th		
232	9.7	359
Pa		
231	$0.8 \cdot 10^{-2}$	$1.9 \cdot 10^{-3}$
233	$1.9 \cdot 10^{-2}$	$1.2 \cdot 10^{-1}$
U		
232	$5.5 \cdot 10^{-2}$	$3.7 \cdot 10^{-3}$
233	1.0	1.0
234	$3.4 \cdot 10^{-1}$	$4.6 \cdot 10^{-1}$
235	$0.7 \cdot 10^{-1}$	$1.2 \cdot 10^{-1}$

In both types of reactors, the fuel ^{233}U and source material ^{232}Th have an important role in supporting the chain reaction. ^{234}U may also be considered as a source material and its role in maintaining the chain reaction cannot be ignored.

In view of the small content of ^{231}Pa and ^{232}U, these isotopes have practically no influence on the chain reaction but form an important part of the toxic radioactive components of the spent fuel.

The role of ^{233}Pa is more complex since, when it decays ^{233}U is formed, increasing the quantity of fuel in the reactor.

In the first stage of the study on the thorium fuel cycle, it is advisable to confine oneself to an analysis of the nuclear database for the six above-mentioned nuclei, examining only those reactions which are characteristic of the role of these nuclei in the reactor:

^{232}Th, ^{233}U and ^{234}U - complete nuclear date files;

^{231}Pa, ^{232}U - reactions responsible for the balance of nuclei in the reactor;

^{233}Pa - reactions responsible for the balance of nuclei and the average number of prompt fission neutrons.

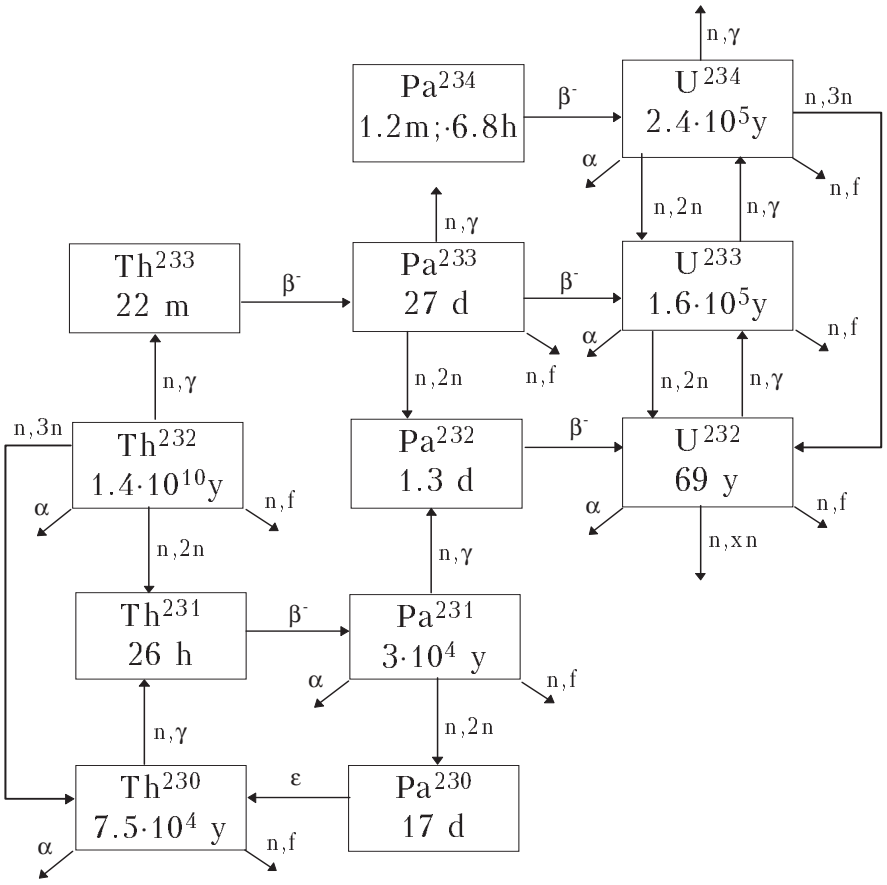

Fig. 1. Scheme of the nuclear transformations in the uranium-thorium fuel cycle

Table 2

Cross-section accuracy requirements (%) in fast reactors

			Minor actinides						
						^{233}Pa			
Reaction cross-section	**^{233}U**	**^{232}Th**	**^{234}U**	**^{232}U**	**^{231}Pa**	$\Phi << \frac{\lambda}{\Sigma_i \sigma_i}$	$\Phi \approx \frac{\lambda}{\Sigma_i \sigma_i}$	$\Phi >> \frac{\lambda}{\Sigma_i \sigma_i}$	$\frac{\Delta k}{k} \approx 0.01$
σ(n,f)	1	1	5	25	20	-	25	13	35
$\bar{\nu}$	0.5	1	3	-	-	-	-	-	25
σ(n,γ)	3	2	5	75	20	-	50	30	35
σ(n,n')	5-10	5	10	-	-	-	-	-	-
σ(n,2n)	10	10	15	-	50	-	-	-	-
σ(tot)	2		5	-	-	-	-	-	-
σ for formation of ^{1}H,^{3}H,^{4}He	15	15	20	-	-	-	-	-	-
Basic role in the reactor	Chain reaction	Chain reaction, ^{233}U production	Chain reaction, ^{235}U production	Ecology	Ecology	Transient kinetics, ^{235}U production			

[The dashes indicate that the accuracy requirements for nuclear data are minimal.]

Let us evaluate the required accuracy of the nuclear data in accordance with the role of the above-mentioned nuclei in the reactor. Nuclear data accuracy requirements for fuel and source materials for fast reactors with a uranium-plutonium fuel cycle have been formulated in Refs [1-4]. These requirements are similar for systems using thorium-based fuel. Table 2 shows the nuclear data accuracy requirements for fast reactors in a one-group approximation.

In determining the permissible errors in the nuclear data for ^{231}Pa, ^{233}Pa and ^{232}U they used as a basis a fairly low requirement of 30% for the error in determining the quantity of these isotopes in the reactor. For ^{233}Pa, three different values of neutron flux Φ were considered:

$$\Phi << \frac{\lambda}{\sum_i \sigma_i}; \qquad \Phi \approx \frac{\lambda}{\sum_i \sigma_i}; \qquad \Phi >> \frac{\lambda}{\sum_i \sigma_i},$$

where λ is the decay constant for ^{233}Pa nuclei, the index i denotes fission reactions (n,f), radiative neutron capture (n,γ) and the reaction (n,2n), i.e. reactions which lead to the disappearance of ^{233}Pa nuclei. In addition, the condition under which the error in the calculated contribution of ^{233}Pa to the multiplication factor of the system may not exceed 1% of its value ($\Delta k/k \approx 0.01$) was also considered. The results are presented in Table 2.

Table 3 shows the nuclear data accuracy requirements for thermal reactors.

Table 3.

Cross-section accuracy requirements (%) for thermal reactors

Reaction cross-section	^{231}Pa	^{232}U	^{233}Pa			
			$\Phi << \frac{\lambda}{\Sigma_i \sigma_i}$	$\Phi \approx \frac{\lambda}{\Sigma_i \sigma_i}$	$\Phi >> \frac{\lambda}{\Sigma_i \sigma_i}$	$\frac{\Delta k}{k} \approx 0.01$
σ(n,f)	-	up to 200	-	-	-	6
σ(n,γ)	20	15	-	50	20	6
σ(n,2n)	-	-	-	-	-	-
$\bar{\nu}$	-	-	-	-	-	12

[The dashes indicate that the accuracy requirements for nuclear data are minimal .]

Status of the nuclear database for the thorium fuel cycle

Figures 12-18 show the evaluated cross-section data from the JEF-2, JENDL-3 and ENDF/B-6 libraries, and the available experimental data for ^{232}Th, ^{231}Pa, ^{233}Pa, ^{232}U, ^{233}U and ^{234}U.

Thorium-232

- *Reaction cross-section* σ_f. Experimental data from numerous studies [5-22] are available for neutron energies below 5MeV, providing a detailed picture of the energy

dependence of the fission cross-section and the structure of the fission cross-section close to the barrier. In the neutron energy range 5-10 MeV data are available in Refs [6, 9, 12, 13, 15, 17, 18, 23-28], the results of which differ by 30% in the region of the (n,n'f) fission reaction threshold, and by 15% above the threshold. In the neutron energy range close to 14 MeV, the mean spread of the experimental results is approximately 15%.

The evaluated data from the JEF-2, JENDL-3 and ENDF/B-6 libraries differ in their description of the structure of the fission cross-section close to the fission barrier by 10 to 20%. In the neutron energy range 5-15 MeV, the data from these libraries diverge by 20-25%.

In the neutron energy range below 5 MeV it is not advisable, at this stage, to perform new measurements of the fission cross-section, since their contribution does not greatly influence the established average value. In this energy range, it is clearly more reliable to carry out the evaluation without a model, using the collection of experimental results. In the neutron energy range above 5 MeV, it is necessary to perform additional measurements of the fission cross-section with greater detail in the 5-12 MeV range.

- *Inelastic neutron scattering.* There are a large number of works on experimental investigation of inelastic neutron scattering [29-47]. They include measurements of the excitation functions of discrete energy levels, total inelastic neutron scattering cross-sections, and angular and energy distributions of secondary neutrons. Unfortunately, many studies were carried out 25-30 years ago, and the technical facilities then available did not provide results that meet present-day requirements. The problem of the systematic divergence of the excitation cross-sections of discrete energy levels, measured on the basis of secondary neutrons and γ-quanta remains unresolved.

The spread of evaluated data for the integral inelastic neutron scattering cross-section from various libraries is 15-50%.

In view of the fundamental role of thorium in the uranium-thorium cycle, there is an urgent need to measure the inelastic scattering cross-sections over a wide energy range (up to 15 MeV), the excitation functions of discrete energy levels, and the spectra and angular distributions of secondary neutrons. Theoretical models for describing the process of inelastic neutron scattering also need to be further developed.

- *Radiative neutron capture cross-section* $\sigma(n,\gamma)$. There is extensive experimental material over the whole energy range important for thermal and fast reactors. The descriptions of the experiments are sufficiently informative.

The evaluated data from different libraries in the energy range 0.05-1.5 MeV differ by 10-30%.

At this stage, for the purpose of the evaluation, it is sufficient to use the existing experimental database with the model description of the cross-section in the neutron energy range above 2 MeV.

- *Reaction cross-section* (n,2n). The experimental data on the energy dependence of the cross-section in the energy range up to 11 MeV from Refs [48] and [49] are quite consistent.

Reference [50] on the whole gives results that are 15-20% lower. For neutron energies close to 14 MeV, experimental data are available from a number of works, with scatter of 30-40%. It should be noted that the majority of experimental measurements of the (n,2n) reaction cross-section were carried out more than 25 years ago.

The evaluated data from various libraries at the peak of the energy dependence σ(n,2n) differ by 10%. In the other energy ranges, the difference is 30-50%.

It would be useful to measure the cross-sections σ(n,2n) at neutron energies from 10 to 20 MeV and to obtain evaluated data taking account of phenomenological systematics.

Protactinium-231

- *Fission cross-sections* σ(n,f). There are several experimental works [51-55] in which the energy dependence of the fission cross-section has been measured over a wide energy range, as well as works describing investigations of structure of the fission cross-section close to the threshold [56-62].

Despite the significant discrepancies in the results of the different works, the set of experimental data enables us to select an ensemble to describe the energy dependence close to the threshold as well as up to the energy range ~10-12 MeV.

The evaluated data, based on different experimental results, diverge by 30-40% in the 1 MeV energy range, and by 10% at neutron energies above 7 MeV.

It is advisable to perform mesurements in the energy range 6-20 MeV, and to carry out an evaluation using a set of experimental results.

- *Reaction cross-section* (n,γ). Experimental data are only available for thermal neutrons.

The evaluated data from the JEF-2.2 and ENDF/B-6 libraries are identical.

It is necessary to perform measurements of the neutron capture cross-section in the fast neutron region range, at least for some energy values, and then to use them for normalization of the calculated data.

- *Reaction cross-section* (n,2n). No experimental data exist. The evaluated data from various libraries differ by 40% and above in the different energy ranges. In this case, it is advisable to use systematics to determine the most realistic evaluated data.

Protactinium-233

- *Fission cross-sections* σ(n,f). Measurements of the fission cross-section have been carried out for neutrons in the fission spectrum (775 ± 190 mb) and for neutrons from a nuclear bomb explosion experiments (numerical data are unavailable). There are no experimental data on the energy dependence of the fission cross-section.

The evaluated data from various libraries differ according to the height of the fission barrier, and the fission cross-sections differ by a factor of two at neutron energies below 6 MeV and by a factor of 1.5 above 6 MeV.

It is not feasible at present to measure the energy dependence of the fission cross-section for ^{233}Pa. A more realistic evaluation may be obtained on the basis ofsystematics, although a more complex fission barrier structure is characteristic for nuclei in the Th-Pa region than for heavier nuclei. As a result of this, extrapolation to the region of Th-Pa nuclei may prove to be inadequate.

- *Radiative neutron capture cross-section* $\sigma(n,\gamma)$. There are data on the results of the measurement of the capture cross-section of reactor spectrum neutrons, neutrons with energy 0.025 eV and neutrons from a nuclear explosion. The energy dependence$\sigma(n,\gamma)$ has not been investigated experimentally.

Adjustment of the evaluated data is complicated by the spread of the experimental data on the capture cross-section in the thermal region.

It is desirable to improve the data for thermal neutrons and measure$\sigma(n,\gamma)$ at least for one energy value in the fast neutron region (or the mean value for the fission spectrum) and then to use them for normalization of the evaluated data obtained on the basis of the model calculations.

- *Reaction cross-section* (n,2n). Experimental data are not available. Evaluated data from various libraries differ in the shape of the energy dependence and the magnitude of the cross-section (by a factor of three). It is to be hoped that this cross-section can be refined on the basis of phenomenologicalsystematics.

Uranium-232

- *Fission cross-section* $\sigma(n,f)$. There are two experimental works covering the neutron energy range above 100 keV (0.13-1.5 MeV) [63] and (0.14-7.4 MeV) [64]. The results of these studies are not consistent below 1.5 MeV, and differ by a factor of 2 at energy ~ 150 keV. The data from the Ref. [64] extrapolate well to the results of the Ref. [65], in which the upper neutron energy limit is 20keV. Combining the results of Refs [64] and [65] gives a sufficiently detailed description of the energy dependence of the fission cross-section up to 7 MeV.

The discrepancy in the evaluated data from various libraries in the neutron energy range above 6 MeV is 100%.

It is advisable to make the evaluation on the basis of a model supported by the experimental studies [64, 65].

- *Radiative capture cross-section* $\sigma(n,\gamma)$. There are experimental works on measurements of the capture cross-section of reactor neutrons, and of neutrons with a Maxwellian spectrum (for example, [66, 67]). All the measurements were performed 25-45 years ago.

The evaluated data from JEF-2.2 have been normalized to $\sigma(n,f) = 78 \pm 4$ b at a neutron energy of 0.025 eV.

It is desirable to perform measurements of $\sigma(n,\gamma)$, at least for one energy in the fast neutron region, in order to normalize the model calculations.

- *Reaction cross-section* (n,2n). Experimental data are not available. The evaluated data from the ENDF/B-6 and JENDL-3 libraries differ by a factor of 10. It is not practicable to measure the reaction cross-section (n,2n) at this stage. Phenomenological systematics must be used to select the most appropriate evaluation.

Uranium-233

- *Fission cross-section* $\sigma(n,f)$. Some works have been carried out with detailed measurements in the fission cross-section ratios of ^{233}U and ^{235}U [68-79].

In a number of works, measurements were performed either of the ratio of the fission cross-sections of ^{233}U and ^{235}U or of the absolute value of the fission cross-section of ^{233}U at neutron energy close to 14 MeV. The spread of the results of these studies is 20%.

On the whole, the set of data is sufficiently representative for evaluating the fission cross-section of ^{233}U in the neutron energy range below 6 MeV. At energies above 6 MeV, there is just one detailed study [49], and it is desirable to perform new measurements in this energy range, although the results of Ref. [73] can be adjudged reliable from their consistency with the results of other works at neutron energies below 6 MeV.

The spread of the evaluated data from the ENDF/B-VI, JENDL-3 and JEF-2 libraries is 5-10% over a wide range of neutron energies up to 20 MeV.

- *Radiative neutron capture cross-section.* Direct measurements of the capture cross-section at neutron energies above 45 keV have not been performed. There are some data derived from the results of two works concerned with measuring the "alpha" value [80-81], which enable us to construct the energy dependence of the radiative capture cross-section in the neutron energy range 0.03-1.0 MeV. However, extrapolation to a higher energy range would be unreliable. The evaluated data at neutron energies above 1MeV differ by a factor of 5 to 10.

Direct measurements of the radiative capture cross-section need to be made over a broad energy range from 0.05 to several MeV.

- *Inelastic neutron scattering.* Direct measurements of the total inelastic scattering cross-section are not available. Data do exist [38] in the energy range 1-3.5 MeV, derived from the cross-section balance. The neutron spectra for inelastic scattering into the continuum region have not been measured. Experimental data on the excitation of discrete energy levels are not available, with the exception of some values for discrete energy points in Ref. [32]. An experimental study of the angular distributions of inelastically scattered neutrons is required. The evaluated data on the total inelastic scattering cross-section from various libraries differ by 40-50%.

Direct measurements of the spectra and angular distributions of inelastically scattered neutrons, total cross-sections and the excitation cross-sections of discrete energy levels are required.

- *Reaction cross-sections* (n,2n). Experimental data on reaction cross-sections (n,2n) are not available.

The evaluated cross-sections in various libraries have a different shape of the energy dependence and differ in magnitude. The spread of the values is 20-100%.

- *Fission neutron spectra*. There are no experimental data on neutron spectra with fission of ^{233}U by fast neutrons. Appropriate measurements at neutron energies 1, 4-5 and 7-8 MeV are required.

Uranium-234

- *Fission cross-section* σ(n,f). More than ten studies (for example [16, 17, 19, 69, 82-87]) exist on experimental investigation of the energy dependence of the cross-section for the fission of ^{234}U nuclei by neutrons. A large number of works are devoted to the study of the fission cross-section close to the fission barrier [5, 88-92].

In addition, there are data on absolute measurements of σ_f at E_n=14 MeV, and for fission spectrum neutrons.

The combined results of these experimental studies, provide a means of constructing the evaluated dependence of the fission cross-section on neutron energy up to 10 MeV, on the basis of experimental data alone, without recourse to model calculations.

There is only one experimental study at higher neutron energies, and evaluation of the cross-section is possible on a model basis.

- *Radiative neutron capture cross-section* σ(n,γ). Experimental data in the fast neutron region are not available. Some studies were undertaken more than 25 years ago on neutrons with a Maxwellian spectrum. The evaluated data from the JEF-2.2 library in the thermal neutron region lie below the experimental results. In order to obtain a more reliable value for the evaluated cross-section σ(n,f), it is advisable to perform measurements of σ(n,γ) for thermal neutrons and at least for 1 to 2 energy values in the fast neutron region.

- *Inelastic scattering cross-section* σ(n,n'). Experimental data are not available. The evaluated data from various libraries differ by 10-30%. A test experiment is highly desirable.

- *Reaction cross-section* (n,2n). Experimental data are not available. The difference in evaluated data from various libraries is 50 to 100%.

In this case, it is hardly possible to expect measurements of the cross-section to be performed. The selection of evaluated data should evidently be based on phenomenological systematics.

The above analysis of the status of the nuclear database for the uranium-thorium fuel cycle shows that the database is extremely poor and does not meet modern requirements in terms of quantity.

- The experimental data are insufficient, and the scatter of the results of measurements of the same quantity performed by various authors exceeds the estimated measurement errors in many cases.

- The majority of the experimental data was obtained in works carried out more than 30 years ago, and their quality frequently falls below modern standards.

- The evaluated data of many files are based solely on model calculations, and the numerical values from various libraries diverge by 50-200%.

All this highlights the need to improve the availability of nuclear data by performing additional measurements, improving the theoretical models and developing phenomenological systematics.

The problem is exacerbated by the fact that the secondary heavy nuclei produced in this cycle possess, as a rule, extremely unpleasant nuclear physics characteristics from the experimentalist's point of view, which greatly complicate experimental investigation of the interaction cross-sections of neutrons with these nuclei.

At this stage it may be concluded that the nuclear database for the uranium-thorium fuel cycle is significantly less reliable than the corresponding base for the uranium-plutonium fuel cycle, and may be used forestimative calculations only.

Before engaging in calculations to be used as a basisprogramme planning or estimating the costs of introducing the new fuel cycle, it is necessary to bring the nuclear database for the uranium-thorium fuel cycle up to the reliability level of that for the uranium-plutonium fuel cycle.

REFERENCES

[1] ZARITSKIJ, S.M., TROYANOV, M.F., Proc. Conf. on the Physics of Fast Reactors, London, BNES (1969) 261.
[2] ZARITSKIJ, S.M., et al., Nejtronnaya Fizika, Vol. 1, Kiev, "Naukova Dumka" (1973) 53 [in Russian].
[3] BOBKOV, Yu.G., USACHEV, L.N., Yadernye Konstanty 16th edition, Moscow, Atomizdat (1975) 5 [in Russian].
[4] USACHEV, L.N., et al., Nejtronnaya Fizika, Part 1, Moscow, Central Scientific Research Institute for Information and Techno-Economic Studies in the Field of Atomic Science and Technology (1976) 64 [in Russian].
[5] WHEELER, Proc. 1st Int. Conf. on the Peaceful Uses of Atomic Energy, Geneva, 2 (1955) 155.
[6] HENKEL, Report LA-2122 (1957).
[7] BATCHELOR, et al., Nucl. Phys. 65 (1965) 236.
[8] BLONS, et al., Phys. Rev. Lett 35 (1975) 1749.
[9] BEHRENS, et al., Nucl. Sci. Eng. 81, 4 (1982) 512.
[10] AUCHAMPAUGH, et al., Phys. Rev. C24, 2 (1981) 503.
[11] PLATTARD, et al., Proc. the Symp. on the Physics and Chemistry of Nuclear Fission, Juelich, §B11 (1979).
[12] MEADOWS, et al., Proc. Conf. on Nuclear Data, Knoxville (1979) 479.
[13] BECKER, et al., Prog. DOE-NDC-27-55 (1982).
[14] Patin. Prog. CEA-N-2284, 90 (1982).
[15] BLONS, et al., Nucl. Phys., A414, 1 (1984) 1.
[16] KANDA, et al., Radiation Effects, 93 (1986) 233.
[17] WATANADE, et al., Annal. Nucl. Energy 14 (1987) 563.
[18] MEADOWS, et al., Rept. ANL-NDM-83 (1983).
[19] FURSOV, B.I., et al., Atomnaya Ehnergiya 71 (1991) 320 [in Russian].
[20] BEHKAMI, et al., Nucl. Phys., A118 (1968) 65.
[21] KONECNY, et al., Zeitschrift f. Physik, 251 (1977) 400.
[22] PEREZ, et al., Phys. Rev., C28 (1983) 1635.
[23] LISOWSKI, et al., Proc. Int. Conf. on Nuclear Data for Science and Technology, Mito (1988) 97.
[24] FOMICHEV, et al., Proc. Conf. on Nuclear Data for Science and Technology, Juelich (1991) 734 [in Russian].
[25] KALININ, et al., Proc. 2nd Int. Conf. on the Peaceful Uses of Nuclear Energy, Geneva, 16 (1958) 136 [in Russian].
[26] PANKRATOV, et al., Atomnaya Ehnergiya 9 (1960) 393, 14 (1963) 177.
[27] NORDBERG, et al., Proc. Int. Conf. on Neutron Physics and Nuclear Data for Reactors and Other Applications, Harwell (1978) 910.
[28] GOVERDOVSKIJ, A.A., et al, Atomnaya Ehnergiya, 61 5 (1986) 380 [in Russian].
[29] BLINOV, et al., Proc. Conf. on Neutron Physics, Kiev, 2 (1983) 308 [in Russian].
[30] LITVINSKIJ, et al, Proc. Conf. on Neutron Physics, Kiev, 2 (1988) 179 [in Russian].
[31] CIARCIA, et al., Nucl. Sci. Eng. 91 (1985) 428.
[32] HAONAT, et al., Nucl. Sci. Eng. 81 (1982) 491.
[33] BUCCINO, et al., Nucl. Phys, 60 (1964) 17.
[34] FUJITA, et al., J. Nucl. Technol, 20 (1969) 983.
[35] HOLMBERG, et al., Nucl. Phys., A127 (1969) 149.
[36] BATCHELOR, et al., Nucl. Phys., 65 (1965) 236.

[37] EGAN, et al., Proc. Conf. on Nuclear Data for Science and Technology, Mito (1988) 63 [in Russian].
[38] SMITH, A., et al., Proc. Conf. on Nuclear Data, Antwerp (1982) 39.
[39] HIRAKAWA, et al., Proc. Conf. on Nuclear Data, Santa Fe (1985) 565.
[40] FILATENKOV, et al., Yadernye Konstanty, 1 (1982) 23.
[41] SMITH, A., et al., Phys. Rev., 126 (1962) 718.
[42] DAVE, et al., Nucl. Sci. Eng., 91 (1985) 187.
[43] GOSWAMI, et al., Nucl. Sci. Eng., 69 (1979) 191.
[44] SAL'NIKOV, O.A., et al., Yaderno-Fizicheskie Issledovaniya, Moscow, 6 (1968) 16 [in Russian].
[45] ZHURAVLEV, B.V., et al., Proc. Conf. on Neutron Physics, Kiev, 1 (1971) 219 [in Russian].
[46] GLAZKOV, N.P., Atomnaya Ehnergiya, 14 (1963) 400 [in Russian].
[47] KANCHROPOL', et al., Yadernaya Fizika, 38 (1983) 1382 [in Russian].
[48] BUTLER, et al., Can. J. Chem., 39 (1961) 689.
[49] RAICS, et al., Phys. Rev., C32 (1985) 87.
[50] TEWES, et al., Rept. UCRL-6028 (1960).
[51] MUIR, et al., Proc. Conf. on Nuclear Cross-Sections for Technology, Knoxville (1971) 292.
[52] KOBAYASHI, et al., Rept. KURRI-TR-8 (1975).
[53] PLATTARD, et al., Proc. Conf. on Nuclear Cross-Sections for Technology, Knoxville (1979) 491.
[54] HOLMBERT, et al., Prog. KDK-37, (1980) 18.
[55] FURSOV, B.I., et al., Atomnaya Ehnergia, 596 56 (1985) 339 [in Russian].
[56] DUBROVINA, et al., Doklady Akad. Nauk, 157 (1961) 561 [in Russian].
[57] SICRE, et al., Rept. CEN(BG) 76, 03 (1976).
[58] IYEK, et al., Prog. BARC-872 (1976) 106.
[59] SICRE, et al., Proc. Symp. on the Physics and Chemistry of Nuclear Fission, Juelich, 1 (1979) 187.
[60] JAMES, et al., Prog. AERE-PR/NP, 26 (1979).
[61] BUDTZ, et al., Prog. INDC(EUR), 12 (1979) 17.
[62] PLATTARD, et al., Phys. Rev. Lett. 46 10 (1981) 633.
[63] VOROTINKOV, P.E., et al., Yadernaya Fizika, 12 (1970) 474 [in Russian].
[64] FURSOV, B.I., et al., Atomnaya Ehnergiya, 61 (1986) 383 [in Russian].
[65] FARRELL, et al., Rept., LA-4420 (1970).
[66] ELSON, et al., Phys. Rev., 89 (1953) 320.
[67] HALPERIN, et al., Nucl. Sci. Eng., 21 (1965) 257.
[68] WHILE, P.H., et al., Proc. Physics and Chemistry of Fission, Vienna, 1965, IAEA (1965) 219.
[69] WHITE, P.H., et al., J. Nucl. Energy, 21 (1967) 671.
[70] NESTEROV, V.G., SMIRENKIN, G.N., Atomnaya Ehnergiya, 24 (1968) 185 [in Russian].
[71] PFLETCHINGER, R., KAPPELER, F., Nucl. Sci. Eng., 40 (1970) 375.
[72] MEADOWS, J.W., Nucl. Sci. Eng., 54 (1974) 317.
[73] CARLSON, et al., Nucl. Sci. Eng., 66 (1978) 205.
[74] FURSOV, B.I., et al., Atomnaya Ehnergiya, 44 (1978) 236 [in Russian].
[75] POENITZ, W.P., Report ANL/NDM-36, Argonne (1979).

[76] SHPAK, D.L., KOROLEV, G.G., Proc. Conf. on Neutron Physics, Kiev, 1980, Central Scientific Research Institute for Information andTechno-Economic Studies in the Field of Atomic Science and Technology, Moscow, 3 (1980) 30 [in Russian].
[77] MOSTOVAYA, T.A., et al., Proc. Conf. on Neutron Physics, Kiev, 1980, ibid., 30 [in Russian].
[78] BERGMAN, A.A., et al., Proc. Conf. on Neutron Physics, Kiev, 1980, ibid., 54.
[79] KANDA, K., et al., Proc. Conf. Nuclear Data for Basic and Applied Science, Santa Fe, USA (1985) 569.
[80] HOPKINS, J.C., DIVEN, B.C., Nucl. Sci. Eng., 12 (1962).
[81] SPIVAK, P.E., et al., Atomnaya Ehnergiya, 1 21 (1956) 169 [in Russian].
[82] LAMPHERE, et al., Nucl. Phys. 38 (1962) 561.
[83] BEHRENS, et al., Nucl. Sci. Eng., 63 (1977) 250.
[84] JAMES, et al., Phys. Rev. C15 (1977) 2083.
[85] MEADOWS, et al., Nucl. Sci. 65 (1978) 171.
[86] GOVERDOVSKIJ, A.A., et al., Yadernaya Fizika, 466 (1987) 1368 [in Russian].
[87] LISOWSKI, et al., Proc. Conf. on Nuclear Data, Juelich, (1991) 732.
[88] LAMPHERE, et al., Phys. Rev., 104 (1956) 1654.
[89] BOUCHARD, et al., Phys. Lett. B61 (1975) 347.
[90] MUELLER, et al., Phys. Lett. B48 (1974) 25.
[91] BARREAY, et al., Proc. Symp. on the Physics and Chemistry of Nuclear Fission, Juelich, §A8 (1979).
[92] GOVERDOVSKIJ, A.A., et al., Atomnaya Ehnergiya, 63 (1987) 60 [in Russian].

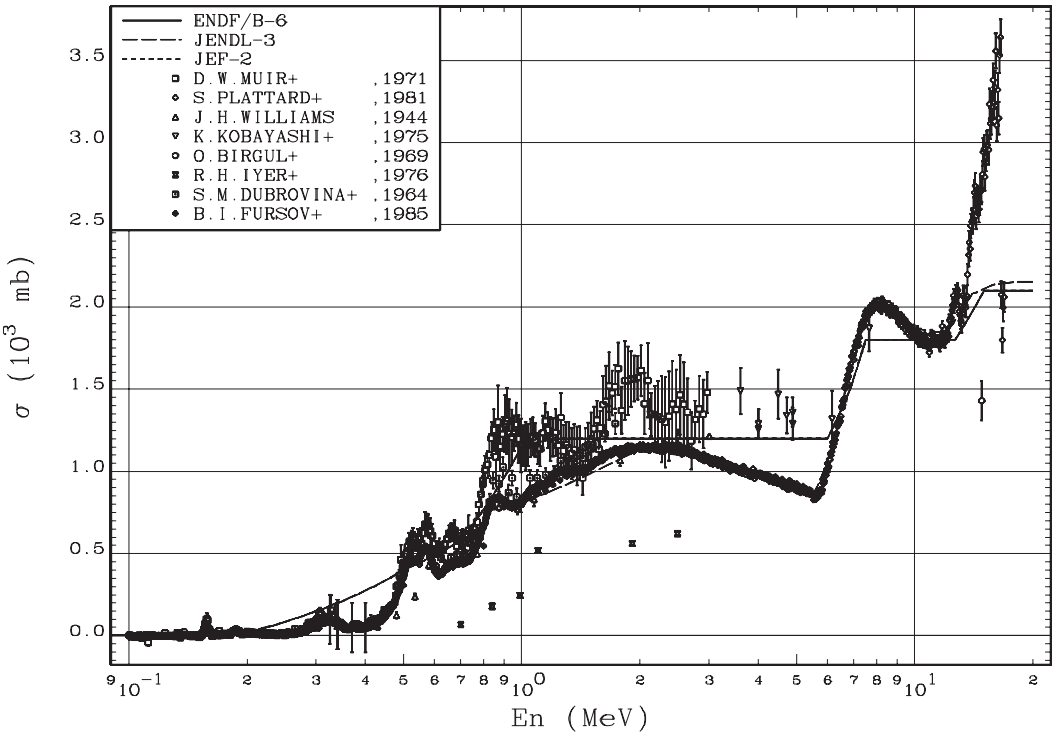

Fig. 2. ^{231}Pa fission cross-section

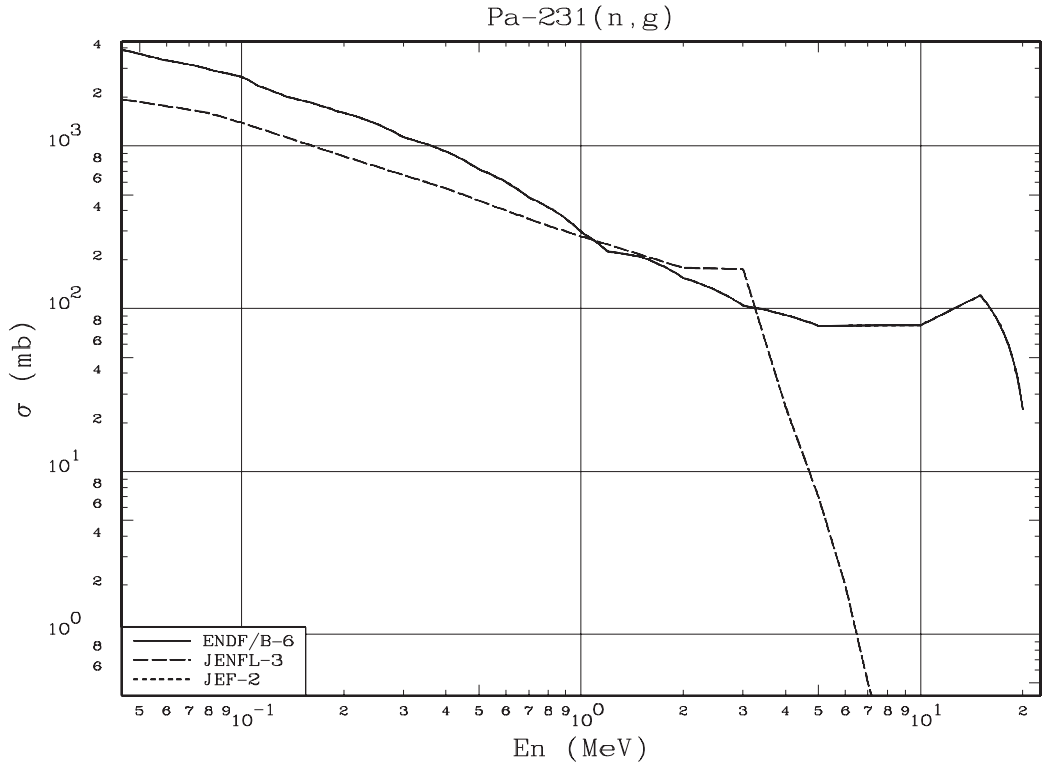

Fig. 3. ^{231}Pa radiative capture cross-section

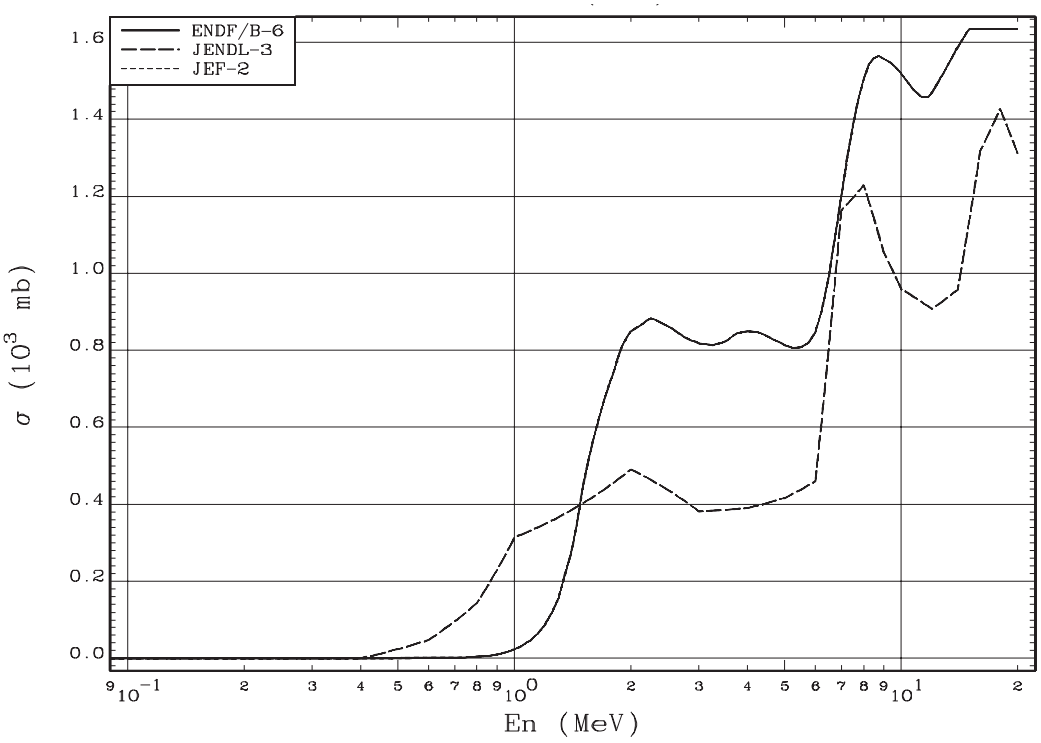

Fig. 4. ^{233}Pa fission cross-section

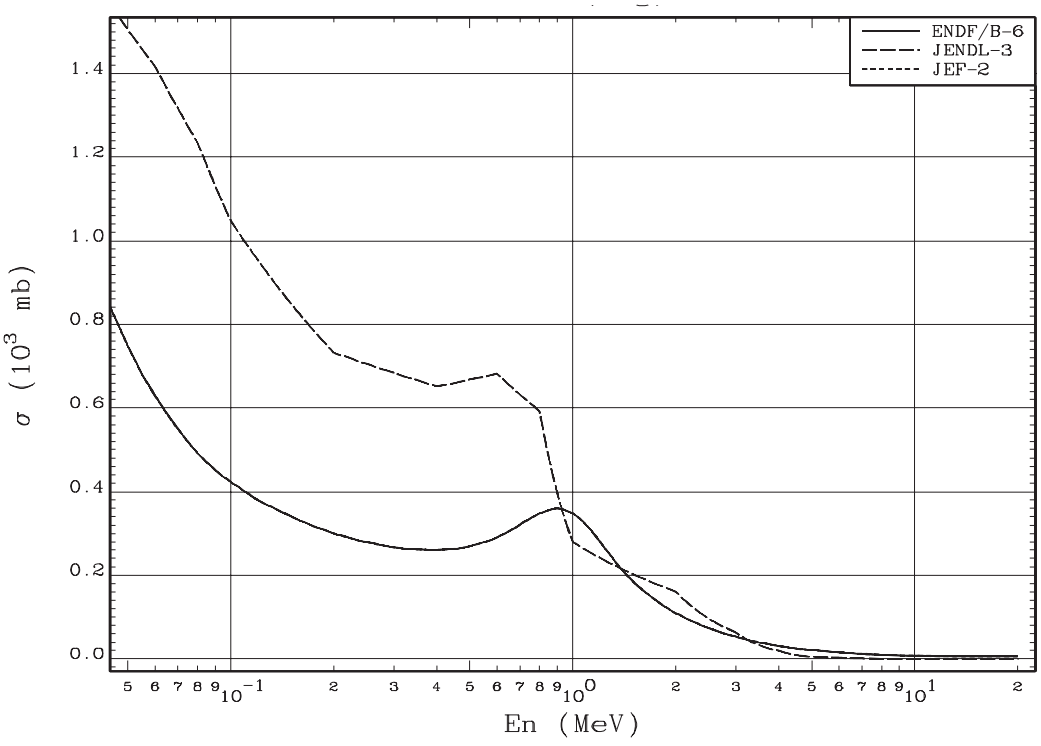

Fig. 5. ^{233}Pa radiative capture cross-section

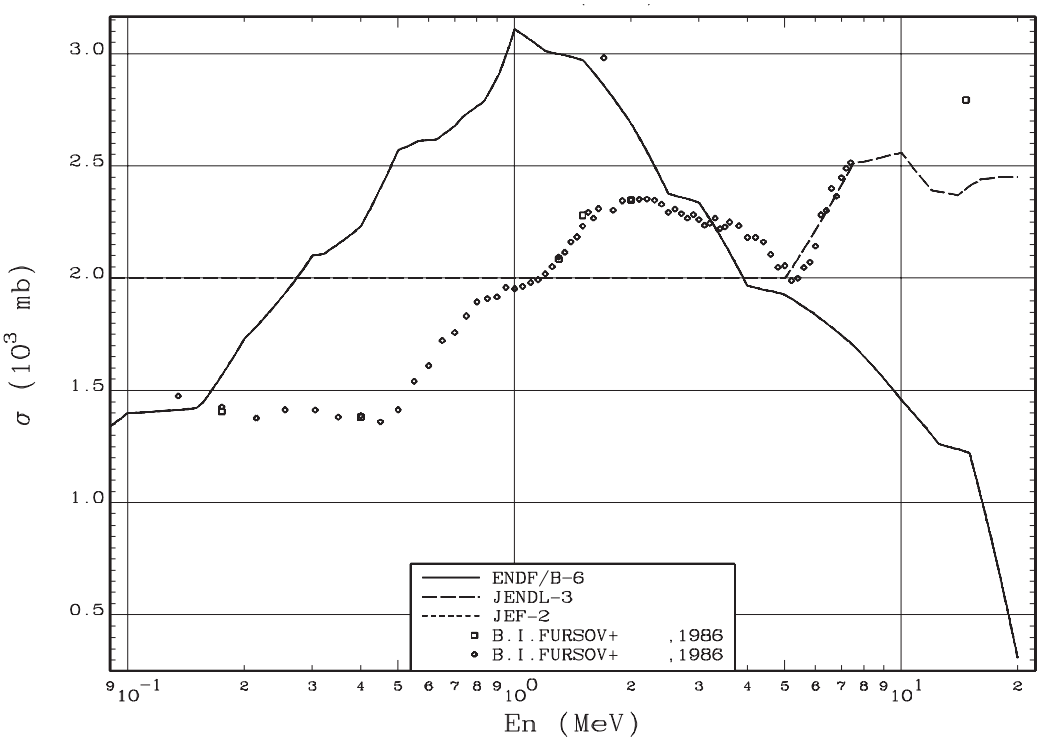

Fig. 6. ^{232}U fission cross-section

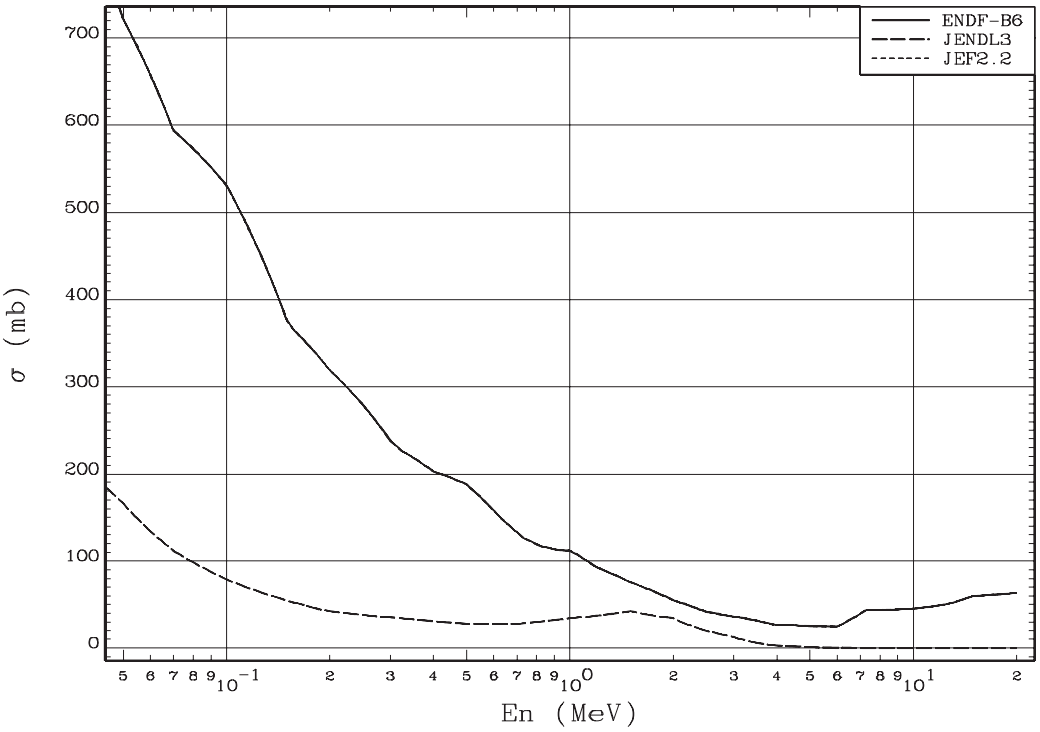

Fig. 7. ^{232}U radiative capture cross-section

a)

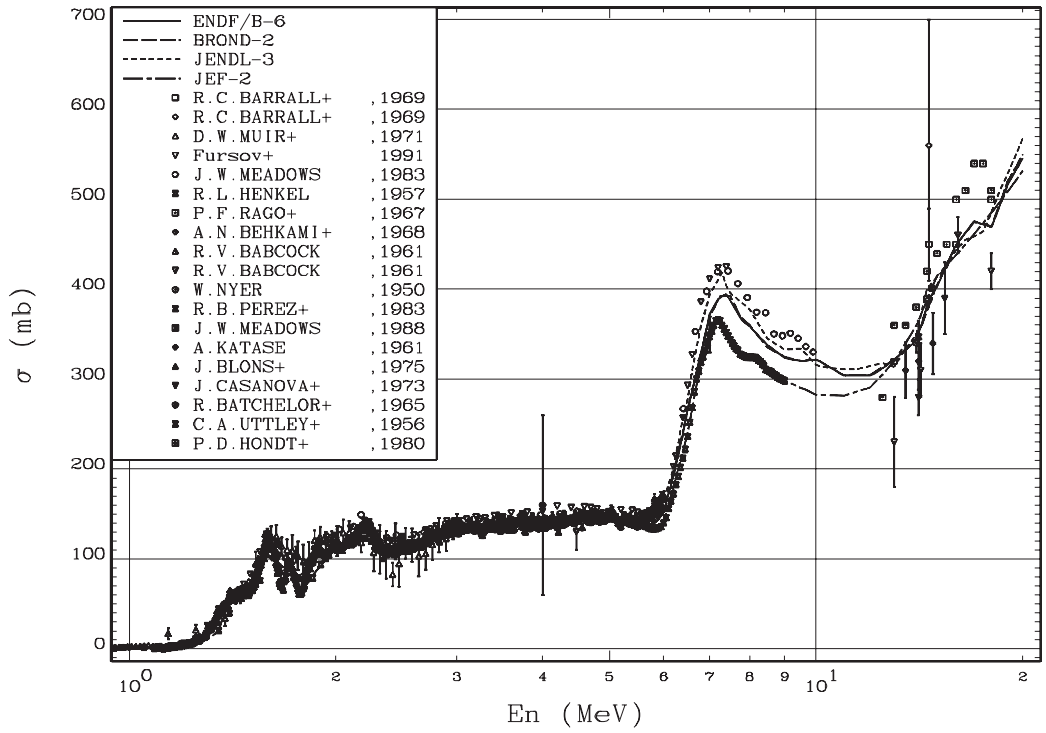

b)

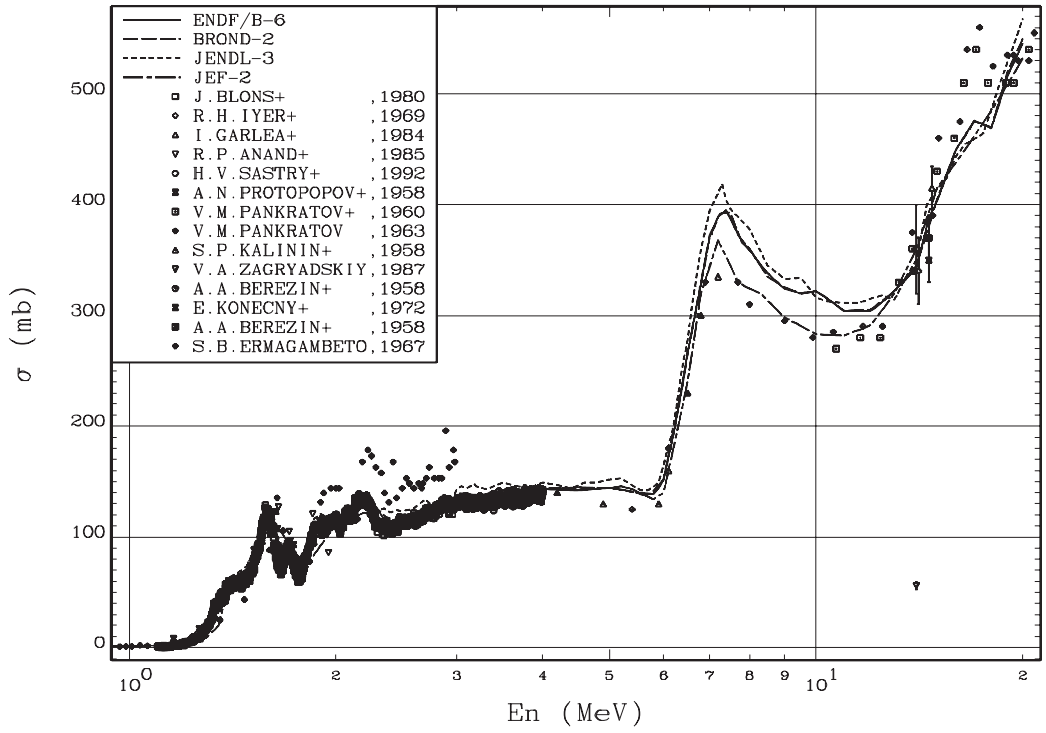

Fig. 8a and b. ^{232}Th fission cross-section

a)

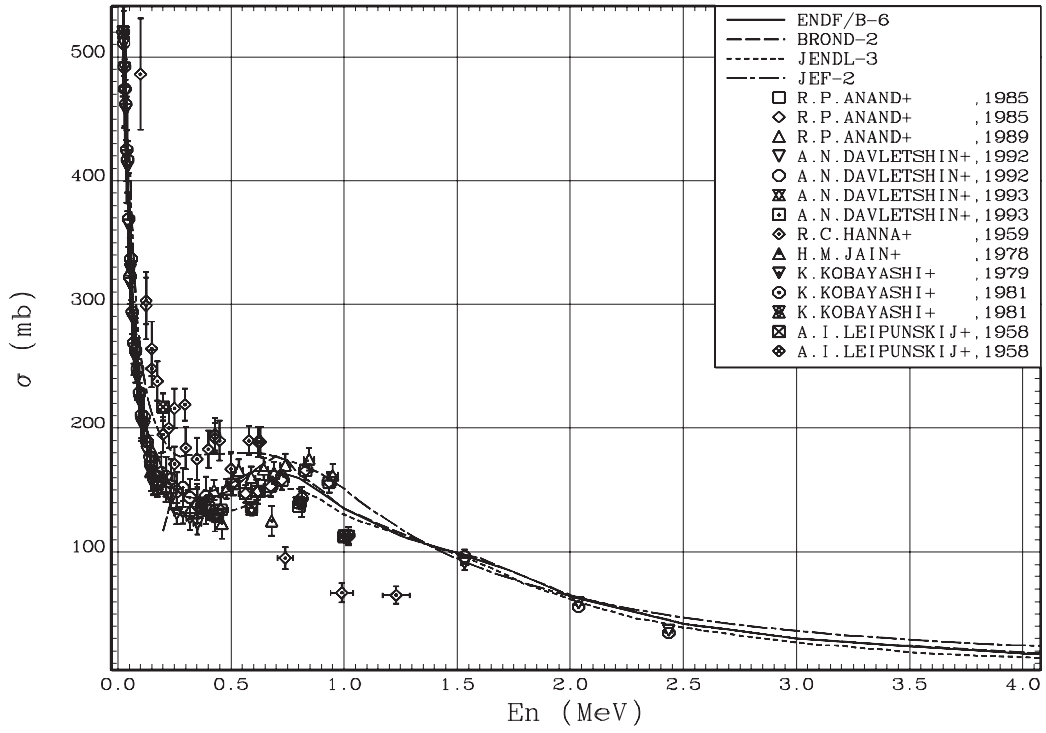

b)

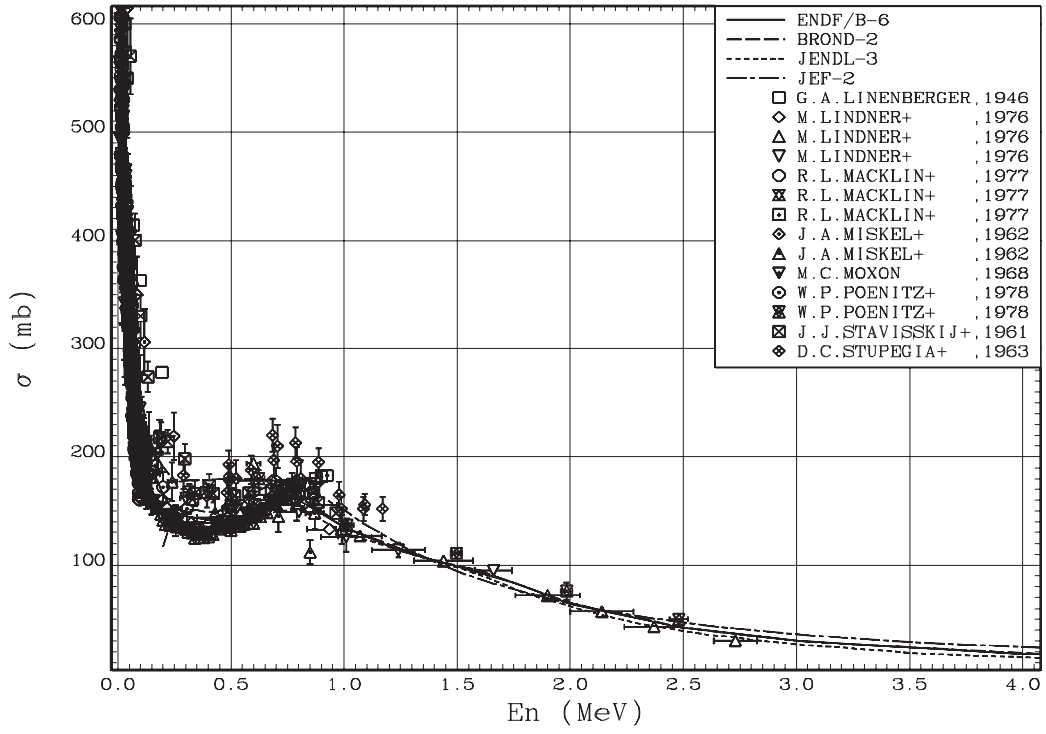

Fig. 9a and b. ^{232}Th radiative capture cross-section

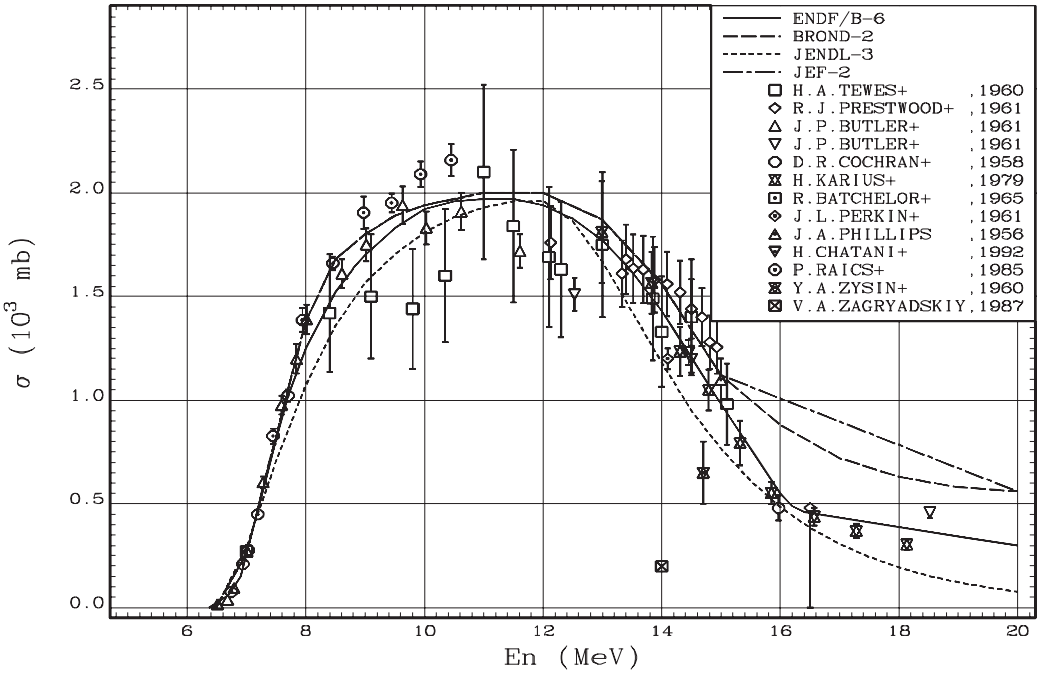

Fig. 10. ^{232}Th(n,2n) reaction cross-section

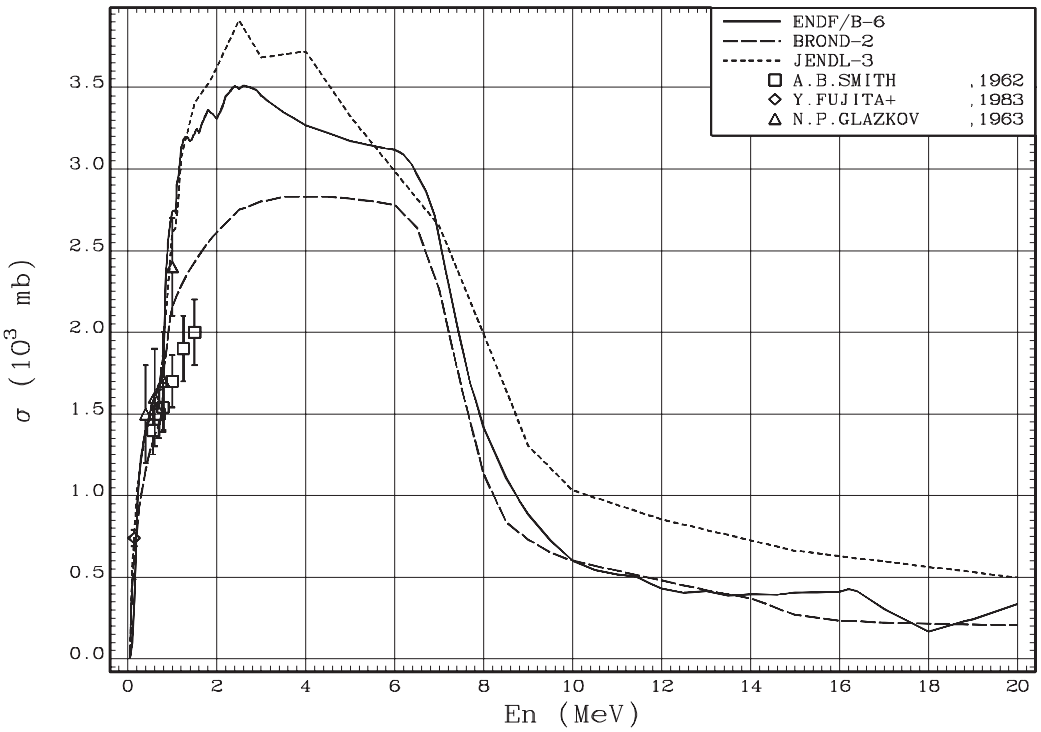

Fig. 11. ^{232}Th inelastic scattering cross-section

a)

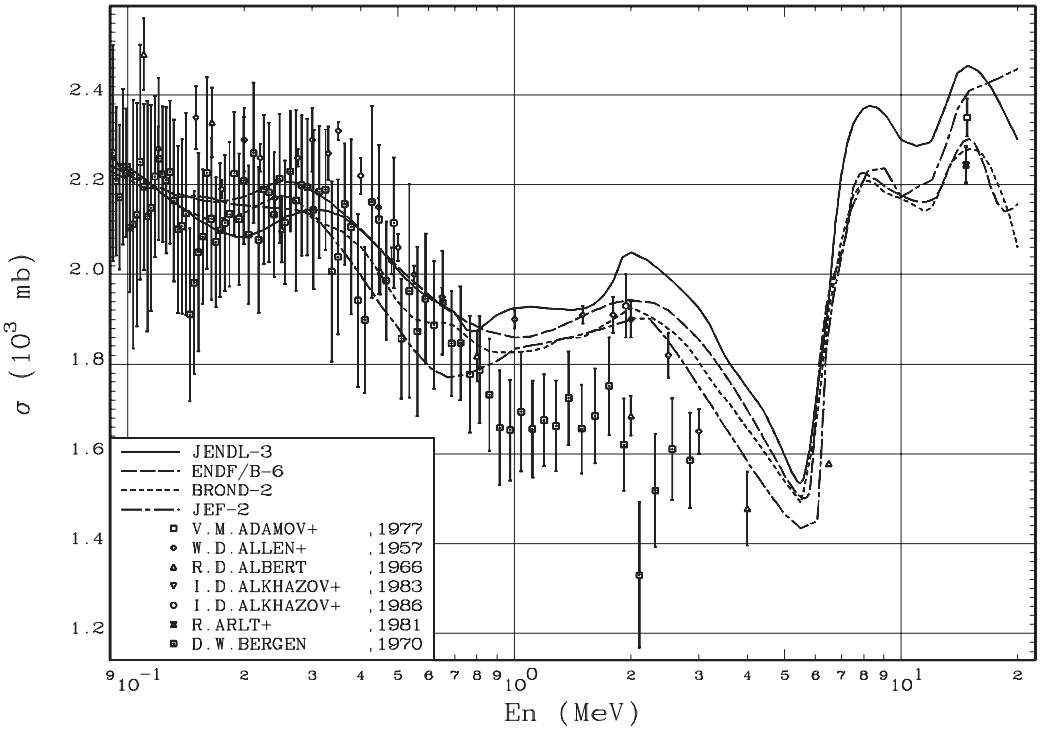

b)

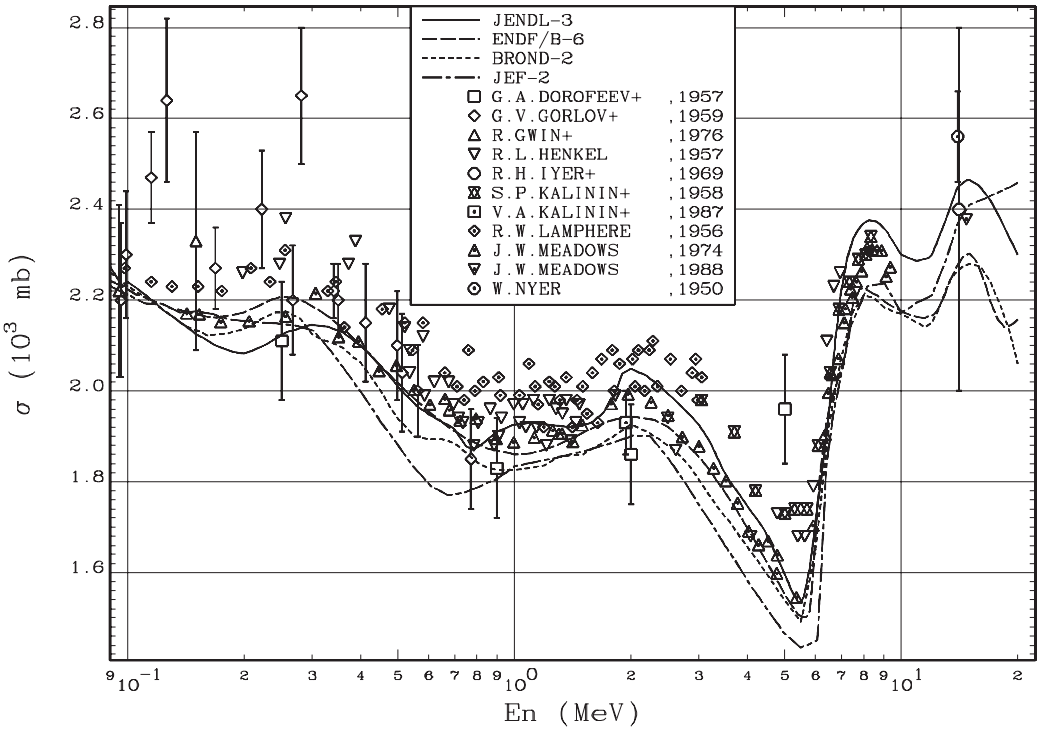

Fig. 12a and b. ^{233}U fission cross-section

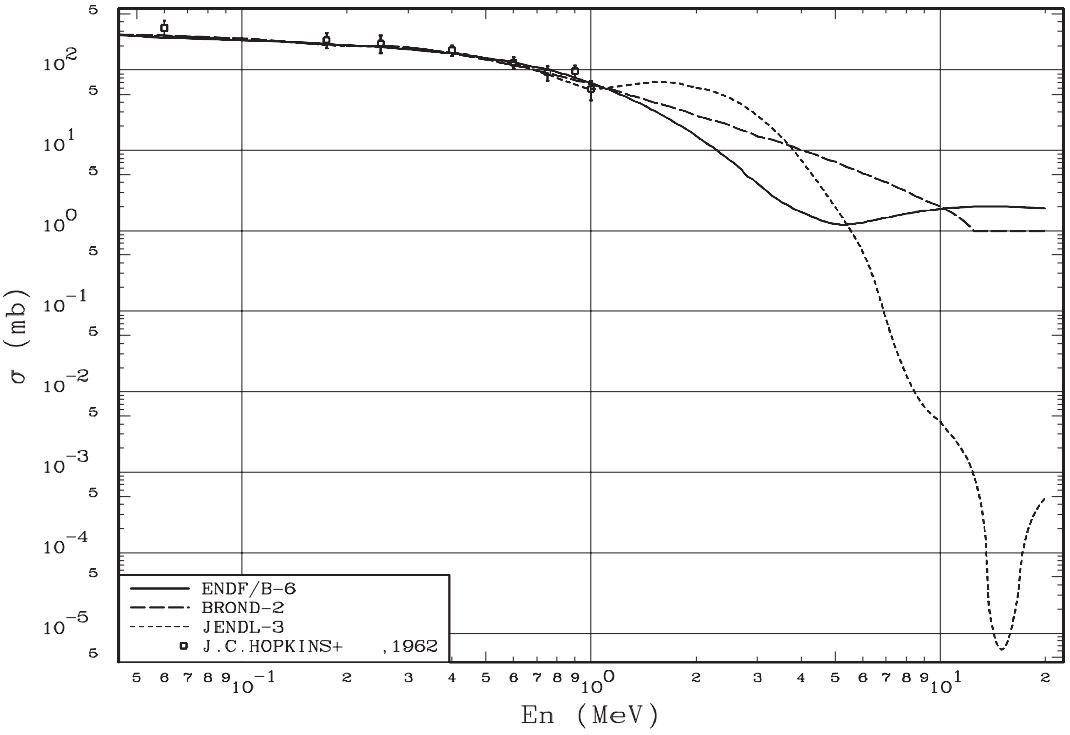

Fig. 13. ^{233}U radiative capture cross-section

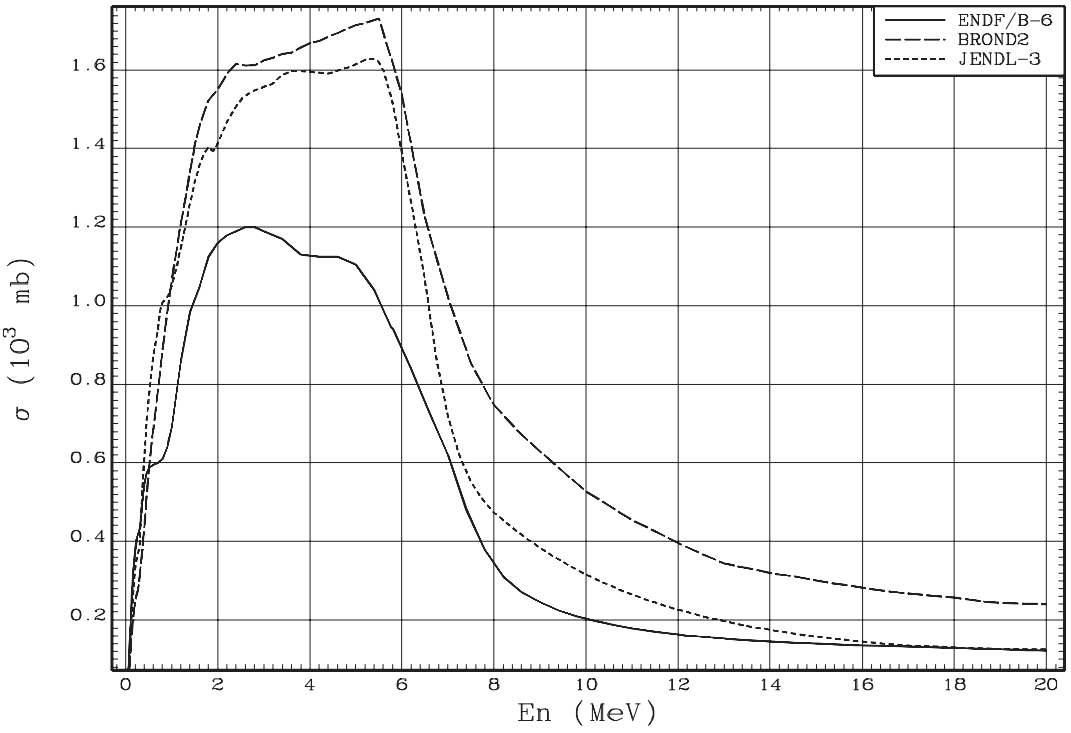

Fig. 14. ^{233}U inelastic scattering cross-section

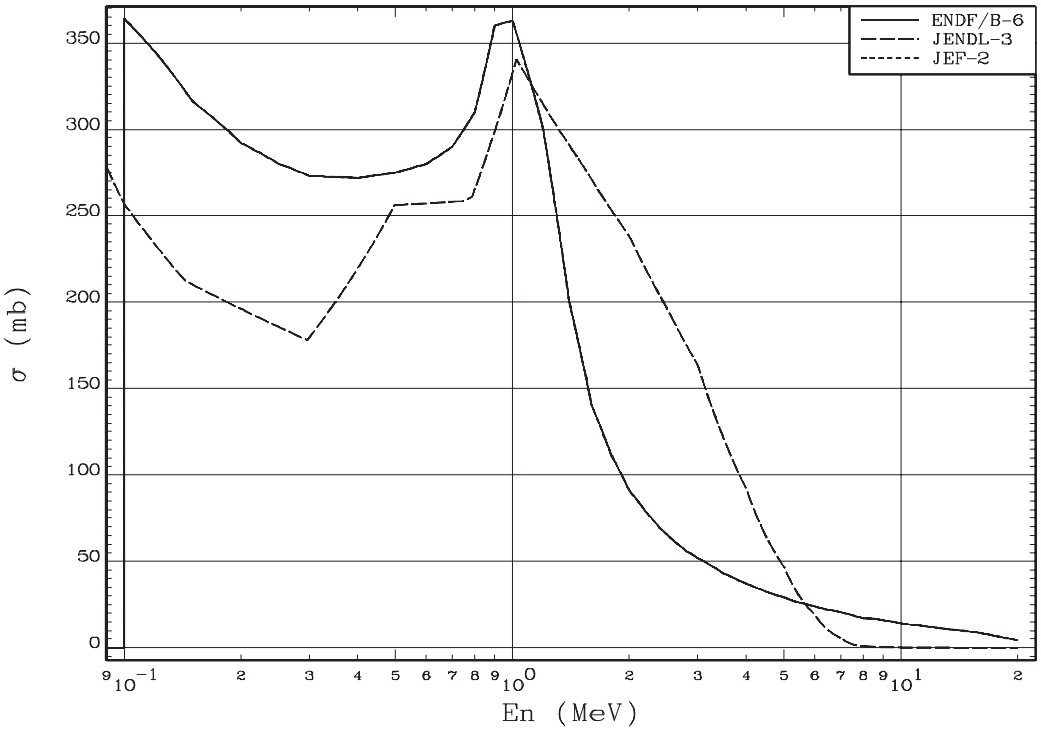

Fig. 15. ^{234}U radiative capture cross-section

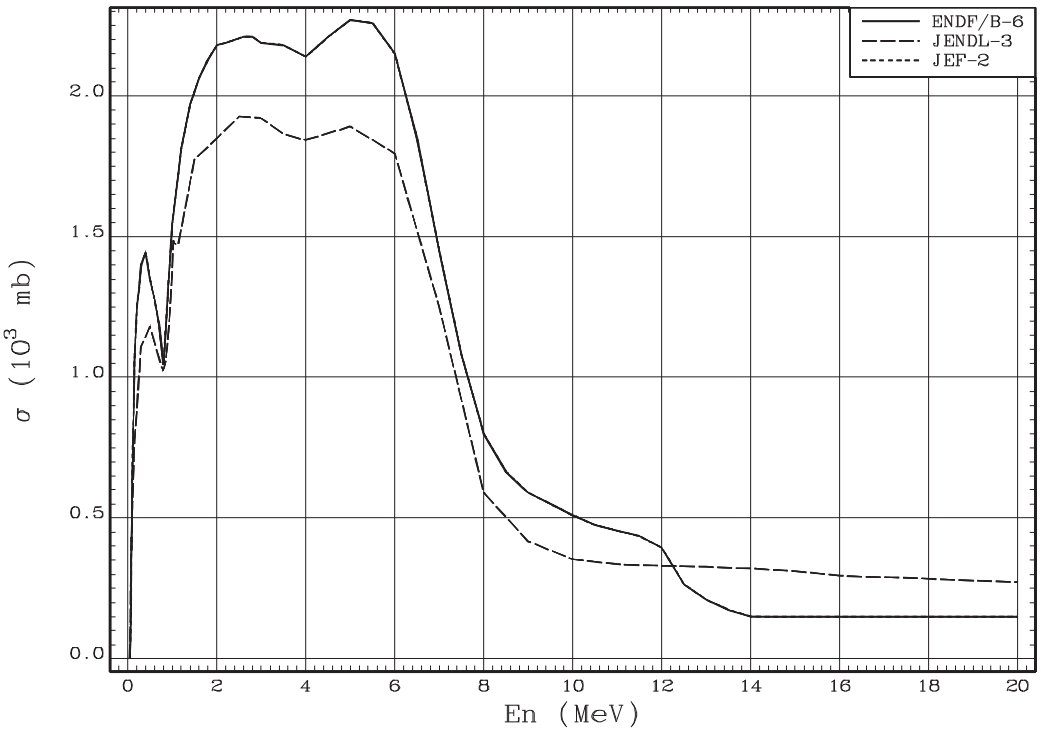

Fig. 16. ^{234}U inelastic scattering cross-section

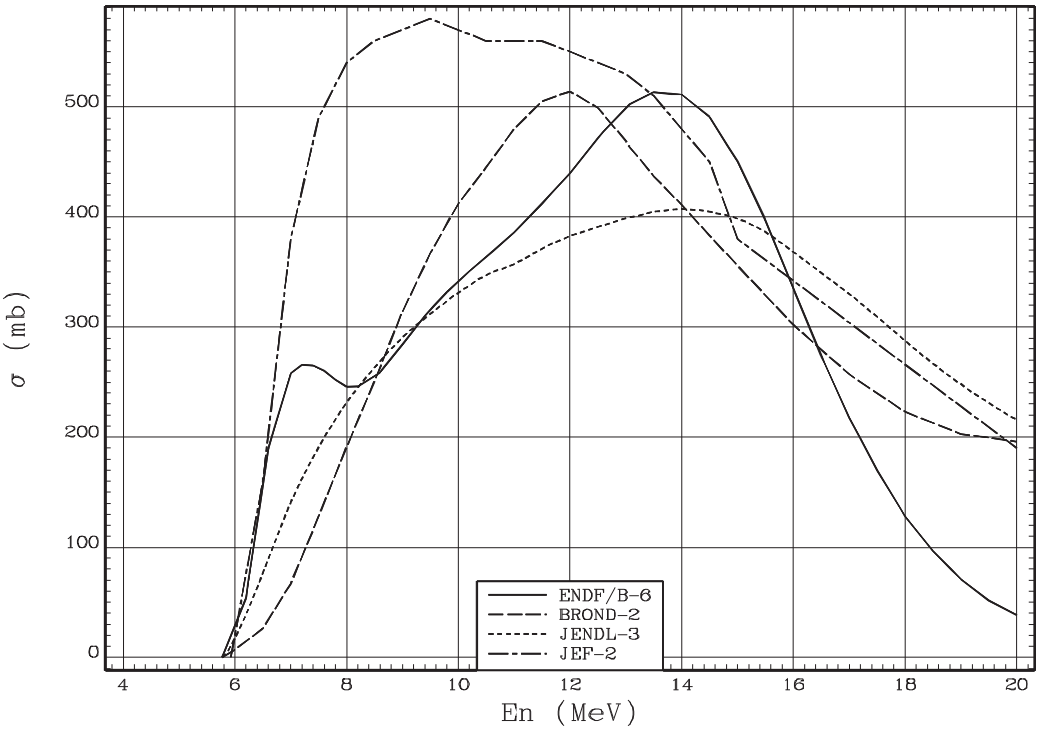

Fig. 17. ^{233}U(n,2n) reaction cross-section

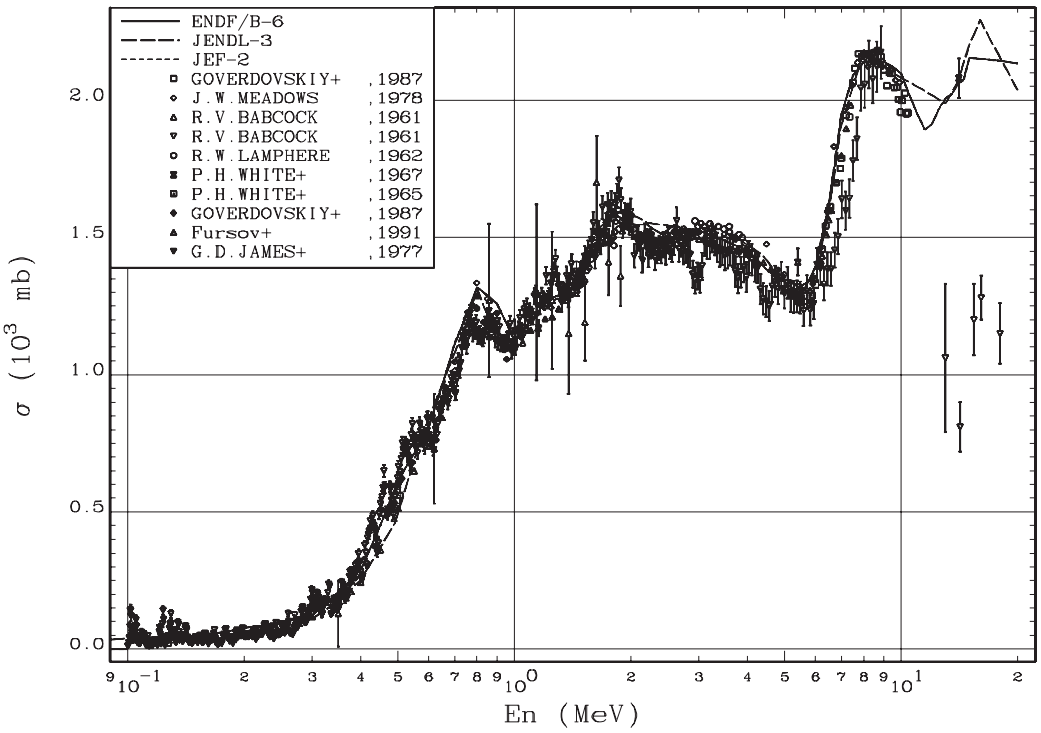

Fig. 18. ^{234}U fission cross-section

98-10985 (70)
Translated from Russian

UDC 539.172

SERIYA: YADERNYE KONSTANTY, Vypusk 3-4, 1997, s. 79
(Series: Nuclear Constants, Issue No. 3-4 1997, p. 79)

NEUTRON RADIATIVE CAPTURE BY THE ^{241}Am NUCLEUS IN THE ENERGY RANGE 1 keV-20 MeV

K.I. Zolotarev, A.V. Ignatyuk, V.A. Tolstikov
G.Ya. Tertychnyj

Russian Federation National Research Centre
Institute of Physics and Power Engineering, Obninsk

ABSTRACT

NEUTRON RADIATIVE CAPTURE FOR ^{241}Am IN THE ENERGY RANGE 1 keV-20 MeV. Production of high actinides leads to many technological problems in the nuclear power. The ^{241}Am(n,γ)^{242}Am reaction is one of the sources of high actinide buildup. So a knowledge of the radiative capture cross-section of ^{241}Am for neutron energies up to 20 MeV is of considerable importance for present day fission reactors and future advanced reactors. The main goal of this paper is the evaluation of the excitation function for the reaction ^{241}Am(n,γ)^{242}Am in the energy range 1 keV-20 MeV. The evaluation was done on the basis of analysed experimental data, data from theoretical model calculations and systematic predictions for 14.5 MeV and 20 MeV. Data from the present evaluation are compared with the cross-section values given in the evaluations carried out earlier.

The reaction of neutron radiative capture by the ^{241}Am nucleus is one of the pathways for the formation of the higher actinides, in particular curium. Accumulation of higher actinides leads to numerous technological problems both during the operation of reactors and in the subsequent chain of spent fuel storage, reprocessing and disposal of long-lived wastes.

To perform a quantitative analysis of the accumulation of actinides it is necessary to have sufficiently accurate data on the energy dependence of the cross-section for radiative capture by ^{241}Am.

The purpose of the present work was to evaluate the excitation function for the reaction ^{241}Am(n,γ)^{242}Am in the neutron energy range 1 keV-20 MeV on the basis of an analysis of published experimental data on the cross-sections for neutron radiative capture in the forbidden resonance region, data from theoretical calculations and systematic predictions of the cross-sections at the points 14.5 and 20 MeV.

1. ANALYSIS OF THE EXPERIMENTAL DATA

1.1. General remarks

All experimental works published so far on research into the cross-sections for absorption and neutron radiative capture by the ^{241}Am nucleus were carried out by the time-of-flight method.

The neutron radiative capture cross-section for ^{241}Am, $\sigma_{n,\gamma}$, or more precisely the absolute values of the ratio of the cross-sections $\sigma_{n,\gamma}{}^{241}\text{Am}/\sigma_{n,\gamma}{}^{197}\text{Au}$ in the energy range 10-250 keV, were measured only in a single paper byWisshak and Käppeler [3].

Weston and Todd [1], Gayter and Thomas [2], and Vanpraet et al. [4] measured the absorption cross-section σ_{abs}, $\sigma_{abs} = \sigma_{n,\gamma} + \sigma_{n,f}$, in the energy range from the thermal region to 200-500 keV. The effect from neutron inelastic scattering was removed by displacement in the gamma detectors.

In the measurements described in Refs [1-3], the americium samples were made from either AmO_2 or Am_2O_3 powders. The weight of the samples was equal to 2 g in the Weston and Todd measurements, 12 g in Gayter and Thomas, and 1.5 g in Wisshak and Käppeler. The samples contained significant impurities of fissionable components.

In the Vanpraet et al. [4] measurements, a sample of pure metallic ^{241}Am weighing 1.74 g was used. This reduced by a factor of more than 8 the gamma background, due largely to (α,n) reactions in oxygen isotopes, and so the systematic error in the background subtraction decreased sharply. In the measurements carried out by Vanpraet et al. [4], an independent normalization of the energy dependence $\sigma_{abs}{}^{241}\text{Am}$ was carried out with respect to the resonance parameters of the saturated resonances at 0.576 and 1.270 eV. The normalization factors agreed to within 0.5%.

In the experiment carried out by Gayter and Thomas [2], only the energy dependence $\sigma_{abs}{}^{241}\text{Am}$ was measured, whereas the absolute normalization was performed on the basis of the Weston and Todd [1] data over the energy range of 1-2 keV, i.e. these two sources are strongly correlated in the "absolute".

In order to make the experimental data listed above comparable, they must be renormalized in terms of both the "absolute" and the energy dependence to uniform standards currently applicable.

In the Weston and Todd [1] measurements the normalization was carried out in terms of $\int_{E_1}^{E_2} \sigma_{abs}\sqrt{E}dE$ (E_1 = 0.02 eV, E_2 = 0.03 eV), which at that time was equivalent to a normalization to 582 barns at 0.0253 eV in accordance with the data published to date.

The energy dependence of the neutron flux up to 2 keV was measured using the $^{10}\text{B}(n,\alpha)$ reaction, and for energies of 2-350 keV using the $^{6}\text{Li}(n,t)^{4}\text{He}$ reaction. It was assumed that the cross-section for the former reaction would change according to a $1/v$ law

with an error of 2%. In relation to the $^{6}Li(n,t)^{4}He$ reaction there are no specific data, only a reference to a program generating these data.

Gayter and Thomas [2] used the $^{6}Li(n,t)^{4}He$ reaction to measure the neutron flux up to 30 keV, and $^{235}U(n,f)$ for higher energies up to 500 keV. From the paper it is not clear what specific data were selected for the reference cross-sections.

Vanpraet et al. [4] measured the neutron flux with the reaction $^{10}B(n,\alpha\gamma)^{7}Li$ over the entire energy range (in terms of averaged cross-sections, from 1 to 500 keV). As in Ref. [2], the authors do not indicate the cross-sections to be used for the monitor reaction.

The foregoing remarks illustrate the difficulty of performing a fully objective renormalization of the measurement data given in Refs [1, 2, 4].

In all five series of measurements carried out by Wisshak and Käppeler [3], as indicated above, absolute values of the ratio $\sigma_{n\gamma}{}^{241}Am/\sigma_{n\gamma}{}^{197}Au$ were determined; hence obtaining absolute values of the excitation function for the reaction $^{241}Am(n,\gamma)^{241}Am$ presented no difficulties.

1.2. Correction of the experimental data

Measurements of Weston and Todd [1]

The cross-section σ_{abs} evaluated by Mughabghab [5] was selected as the renormalization cross-section for 0.0253 eV. For this energy Mughabghab gives a value of the cross-section $\sigma_{n,\gamma} + \sigma_{n,f} = 587\ b + 3\ b = 590 \pm 12\ b$ with an error of ~ 2%. The argument for selecting this value was that it was obtained on the basis of data from time-of-flight measurements for 0.0253 eV. We were reluctant to take data from the ENDF/B-VI evaluation because it is partly based on experiments in thermal columns with insufficiently well-known spectra.

The normalization coefficient linked with the new value of the standard for σ_{abs} in the thermal point was thus determined from the ratio 590/582 = 1.0137.

In order to obtain the cross-section for neutron radiative capture in pure form the contribution of the $\sigma_{n,f}$ component to σ_{abs} at each energy point was subtracted. Data on the cross-section for the reaction $^{241}Am(n,f)$ were taken from Ref. [6]. The contribution of the fission cross-section to σ_{abs} grows with increasing neutron energy. At 1.25 keV it amounts to 0.57%, increasing to 4.93% at E_n = 325 keV.

The total error in the neutron radiative capture cross-section $\sigma_{n,\gamma}$ for the Weston and Todd data was calculated by the formula:

$$\Delta\sigma_{n,\gamma}(\%) = \sqrt{\Delta\sigma_1^2 + \Delta\sigma_2^2 + \Delta\sigma_3^2 + \Delta\sigma_4^2}$$

where $\Delta\sigma_1$ is the systematic error taken from Weston and Todd [1]; $\Delta\sigma_2$ is the error in the normalization cross-section in the point 0.0253 eV, $\Delta\sigma_3$ = 2%, $\Delta\sigma_3$ is the error in the energy

dependence of the reference cross-sections: 1% for the $^{10}B(n,\alpha)$ reaction up to 2 keV; 2% for the $^{6}Li(n,t)^{4}He$ reaction in the range 2-350 keV, and $\Delta\sigma_4$ is the error in the determination of the contribution of the fission cross-section to σ_{abs}.

This is an evaluation of the "minimum" error. In fact, for E_n > 8-12 keV it is somewhat higher owing to the indeterminacy in the data used for the monitor reaction $^{6}Li(n,t)^{4}He$.

Measurements of Gayter and Thomas [2]

The description of the experiment given in Ref. [2] does not contain all the information needed for analysis. The measurement results are given by the authors only in a graphic representation. For this reason, we took numerical data on the cross-section obtained by Gayter and Thomas from the EXFOR library [7]. As indicated above, no independent absolute normalization was carried out by these authors, who made an "adaptation" to the data of Ref. [1]. Accordingly, for the reasons given above, we multiplied the data of Gayter and Thomas by a coefficient1.0137.

To determine the neutron radiative capture cross-sections in pure form, as for the Weston and Todd data, we subtracted the contribution of the $\sigma_{n,f}$ component to σ_{abs} at each energy point. Over the range 1.0-1.5 keV it was equal to 0.59%, increasing to 8.1% at E_n = 400-500 keV. In addition, we introduced a correction into the Gayter and Thomas data to take into account the contribution from fission of ^{239}Pu, which is present in the americium specimen as an impurity of 1.5% (by weight). The correction for the contribution from ^{239}Pu fission, like that for the contribution from ^{241}Am fission, grows with increasing neutron energy, but more slowly. In the ranges 1.0-1.5 keV and 400-450 keV it is equal to 0.76% and 2.55%, respectively. To calculate the correction, we took data on the cross-section for the $^{239}Pu(n,f)$ reaction from the JENDL-3.2 library[8].

The Gayter and Thomas paper does not indicate clearly which cross-sections were selected for the monitor reactions: $^{6}Li(n,t)^{4}He$ in the range 0.125-27.5 keV and $^{235}U(n,f)$ in the range 30-450 keV.

We determined that the authors used cross-sections from the ENDF/B-IV library for both monitor reactions and renormalized their original data to cross-sections from the ENDF/B-VI library, since the data of this library are now recommended as a standard for both the $^{6}Li(n,t)^{4}He$ and the $^{235}U(n,f)$ reaction [9].

Using cross-sections from the ENDF/B-VI library [10] for the monitor reaction $^{6}Li(n,t)^{4}He$ leads to a reduction in the value of σ_{abs} ^{241}Am by 0.1-1.2% in the range 0.85-1.7 keV and by 1.3-2.3% in the range 20-30 keV.

The transition from the ENDF/B-IV [11] to the ENDF/B-VI [12] standard for the $^{235}U(n,f)$ reaction leads (except at three points) to a reduction in σ_{abs} ^{241}Am by 0.3-4.5%. At neutron energies of 35, 45 and 225 keV the ratio of the ENDF/B-IV cross-section to the ENDF/B-VI cross-section for the $^{235}U(n,f)$ reaction equals 1.0045, 1.0045 and 1.0015, respectively.

The error in the experimental data of 12% as given by Gayter and Thomas does not include the error due to the obtaining of absolute values of the cross-sections. The error in the absolute normalization comprises two components. The error in the data of Weston and Todd [1] in the range 1-2 keV is ~ 7.5% and the error in the value of the renormalized cross-section for 0.0253 eV taken from Ref. [5] is 2.1%. The total normalization error evaluated this way is 7.8%.

Measurements of Vanpraet et al. [4]

The flux of irradiating neutrons was measured from the reaction $^{10}B(n,\alpha\gamma)^{7}Li$ using the same gamma detectors recording prompt gamma quanta from capture, with the ^{241}Am sample being replaced by a $^{10}B_4C$ one. Note that no correction for self-shielding was made in the data.

The self-shielding correction may be evaluated on the basis of the Wisshak and Käppeler [3] data. In the overlapping neutron energy ranges it did not exceed ~ 4%, but since the sample thickness in the case of Vanpraet et al. was about three times less than that of Wisshak and Käppeler, the value of this correction was evidently no more than 1.5%. Since it enters into the calculation formula in the form of a ratio with an appropriate value for a ^{10}B detector, they are to some extent compensated and do not substantially change either the value of the cross-section σ_{abs} or its total error. The latter, according to our calculations, was about 11.2% over the measurement range.

The paper does not clearly state from what evaluation the values of the cross-sections for the monitor reaction $^{10}B(n,\alpha\gamma)^{7}Li$ were taken. Judging from the date of publication, the cross-sections were most probably taken from the ENDF/B-V library. We renormalized the data of Vanpraet et al. using cross-sections for the monitor reaction from the ENDF/B-VI library [13]. Renormalization led to an increase in the data of Vanpraet et al. by ~ 1-3% on average.

In making the transition from the neutron absorption cross-section to the neutron radiative capture cross-section the data of Vanpraet were corrected in the same way as those of Ref. [1]. The maximum contribution from ^{241}Am fission to σ_{abs} for the Vanpraet et al. data was 1.84% in the range 150-200 keV.

Measurements of Wisshak and Käppeler [3]

In order to obtain absolute values of the excitation function for the reaction $^{241}Am(n,\gamma)^{242}Am$ we took data on the cross-section for neutron radiative capture by gold from the ENDF/B-VI library [14]. The excitation function for the reaction $^{197}Au(n,\gamma)^{198}Au$ given in ENDF/B-VI is recommended nowadays as a standard for the thermal point and for incident neutron energies of 0.2-2.5 MeV [9].

To complete the analysis of the experimental data on the cross-section for the reaction $^{241}Am(n,\gamma)^{242}Am$ we may draw the following conclusions:

1. The values of the excitation function for the reaction ^{241}Am(n,γ)^{242}Am are measured in greatest detail and with the smallest error in the paper by Wisshak and Käppeler [3].
2. The fact that Weston and Todd's data for the energy range 25-95 keV are systematically lower than all the other measurements may be due to the value they used for the cross-section for the reference reaction ^{6}Li(n,t)^{4}He. However, it should be noted that in the neutron energy region above 0.1 MeV, where use of ^{6}Li(n,t)^{4}He as the reference reaction is not recommended because of the resonance in the cross-section, the discrepancy between the Weston and Todd data and the other measurements is not great.

3. The discrepancies existing in Refs [1-4] with small exceptions lie within the limits of the measurement error. For this reason we consider that an evaluation of the excitation function for the reaction ^{241}Am(n,γ)^{242}Am over the range 1-450 keV should take into account the data from all four papers.

Original and corrected experimental data from Refs [1-4] on the excitation function for the reaction ^{241}Am(n,γ)^{242}Am for incident neutron energies of 1-450 keV are given in Table 1. The values of the cross-sections and their errors are given in ascending order of neutron energy.

2. CALCULATION OF THE EXCITATION FUNCTION FOR THE REACTION ^{241}Am(n,γ)^{242}Am

The calculation of the cross-section for the ^{241}Am(n,γ) reaction was performed using the GNASH program [15], the theoretical basis of which is the Hauser-Feshbach statistical theory of nuclear reactions with special account being taken of pre-equilibrium emission of secondary particles in an exciton model.

The choice of basic parameters for the model - the parameters of level density, the optical model and fission barriers - was based on a mutually harmonized description of all competing reactions included in the calculation, (n,n'), (n,2n), (n,3n), (n,f) and (n,γ), with an adaptation to the known experimental data. The optical neutron transparency coefficients and the cross-sections for direct neutron inelastic scattering with excitation of the first four collective rotation levels were calculated using the coupled channel method (CCROT program).

An important characteristic entering into the calculation of the cross-section for the (n,γ) reaction is the radiative strength function $f(E_\gamma) = \sum_{XL} f_{XL}(E_\gamma)$. Its dipole component f_{E1} we chose in the form of the generalized Lorentzian of Kopetskij-Uhl [15], with the parameters of the giant E1 resonance being taken as for the ^{237}Np nucleus, for which experimental data exist [16]. In addition, we took into account the contribution of the E1 pygmy resonance with energy E = 5.5 MeV and width Γ = 1.5 MeV, exhausting ~ 1.5% of the dipole sum rule. f_{E2} and f_{M1}, components of the total strength function, were selected in the Axel-Brink form with the parameterization given in Ref. [15].

The total strength function was normalized to achieve agreement between the calculated and experimental [1-4] values of the cross-sections in the energy range E_n < 450 keV. Note, however, that since the GNASH program does not take nucleon width correlations into account, this leads to an exaggeration of the calculated cross-sections in the range indicated by an average of 20%.

As indicated above, the cross-sections for the (n,γ) reaction were calculated taking into account a pre-equilibrium component - the so-called direct-semidirect reaction mechanism - which is dominant in the neutron energy region corresponding to excitation of the giant E1 resonance. In the case under discussion this is the region E_n > 8 MeV. Leaving it out of consideration leads to a sharp drop in the cross-section in this energy region, which contradicts the available experimental data for the ^{238}U nucleus [17] and the systematic cross-section data for the points 14.5 and 20 MeV [18].

The excitation function for the reaction ^{241}Am(n,γ)^{242}Am in the incident neutron energy range 20 keV-20 MeV obtained by calculation using the GNASH program is given in Fig. 1. This figure also gives, for comparison, corrected experimental cross-section data [1-4] and systematic data for the points 14.5 and 20 MeV [18]. It can be seen that below 100 keV the GNASH data are systematically higher than the measured cross-section values, which - as already noted above - is due to not taking the neutron width correlation into account. It may also be seen that the data obtained by calculation using the GNASH program agree well with the experimental data above 100 keV and the systematic data for neutron energies of 14.5 and 20 MeV.

3. INITIAL DATA USED TO EVALUATE THE EXCITATION FUNCTION FOR THE REACTION ^{241}Am(n,γ)^{242}Am IN THE NEUTRON ENERGY RANGE 1 keV-20 MeV

In the neutron energy range from 1 to 400 keV only experimental data were used for the evaluation of the excitation function for the reaction of radiative neutron capture by ^{241}Am. The initial data set as a basis for evaluating the excitation function included the corrected cross-section data from all the experimental work reviewed above [1-4]. In the neutron energy region 400 keV-20 MeV, where there are no experimental data above 450 keV, information on the energy dependence of the cross-section for the reaction ^{241}Am(n,γ)^{242}Am was taken from two sources. Data from the calculation performed using the GNASH program (see Section 2) were used for the whole neutron energy range 400 keV-20 MeV. In addition to the calculated values of the excitation function, the initial data set also included cross-section values for the points 14.5 and 20 MeV which we took from the systematic data in Ref. [18].

The values for the errors in the experimental data were taken as evaluated in our analysis. An error of 10-30% was assigned to the data obtained by calculation using the GNASH program. We evaluated the error in the cross-section values obtained by the GNASH program by comparing calculated and experimental data in the energy range 40-450 keV on the assumption that the error in the data gradually grows as the incident neutron energy increases. The tendency for the error in calculated data to increase is confirmed when the calculated data are compared with data obtained from systematic radiative capture cross-sections for neutron energies above 10 MeV. The data from systematics [18] give a value of

the cross-section for the reaction $^{241}Am(n,\gamma)^{242}Am$ at the point 14.5 MeV with an error of the order of 25%. At a neutron energy of 20 MeV the error in the data from systematics increases to 30%.

In addition to information on the reaction cross-section and total error the initial dataset also included information on the structure of the error. Altogether the dataset comprised information on the cross-section values at 250 incident neutron energy points.

4. METHOD OF EVALUATING THE EXCITATION FUNCTION FOR THE REACTION $^{241}Am(n,\gamma)^{242}Am$

The method of statistical analysis of correlated data to be used in evaluating the excitation function for the reaction $^{241}Am(n,\gamma)^{242}Am$ is described in some detail in Refs [19, 20]. Accordingly we shall only look at the main characteristics of the method.

The statistical analysis of the available reaction cross-section data was carried out in the framework of the non-linear regression model. The model function used was the rational function (Padé approximation):

$$f(E) = C + \sum_{i=1}^{l_1} \frac{a_i}{E - r_i} + \sum_{k=1}^{l_2} \frac{a_k (E - \varepsilon_k) + \beta_k}{(E - \varepsilon_k)^2 + \gamma_k^2}, \qquad (1)$$

where E is the value of the neutron energy; C, a_i, r_i, α_k, β_k, ε_k, and γ_k are the parameters being evaluated. The total number of parameters in the Padé approximation is: $L = 2l_1 + 4l_2 + 1$.

The model function parameters can be found from the condition for the minimum of a functional:

$$S(\vec{\beta}) = (\vec{\sigma} - \vec{f})^T (DPD)^{-1} (\vec{\sigma} - \vec{f}). \qquad (2)$$

In expression (2) for a functional that is to be minimized, $\vec{\beta}$ is the vector of the parameters being evaluated; $\vec{\sigma}$ is the vector of the cross-sections from the dataset; D is the diagonal matrix of the error in the cross-sections from the dataset; P is the correlation matrix of the experimental (calculated) data to be used to evaluate the excitation function; and T indicates that the matrix is transposed.

The technical side of the minimization process based on the method of discrete optimization and the Newton-Gauss algorithm is described in detail in Ref. [21].

The algorithm used to minimize the functional (2) involved two approximations which significantly simplified the calculation:

(1) Cross-section data obtained in different experiments (calculations) were considered uncorrelated;

(2) Correlations between cross-sections obtained in a single experiment (calculation) were described using the mean correlation coefficient.

The covariation matrix of the errors of the evaluated parameters W($\hat{\bar{\beta}}$) and the errors in the value of the evaluated function at the point $\Delta f(E_{i_k}^k \hat{\bar{\beta}})$ were determined from the relationships

$$W\left(\hat{\bar{\beta}}\right) = \frac{s}{n-L}\left(X^T V^{-1} X\right)^{-1},$$

$$\Delta f\left(E_{i_k}, \hat{\bar{\beta}}\right) = \sum_{m=1}^{L}\sum_{j=1}^{L} X_{i_k m}^k X_{i_k j}^k W_{mj},$$

where n is the total number of reaction cross-section data to be used in the analysis; X is the $(n \times L)$ matrix of coefficients of sensitivity of the rational function to change in the parameters ($X_{i_k m} = \frac{\partial f\left(E_{i_k}, \hat{\bar{\beta}}\right)}{\partial \beta_m}$), and $\bar{\beta}$ is the vector of the values of the evaluated parameters.

The average correlation coefficients were determined by analysing the structure of the errors of all the experimental data.

The value of the average correlation coefficient $\bar{p}^k$ for a *k* experiment containing information on the n_k values of the reaction excitation function was determined by the formula:

$$\bar{p}^k = \frac{2}{(n_k - 1)n_k}\sum_{i=1}^{n_k-1}\sum_{j=i+1}^{n_k}\frac{\sum_{m=1}^{l} P_{ij}^m e_i^m e_j^m}{e_i e_j}, \qquad (3)$$

where $e_i(e_j)$ is the total error (standard deviation) of the cross-section at the i-th (j-th) point, corresponding to a standard deviation of 1σ; $e_i^m(e_j^m)$ is the m-th component of the systematic error in the cross-section at the i-th (j-th) point; P_{ij}^m is the correlation coefficient between the *m*-th components of the systematic error in the i-th and j-th points; and l is the number of components in the systematic error.

The values of the average correlation coefficients for the data $^{241}Am(n,\gamma)^{242}Am$ reaction cross-section data to be used are given in Table 2. The data from the Wisshak and Käppeler [3] measurements were included by us in the initial data set in the form of five separate series of measurements, i.e. as they were given by the authors themselves. The difference in the average correlation coefficients obtained for the Wisshak and Käppeler measurements is explained largely by the different values of the statistical components of the error.

5. RESULTS OF THE EXCITATION FUNCTION EVALUATION

Statistical analysis of the dataset showed that the rational function (1) with the parameters:

$1_1 = 2$, $1_2 = 3$, C = -0.405523

a_1 = 2.42171E+02	r_1 = -6.27624E-02		
a_2 = 8.25765E+00	r_2 = -1.19556E-04		
α_1 = -1.77498E+02	β_1 = 1.44237E+02	ε_1 = 1.27069E+00	γ_1 = 1.79874E+00
α_2 = -2.62298E+01	β_2 = 1.84433E-01	ε_2 = -3.89656E-03	γ_2 = 7.51044E-03
α_3 = -2.33123E+01	β_3 = 3.11122E+00	ε_3 = 6.50979E-01	γ_3 = 2.13515E-01

describes best, from a physics point of view, the excitation function of the reaction ^{241}Am(n,γ)^{242}Am over the entire range of incident neutron energies from 1 keV to 20 MeV. The cross-sections to be calculated by formula (1) with the parameters indicated are measured in millibarns (mb). The neutron energy *E* is given in megaelectronvolts (MeV). The value of the functional (2) corresponding to the rational function selected is*S* = 1.24592.

The results of the evaluation of the excitation function for the reaction ^{241}Am(n,γ)^{242}Am are given in Figs 2 and 3, which also show experimental data and indicate the lower and upper limits of the error band for the evaluated curve corresponding to a standard deviation of 2σ.

Data on the error in the evaluated excitation function for the reaction ^{241}Am(n,γ)^{242}Am in the various energy groups are given in Table 3, from which it is apparent that the highest accuracy in the evaluation of the excitation function for the reaction, namely 4.62-5.46%, is achieved for the energy range 20-100 keV, where most of the experimental data on the reaction cross-section are.

A correlation matrix of the evaluated group cross-sections is given in Table 4. The strong positive correlation between the cross-section values in the 18th to 42nd energy groups (0.4-20.0 MeV) is due to the fact that a dominant role is played in the evaluation of the cross-sections in this region by data obtained from a single source - namely calculation using the GNASH program.

6. COMPARISON OF THE EVALUATED EXCITATION FUNCTION FOR THE REACTION ^{241}Am(n,γ)^{242}Am WITH DATA FROM OTHER EVALUATIONS

Our evaluation of the total cross-section for the reaction of radiative neutron capture by ^{241}Am in the energy range 1 keV-20 MeV was compared with three other recent evaluations using data from Maslov et al. [22], JENDL-3.2 [23] and ENDF/B-VI [24]. The results of this comparison for the incident neutron energy ranges 1-100 keV and 0.1-20 MeV are given in Figs 4 and 5, respectively. These figures also show corrected experimental cross-section data from Refs [1-4].

Comparison of the data from the four evaluations shows that in the neutron energy range 1 keV-0.8 MeV the evaluated cross-section values for the $^{241}Am(n,\gamma)^{242}Am$ reaction agree to within 30%. It is apparent that the JENDL-3.2 and ENDF/B-VI evaluations were carried out by and large with an orientation towards the experimental data of Weston and Todd [1] and Vanpraet et al. [4]. It is also apparent that the data of Maslov et al. in the range 1-20 keV are systematically lower than the data of the three other evaluations. At the point 1.5 keV, our evaluation, as well as the JENDL-3.2 and ENDF/B-VI evaluations, gives a radiative capture cross-section value 17% higher than Maslov et al.

In the neutron energy range above 0.8 MeV, where there are no experimental data on the cross-section, the evaluations of the excitation function for the $^{241}Am(n,\gamma)^{242}Am$ reaction diverge significantly. Comparatively satisfactory agreement up to an energy of 3.5 MeV and at the point 14.5 MeV is observed only between the data of our evaluation and those of Maslov et al. The sharp drop in the reaction cross-section for the $^{241}Am(n,\gamma)^{242}Am$ reaction seen in the ENDF/B-VI data beyond 0.8 MeV, in the JENDL-3.2 data beyond 1.2 MeV and in Maslov et al. beyond 3.5 MeV would appear to be due to incomplete account being taken of all gamma transitions in the calculation. In the JENDL-3.2 evaluation no account was apparently also taken of direct-semidirect processes, which for the $^{241}Am(n,\gamma)^{242}Am$ reaction are dominant at neutron energies $E_n > 8$ MeV.

Since our new evaluation of the excitation function for the reaction $^{241}Am(n,\gamma)^{242}Am$ was performed on the basis of statistical analysis of cross-sections from a data set which included all available information on the cross-section, it agrees better than the two other comparable evaluations with the experimental data and the data from systematics for the points 14.5 and 20 MeV.

At this time, we believe, there are insufficient reliable integral experimental data on the cross-section for the reaction $^{241}Am(n,\gamma)^{242}Am$. Therefore the evaluated excitation functions were not tested against the integral experimental data.

More accurate values of the excitation function for the $^{241}Am(n,\gamma)^{242}Am$ reaction at neutron energies above 450 keV can be obtained only by measuring microscopic cross-sections in that energy range. It may also be helpful in achieving these accurate values to measure the mean cross-sections for this reaction in the ^{235}U fission neutron spectrum, the ^{252}Cf spontaneous fission neutron spectrum and several other standard neutron fields.

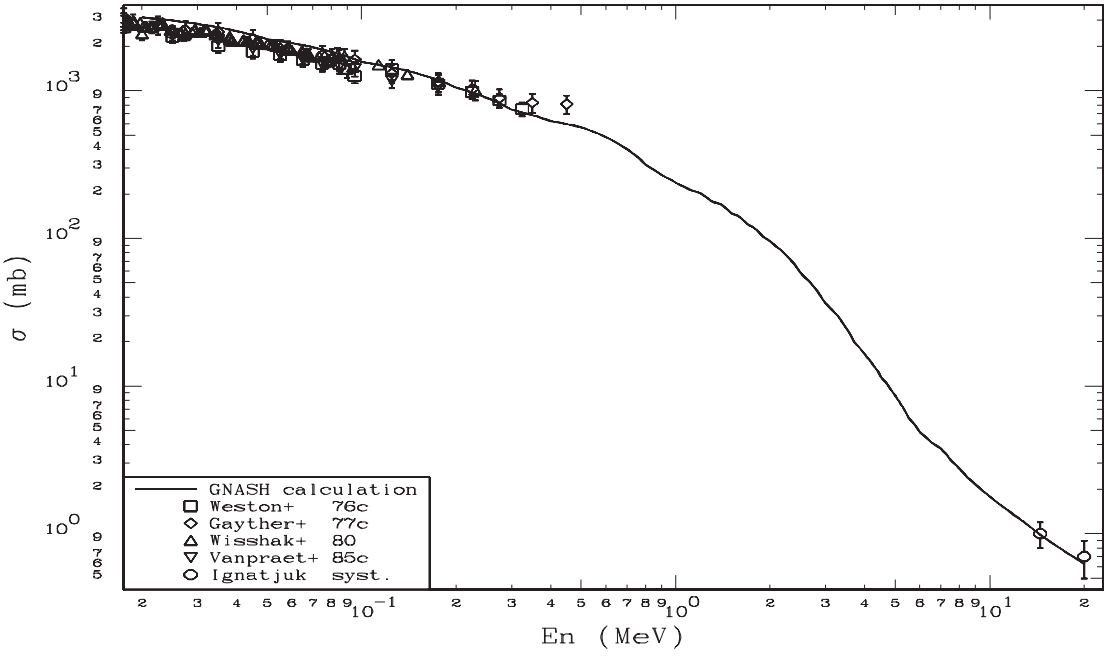

Fig. 1. Excitation function for the reaction $^{241}Am(n,\gamma)^{242}Am$ in the neutron energy range 20 keV-20 MeV, obtained by calculation using the GNASH program, compared with experimental data and data from systematics.

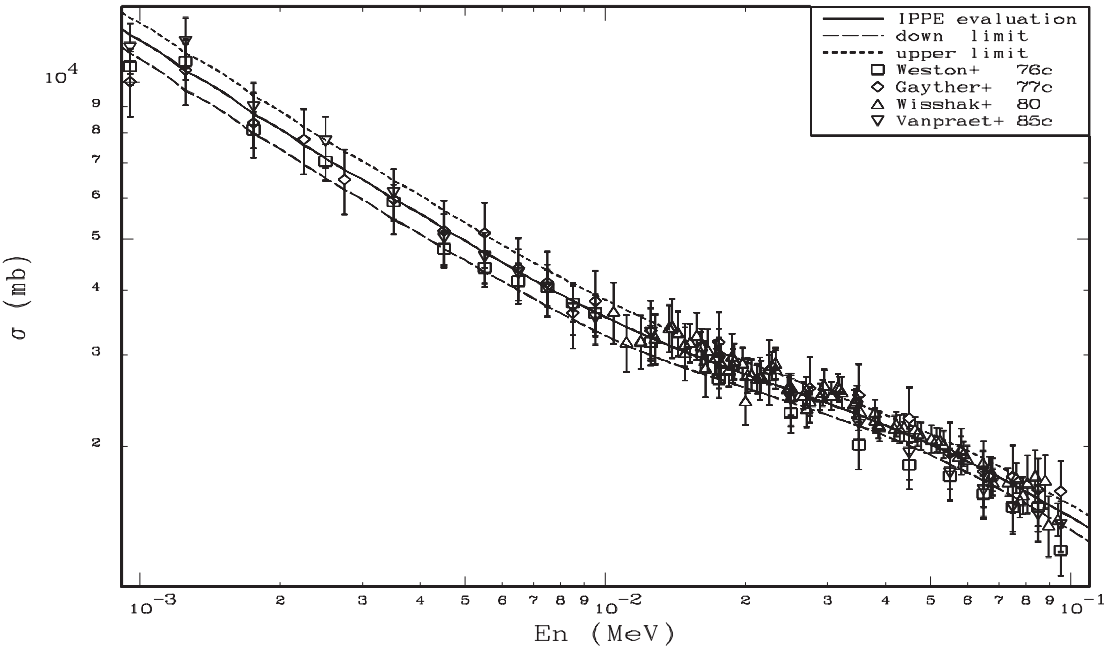

Fig. 2. Evaluated excitation function for $^{241}Am(n,\gamma)^{242}Am$ in the neutron energy range 1-100 keV. The dotted lines give the upper and lower limits of the error band for the evaluated cross-sections.

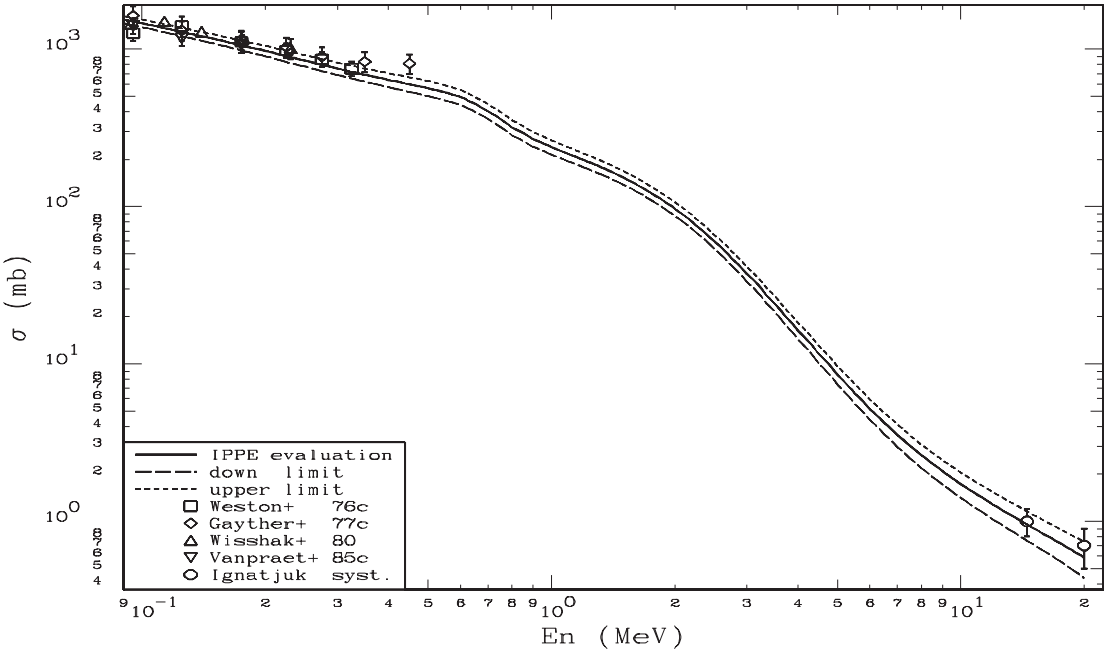

Fig. 3. Evaluated excitation function for $^{241}Am(n,\gamma)^{242}Am$ in the neutron energy range 0.1-20 MeV. The dotted lines give the upper and lower limits of the error band for the evaluated cross-sections.

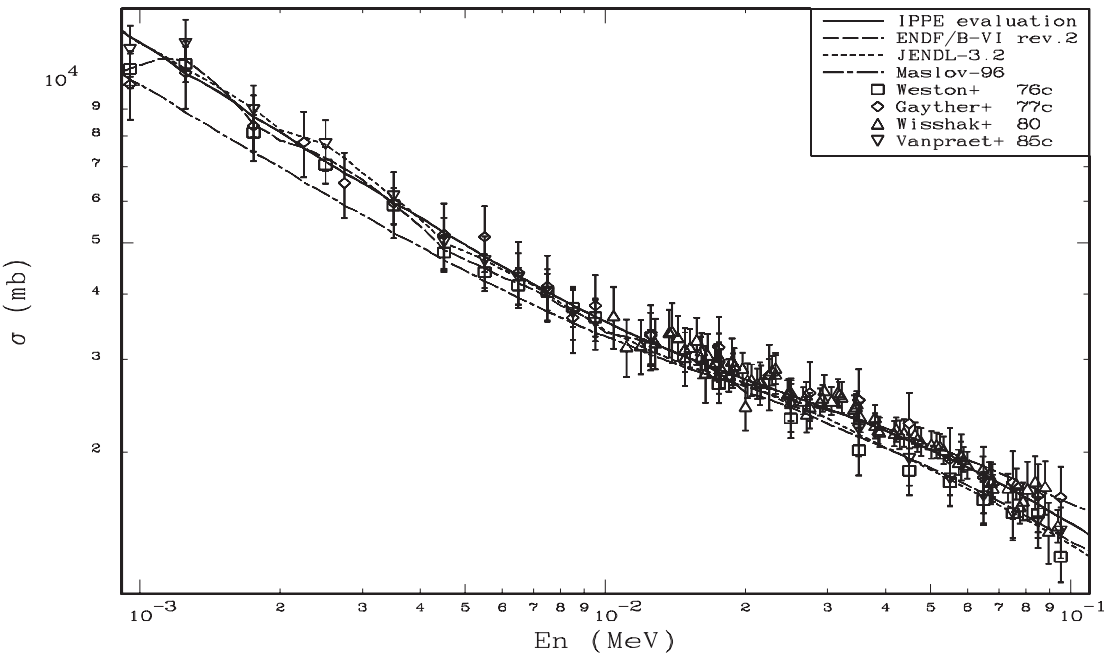

Fig. 4. Evaluated excitation function for $^{241}Am(n,\gamma)^{242}Am$ compared with data from other evaluations and experimental data. Neutron energy range 1-100 keV.

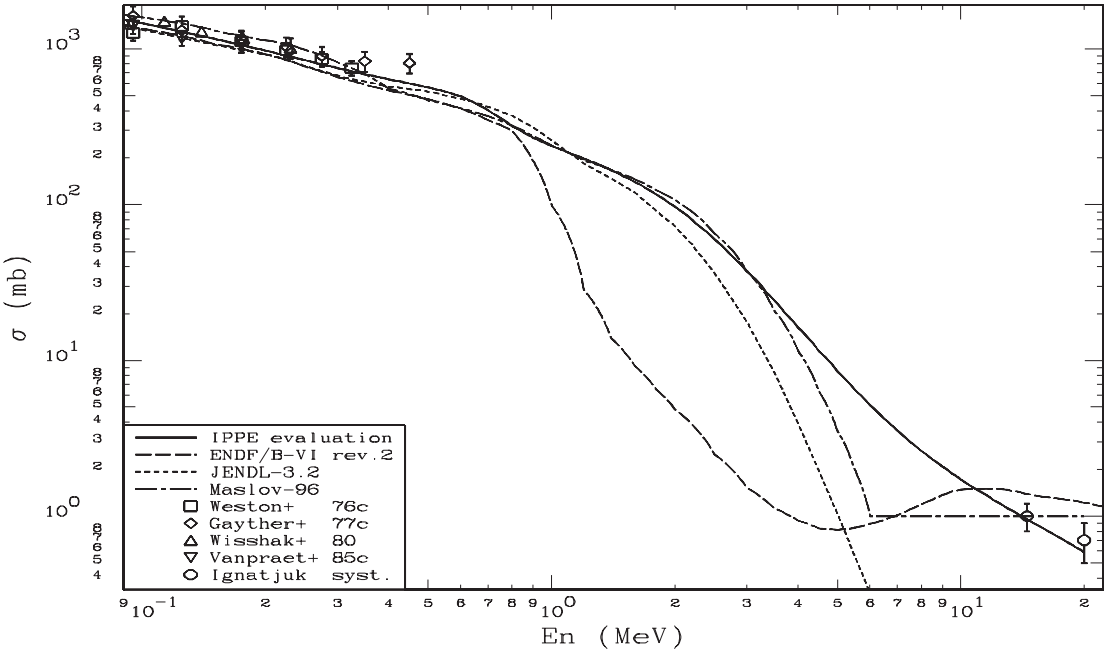

Fig. 5. Evaluated excitation function for $^{241}Am(n,\gamma)^{242}Am$ compared with data from other evaluations and experimental data. Neutron energy range 0.1-20 MeV.

Table 1

Experimental data on the cross-section for the $^{241}Am(n,\gamma)^{242}Am$ reaction in the neutron energy range 1-500 keV

No.	E_n (keV)	Resol. (keV)	σ (orig) (barns)	Δσ (orig) (barns)	Data correction	σ (corr.) (barns)	Δσ (corr.) (barns)	Authors	
1	1,25	0,25	10,90000	0,80006	1;6	10,98700	0,86687	Weston+	76
2	1,25	0,25	10,59000	1,30045	1;5;6	10,57500	1,53972	Gayther+	77
3	1,25	0,25	11,69300	1,30962	1;6	11,99100	1,34299	Vanpraet+	85
4	1,75	0,25	8,06000	0,59966	1;6	8,12000	0,64879	Weston+	76
5	1,75	0,25	8,37000	1,00022	1;5;6	8,36700	1,19481	Gayther+	77
6	1,75	0,25	8,94700	1,00206	1;6	8,97300	1,00498	Vanpraet+	85
7	2,25	0,25	7,78000	0,93049	1;5;6	7,78100	1,11191	Gayther+	77
8	2,50	0,50	7,00000	0,52010	1;6	7,05500	0,56299	Weston+	76
9	2,50	0,50	7,69000	0,86128	1;6	7,72000	0,86464	Vanpraet+	85
10	2,75	0,25	6,53000	0,78034	1;5;6	6,50700	0,92920	Gayther+	77
11	3,50	0,50	5,85000	0,43992	1;6	5,89600	0,47522	Weston+	76
12	3,50	0,50	5,99000	0,72000	1;5;6	5,96700	0,85567	Gayther+	77
13	3,50	0,50	6,11100	0,68443	1;6	6,13700	0,68734	Vanpraet+	85
14	4,50	0,50	4,76000	0,35986	1;6	4,79500	0,38840	Weston+	76
15	4,50	0,50	5,21000	0,63041	1;5;6	5,19200	0,74817	Gayther+	77
16	4,50	0,50	5,00700	0,56078	1;6	5,02700	0,56302	Vanpraet+	85
17	5,50	0,50	4,37000	0,32994	1;6	4,40200	0,35612	Weston+	76
18	5,50	0,50	5,16000	0,62023	1;5;6	5,13700	0,73665	Gayther+	77
19	5,50	0,50	4,60800	0,51610	1;6	4,62700	0,51822	Vanpraet+	85
20	6,50	0,50	4,12000	0,30982	1;6	4,15100	0,33457	Weston+	76
21	6,50	0,50	4,41000	0,53008	1;5;6	4,39200	0,62981	Gayther+	77
22	6,50	0,50	4,28000	0,47936	1;6	4,29700	0,48126	Vanpraet+	85
23	7,50	0,50	4,01000	0,29995	1;6	4,04100	0,32409	Weston+	76
24	7,50	0,50	4,16000	0,50003	1;5;6	4,13300	0,59267	Gayther+	77
25	7,50	0,50	3,99200	0,44710	1;6	4,00900	0,44901	Vanpraet+	85
26	8,50	0,50	3,74000	0,28013	1;6	3,76800	0,30257	Weston+	76
27	8,50	0,50	3,63000	0,43996	1;5;6	3,60300	0,51955	Gayther+	77
28	8,50	0,50	3,67000	0,41104	1;6	3,68500	0,41272	Vanpraet+	85
29	9,50	0,50	3,58000	0,26993	1;6	3,60700	0,29145	Weston+	76
30	9,50	0,50	3,82000	0,45993	1;5;6	3,79800	0,54539	Gayther+	77
31	9,50	0,50	3,51200	0,39334	1;6	3,52700	0,39502	Vanpraet+	85
32	10,40	0,60	3,63400	0,48841	0	3,63400	0,48841	Wisshak+	80
33	11,10	0,70	3,17500	0,39878	0	3,17500	0,39878	Wisshak+	80
34	11,90	0,70	3,18700	0,37862	0	3,18700	0,37862	Wisshak+	80
35	12,50	2,50	3,14000	0,22985	1;6	3,16300	0,24893	Weston+	76
36	12,50	2,50	3,36000	0,40018	1;5;6	3,33200	0,47514	Gayther+	77
37	12,50	2,50	3,29900	0,36949	1;6	3,31100	0,37083	Vanpraet+	85
38	12,80	0,80	3,22800	0,35573	0	3,22800	0,35573	Wisshak+	80
39	13,70	0,80	3,37800	0,35266	0	3,37800	0,35266	Wisshak+	80
40	13,90	0,60	3,39400	0,44292	0	3,39400	0,44292	Wisshak+	80
41	14,30	0,70	3,30500	0,32620	0	3,30500	0,32620	Wisshak+	80
42	14,80	0,70	3,02500	0,35362	0	3,02500	0,35362	Wisshak+	80
43	14,80	0,90	3,14200	0,30100	0	3,14200	0,30100	Wisshak+	80
44	15,20	0,80	3,16500	0,25004	0	3,16500	0,26744	Wisshak+	80
45	15,70	0,70	3,26600	0,33770	0	3,26600	0,33770	Wisshak+	80
46	16,00	1,00	3,03700	0,27667	0	3,03700	0,27667	Wisshak+	80
47	16,10	0,80	3,11600	0,24866	0	3,11600	0,24866	Wisshak+	80
48	16,40	0,80	2,82900	0,34995	0	2,82900	0,34995	Wisshak+	80
49	16,60	0,80	3,05900	0,29305	0	3,05900	0,29305	Wisshak+	80
50	17,20	0,90	2,96600	0,21770	0	2,96600	0,21770	Wisshak+	80
51	17,30	1,10	2,96700	0,23410	0	2,96700	0,23410	Wisshak+	80
52	17,50	2,50	2,67000	0,19998	1;6	2,68900	0,21593	Weston+	76
53	17,50	2,50	3,20000	0,38016	1;5;6	3,16600	0,45052	Gayther+	77
54	17,50	0,90	3,04100	0,32052	0	3,04100	0,32052	Wisshak+	80
55	17,50	2,50	2,89700	0,32446	1;6	2,90800	0,32570	Vanpraet+	85

No.	E_n (keV)	Resol. (keV)	σ (orig) (barns)	Δσ (orig) (barns)	Data correction	σ (corr.) (barns)	Δσ (corr.) (barns)	Authors	
56	17,70	0,90	2,89200	0,24698	0	2,89200	0,24698	Wisshak+	80
57	18,40	1,00	2,80100	0,19803	0	2,80100	0,19803	Wisshak+	80
58	18,70	0,90	2,98100	0,30555	0	2,98100	0,30555	Wisshak+	80
59	18,80	1,20	2,86100	0,21515	0	2,86100	0,21515	Wisshak+	80
60	18,90	0,90	2,91900	0,23031	0	2,91900	0,23031	Wisshak+	80
61	19,70	1,00	2,88900	0,20165	0	2,88900	0,20165	Wisshak+	80
62	20,00	1,00	2,44300	0,24797	0	2,44300	0,24797	Wisshak+	80
63	20,20	1,00	2,73900	0,20871	0	2,73900	0,20871	Wisshak+	80
64	20,60	1,40	2,74500	0,19160	0	2,74500	0,19160	Wisshak+	80
65	21,20	1,10	2,70200	0,17887	0	2,70200	0,17887	Wisshak+	80
66	21,50	1,10	2,70700	0,25175	0	2,70700	0,25175	Wisshak+	80
67	21,60	1,10	2,72300	0,19497	0	2,72300	0,19497	Wisshak+	80
68	22,50	2,50	2,84000	0,33995	1;5;6	2,79800	0,40039	Gayther+	77
69	22,50	1,50	2,81600	0,18389	0	2,81600	0,18389	Wisshak+	80
70	22,80	1,20	2,85800	0,18406	0	2,85800	0,18406	Wisshak+	80
71	23,20	1,20	2,89000	0,19912	0	2,89000	0,19912	Wisshak+	80
72	23,20	1,20	2,81900	0,24074	0	2,81900	0,24074	Wisshak+	80
73	24,60	1,40	2,58000	0,15480	0	2,58000	0,15480	Wisshak+	80
74	24,80	1,70	2,59300	0,16466	0	2,59300	0,16466	Wisshak+	80
75	25,00	5,00	2,30000	0,18009	1;6	2,31600	0,19339	Weston+	76
76	25,00	1,30	2,60000	0,16068	0	2,60000	0,16068	Wisshak+	80
77	25,00	1,40	2,49200	0,20360	0	2,49200	0,20360	Wisshak+	80
78	25,00	5,00	2,45300	0,27474	1;6	2,45900	0,27542	Vanpraet+	85
79	26,60	1,50	2,50500	0,15030	0	2,50500	0,15030	Wisshak+	80
80	27,00	1,50	2,56800	0,15203	0	2,56800	0,15203	Wisshak+	80
81	27,10	1,50	2,36200	0,18636	0	2,36200	0,18636	Wisshak+	80
82	27,50	2,50	2,64000	0,31997	1;5	2,59000	0,37374	Gayther+	77
83	27,50	2,00	2,44000	0,15274	0	2,44000	0,15274	Wisshak+	80
84	28,90	1,70	2,49100	0,14747	0	2,49100	0,14747	Wisshak+	80
85	29,30	1,70	2,53600	0,14785	0	2,53600	0,14785	Wisshak+	80
86	29,50	1,70	2,61800	0,18509	0	2,61800	0,18509	Wisshak+	80
87	30,60	2,30	2,50400	0,15475	0	2,50400	0,15475	Wisshak+	80
88	31,60	1,90	2,59900	0,14944	0	2,59900	0,14944	Wisshak+	80
89	31,80	1,80	2,57500	0,14575	0	2,57500	0,14575	Wisshak+	80
90	32,20	1,90	2,54600	0,17542	0	2,54600	0,17542	Wisshak+	80
91	34,20	2,60	2,41500	0,14707	0	2,41500	0,14707	Wisshak+	80
92	34,60	2,10	2,44000	0,13615	0	2,44000	0,13615	Wisshak+	80
93	34,70	2,00	2,47300	0,13799	0	2,47300	0,13799	Wisshak+	80
94	35,00	5,00	2,00000	0,20000	1;6	2,01300	0,20955	Weston+	76
95	35,00	5,00	2,50000	0,30000	1;5;6	2,50700	0,36652	Gayther+	77
96	35,00	5,00	2,19900	0,24629	1;6	2,20700	0,24718	Vanpraet+	85
97	35,30	2,10	2,33200	0,15228	0	2,33200	0,15228	Wisshak+	80
98	38,00	2,30	2,24400	0,12522	0	2,24400	0,12522	Wisshak+	80
99	38,00	2,40	2,32700	0,12985	0	2,32700	0,12985	Wisshak+	80
100	38,60	3,10	2,20200	0,13212	0	2,20200	0,13212	Wisshak+	80
101	38,80	2,40	2,18300	0,14059	0	2,18300	0,14059	Wisshak+	80
102	41,80	2,60	2,16800	0,11902	0	2,16800	0,11902	Wisshak+	80
103	42,10	2,70	2,20800	0,11945	0	2,20800	0,11945	Wisshak+	80
104	42,90	2,70	2,16100	0,13528	0	2,16100	0,13528	Wisshak+	80
105	43,80	3,60	2,17600	0,13056	0	2,17600	0,13056	Wisshak+	80
106	45,00	5,00	1,83000	0,18007	1;6	1,84100	0,18889	Weston+	76
107	45,00	5,00	2,26000	0,27007	1;5;6	2,26300	0,32995	Gayther+	77
108	45,00	5,00	1,93400	0,21661	1;6	1,94000	0,21728	Vanpraet+	85
109	46,20	3,00	2,15600	0,11836	0	2,15600	0,11836	Wisshak+	80
110	46,80	3,20	2,11500	0,11442	0	2,11500	0,11442	Wisshak+	80
111	47,60	3,20	2,09200	0,12740	0	2,09200	0,12740	Wisshak+	80
112	50,20	4,40	2,06600	0,12396	0	2,06600	0,12396	Wisshak+	80
113	51,40	3,50	2,05900	0,11304	0	2,05900	0,11304	Wisshak+	80
114	52,30	3,70	2,05300	0,11107	0	2,05300	0,11107	Wisshak+	80
115	53,30	3,70	2,01700	0,12102	0	2,01700	0,12102	Wisshak+	80
116	55,00	5,00	1,74000	0,17000	1;6	1,75000	0,17833	Weston+	76
117	55,00	5,00	2,00000	0,24000	1;5;6	1,93500	0,28290	Gayther+	77

No.	E_n (keV)	Resol. (keV)	σ (orig) (barns)	Δσ (orig) (barns)	Data correction	σ (corr.) (barns)	Δσ (corr.) (barns)	Authors	
118	55,00	5,00	1,77000	0,19824	1;6	1,77800	0,19914	Vanpraet+	85
119	57,40	4,00	1,91200	0,10497	0	1,91200	0,10497	Wisshak+	80
120	58,00	5,30	1,97100	0,11826	0	1,97100	0,11826	Wisshak+	80
121	58,10	4,00	1,96100	0,19904	0	1,96100	0,19904	Wisshak+	80
122	58,80	4,30	1,93600	0,10474	0	1,93600	0,10474	Wisshak+	80
123	59,90	4,40	1,89000	0,11189	0	1,89000	0,11189	Wisshak+	80
124	64,70	4,70	1,85500	0,10184	0	1,85500	0,10184	Wisshak+	80
125	65,00	5,00	1,61000	0,16003	1;6	1,61800	0,16746	Weston+	76
126	65,00	5,00	1,85000	0,22015	1;5;6	1,78600	0,25968	Gayther+	77
127	65,00	5,00	1,63500	0,18312	1;6	1,64600	0,18435	Vanpraet+	85
128	66,70	5,10	1,81100	0,09798	0	1,81100	0,09798	Wisshak+	80
129	67,40	4,90	1,74900	0,15933	0	1,74900	0,15933	Wisshak+	80
130	67,90	6,70	1,76700	0,12811	0	1,76700	0,12811	Wisshak+	80
131	68,00	5,20	1,70700	0,10105	0	1,70700	0,10105	Wisshak+	80
132	73,30	5,60	1,70800	0,10555	0	1,70800	0,10555	Wisshak+	80
133	75,00	5,00	1,52000	0,15002	1;6	1,52700	0,15713	Weston+	76
134	75,00	5,00	1,81000	0,22010	1;5;6	1,74700	0,25768	Gayther+	77
135	75,00	5,00	1,51300	0,16946	1;6	1,52700	0,17102	Vanpraet+	85
136	76,30	6,10	1,74000	0,11675	0	1,74000	0,11675	Wisshak+	80
137	77,70	6,10	1,57500	0,11702	0	1,57500	0,11702	Wisshak+	80
138	78,90	6,10	1,61300	0,13178	0	1,61300	0,13178	Wisshak+	80
139	80,70	8,40	1,70000	0,21522	0	1,70000	0,21522	Wisshak+	80
140	83,80	6,70	1,75500	0,20516	0	1,75500	0,20516	Wisshak+	80
141	85,00	5,00	1,52000	0,15002	1;6	1,52600	0,15703	Weston+	76
142	85,00	5,00	1,71000	0,20999	1;5;6	1,64800	0,24473	Gayther+	77
143	85,00	5,00	1,45700	0,16318	1;6	1,47500	0,16520	Vanpraet+	85
144	88,10	7,40	1,71900	0,20095	0	1,71900	0,20095	Wisshak+	80
145	89,70	7,50	1,41200	0,18836	0	1,41200	0,18836	Wisshak+	80
146	93,90	7,70	1,44600	0,10353	0	1,44600	0,10353	Wisshak+	80
147	95,00	5,00	1,26000	0,13003	1;6	1,26200	0,13529	Weston+	76
148	95,00	5,00	1,70000	0,20009	1;5;6	1,63700	0,23622	Gayther+	77
149	95,00	5,00	1,38700	0,15534	1;6	1,40900	0,15781	Vanpraet+	85
150	113,4	10,20	1,50200	0,09943	0	1,50200	0,09943	Wisshak+	80
151	125,0	25,00	1,40000	0,21000	1;6	1,40300	0,21438	Weston+	76
152	125,0	25,00	1,37000	0,16002	1;5;6	1,31600	0,18582	Gayther+	77
153	125,0	25,00	1,15900	0,12981	1;6	1,17600	0,13171	Vanpraet+	85
154	139,8	13,70	1,29200	0,07868	0	1,29200	0,07868	Wisshak+	80
155	175,0	25,00	1,12000	0,17002	1;6	1,11500	0,17227	Weston+	76
156	175,0	25,00	1,19000	0,14006	1;5;6	1,15100	0,16333	Gayther+	77
157	175,0	25,00	1,05400	0,11805	1;6	1,06500	0,11928	Vanpraet+	85
158	176,6	19,30	1,16400	0,06984	0	1,16400	0,06984	Wisshak+	80
159	225,0	25,00	0,99400	0,10000	1;6	0,98200	0,10282	Weston+	76
160	225,0	25,00	1,06000	0,13006	1;5;6	1,02900	0,15034	Gayther+	77
161	230,1	28,40	1,01400	0,15017	0	1,01400	0,15017	Wisshak+	80
162	275,0	25,00	0,88200	0,08996	1;6	0,86300	0,09148	Weston+	76
163	275,0	25,00	0,98000	0,12005	1;5;6	0,89700	0,13087	Gayther+	77
164	325,0	25,00	0,78000	0,08003	1;6	0,75200	0,08016	Weston+	76
165	350,0	50,00	0,89000	0,11000	1;5;6	0,83300	0,12237	Gayther+	77
166	450,0	50,00	0,92000	0,11003	1;5;6	0,81200	0,11652	Gayther+	77

Data correction:

0 - experimental data were not corrected;

1 - experimental data were corrected taking into account new recommended data on the cross-section for the monitor reaction;

5 - additional error components not taken into account in the original experimental data have been included;

6 - special correction, see text for details.

Table 2

Mean correlation coefficients for data to be used in evaluating the excitation function for the reaction $^{241}Am(n,\gamma)^{242}Am$

No.	Data		p^k
1.	Weston	76	0,38
2.	Gayther	77	0,29
3.	Wisshak	80	0,45
4.	Wisshak	80	0,49
5.	Wisshak	80	0,47
6.	Wisshak	80	0,35
7.	Wisshak	80	0,42
8.	Vanpraet	85	0,38
9.	GNASH-K	97	0,96
10.	Ignatyuk	97	0,96

Table 3

Group cross-sections and their errors for the $^{241}Am(n,\gamma)^{242}Am$ reaction

Group No.	Energy range (MeV)		Cross-section (mb)	Error (mb)	Error (%)
1	0,001	0,002	9658,84	788,66	8,17
2	0,002	0,004	6586,81	543,87	8,26
3	0,004	0,006	4969,54	408,54	8,22
4	0,006	0,008	4179,91	328,01	7,85
5	0,008	0,010	3711,12	294,56	7,94
6	0,010	0,020	3061,37	205,39	6,71
7	0,020	0,030	2568,04	136,43	5,31
8	0,030	0,040	2299,33	109,85	4,78
9	0,040	0,050	2100,79	97,12	4,62
10	0,050	0,060	1939,79	91,65	4,72
11	0,060	0,070	1804,35	88,55	4,91
12	0,070	0,080	1688,17	86,02	5,10
13	0,080	0,090	1587,23	83,79	5,28
14	0,090	0,100	1498,65	81,90	5,46
15	0,100	0,200	1175,39	75,63	6,43
16	0,200	0,300	849,03	71,10	8,37
17	0,300	0,400	689,69	65,73	9,53
18	0,400	0,500	599,23	63,22	10,55
19	0,500	0,600	532,66	58,34	10,95
20	0,600	0,700	450,64	48,12	10,68
21	0,700	0,800	357,55	38,40	10,74
22	0,800	0,900	291,51	31,47	10,80
23	0,900	1,000	252,29	26,50	10,50
24	1,000	1,500	190,72	19,11	10,02
25	1,500	2,000	122,95	12,19	9,91
26	2,000	3,000	62,24	6,30	10,12
27	3,000	4,000	24,95	2,79	11,20
28	4,000	5,000	11,76	1,49	12,68
29	5,000	6,000	6,60	0,94	14,23
30	6,000	7,000	4,26	0,66	15,62
31	7,000	8,000	3,04	0,51	16,80
32	8,000	9,000	2,34	0,42	17,86
33	9,000	10,000	1,89	0,36	18,88
34	10,000	12,000	1,47	0,30	20,32
35	12,000	13,000	1,20	0,26	21,82
36	13,000	14,000	1,06	0,24	22,78
37	14,000	15,000	0,96	0,23	23,76
38	15,000	16,000	0,87	0,21	24,80
39	16,000	17,000	0,79	0,20	25,93
40	17,000	18,000	0,72	0,20	27,18
41	18,000	19,000	0,66	0,19	28,61
42	19,000	20,000	0,61	0,19	30,25

Table 4

Correlation matrix of group cross-sections for the evaluated excitation function of the $^{241}Am(n,\gamma)^{242}Am$ reaction (correlations given in %)

Energy range (MeV)	Group No.	1	2	3	4	5	6	7	8	9	10	11	12	13	14	15	16	17	18	19	20	21	22	23	24	25	26	27	28	29	30	31	32	33	34	35	36	37	38	39	40	41	42
0.001 - 0.002	1	100																																									
0.002 - 0.004	2	76	100																																									
0.004 - 0.006	3	46	85	100																																								
0.006 - 0.008	4	40	60	87	100																																							
0.008 - 0.010	5	40	38	64	93	100																																					
0.010 - 0.020	6	45	26	38	69	87	100																																				
0.020 - 0.030	7	40	33	32	42	52	81	100																																			
0.030 - 0.040	8	38	36	36	42	47	70	95	100																																		
0.040 - 0.050	9	41	35	38	49	55	69	85	96	100																																	
0.050 - 0.060	10	43	32	38	54	62	70	75	87	97	100																																
0.060 - 0.070	11	45	31	37	56	66	70	68	79	92	98	100																															
0.070 - 0.080	12	46	30	37	57	67	70	62	72	86	95	99	100																														
0.080 - 0.090	13	47	31	37	57	67	69	58	66	80	91	96	99	100																													
0.090 - 0.100	14	47	31	36	56	65	67	55	61	75	86	93	97	99	100																												
0.100 - 0.200	15	43	35	36	46	51	55	46	44	51	61	70	78	85	90	100																											
0.200 - 0.300	16	32	35	32	30	29	36	34	28	27	32	39	48	57	65	90	100																										
0.300 - 0.400	17	26	32	28	23	21	26	28	21	18	21	26	33	41	48	75	95	100																									
0.400 - 0.500	18	21	26	23	19	17	21	23	18	15	16	20	25	30	36	58	80	94	100																								
0.500 - 0.600	19	20	22	21	18	17	20	20	17	15	17	20	24	29	34	52	69	83	95	100																							
0.600 - 0.700	20	21	25	23	19	17	22	23	17	15	17	22	28	34	40	61	74	79	81	90	100																						
0.700 - 0.800	21	21	26	23	19	16	21	23	17	15	16	20	26	32	38	60	77	84	81	79	90	100																					
0.800 - 0.900	22	20	24	22	19	17	21	21	17	15	17	21	25	30	35	55	73	84	88	83	80	94	100																				
0.900 - 1.000	23	21	25	22	20	18	22	22	18	16	18	22	27	33	38	58	74	85	89	87	81	87	97	100																			
1.000 - 1.500	24	23	28	25	20	18	23	25	19	16	18	23	29	35	42	65	81	88	89	88	87	86	90	96	100																		
1.500 - 2.000	25	22	26	24	20	18	22	24	18	16	18	22	28	34	40	62	80	89	91	88	87	89	90	91	96	100																	
2.000 - 3.000	26	22	26	23	20	18	22	23	18	17	18	23	28	34	39	61	78	88	91	89	86	88	91	92	94	98	100																
3.000 - 4.000	27	22	27	24	20	18	23	24	19	16	18	23	29	35	42	65	81	88	89	88	87	87	89	92	94	94	97	100															
4.000 - 5.000	28	22	27	24	20	18	22	24	19	16	18	22	28	35	41	64	81	88	89	88	87	87	89	92	95	94	95	98	100														
5.000 - 6.000	29	22	26	24	20	18	22	24	18	16	18	22	28	34	40	62	80	88	90	88	86	88	89	91	94	94	94	95	98	100													
6.000 - 7.000	30	22	26	23	20	18	22	23	18	16	18	22	28	33	39	60	78	88	90	88	86	88	89	91	93	95	93	93	96	97	100											
7.000 - 8.000	31	22	25	23	20	18	22	23	18	16	18	22	28	33	39	60	77	87	89	87	85	87	89	90	93	94	93	92	94	96	96	100										
8.000 - 9.000	32	22	25	23	20	18	22	23	18	16	18	22	27	33	39	60	77	86	88	87	84	86	88	90	92	93	92	91	92	93	94	94	100									
9.000 - 10.000	33	21	25	23	20	18	22	23	18	16	18	22	27	33	39	60	77	85	87	85	83	85	87	88	91	92	91	90	90	91	92	92	91	100								
10.000 - 12.000	34	21	25	23	19	17	21	23	17	15	17	21	27	33	38	60	76	83	84	83	82	82	84	86	89	89	89	88	88	88	88	89	89	88	100							
12.000 - 13.000	35	21	25	22	18	16	21	22	17	15	16	21	26	32	38	59	74	81	82	81	80	80	82	84	87	87	87	87	86	85	85	86	86	85	84	100						
13.000 - 14.000	36	20	25	22	18	16	20	22	17	14	16	20	26	32	37	58	73	80	81	80	79	79	81	83	85	85	86	85	84	84	84	84	84	84	82	80	100					
14.000 - 15.000	37	20	24	22	18	16	20	22	17	14	16	20	25	31	37	57	72	79	79	78	78	78	80	82	84	84	85	84	83	83	83	83	83	82	81	79	77	100				
15.000 - 16.000	38	20	24	21	18	16	20	21	16	14	16	20	25	31	36	56	71	78	78	77	76	77	78	81	83	83	83	83	83	82	82	82	81	80	79	77	76	74	100			
16.000 - 17.000	39	19	23	21	17	15	19	21	16	14	15	19	24	30	35	55	70	76	77	76	75	76	77	79	82	82	82	82	82	81	81	80	80	79	77	75	74	73	71	100		
17.000 - 18.000	40	19	23	20	17	15	19	20	16	14	15	19	24	29	34	53	68	75	76	75	74	75	76	78	80	81	80	80	80	80	80	79	78	77	75	73	72	71	70	69	100	
18.000 - 19.000	41	18	22	20	17	15	19	20	15	14	15	19	23	28	33	51	66	73	75	74	72	73	75	76	78	79	79	78	79	79	79	78	76	75	73	71	70	69	68	67	66	100
19.000 - 20.000	42	18	21	19	17	15	18	19	15	13	15	18	23	27	32	49	64	72	74	72	70	72	73	74	77	78	77	76	78	78	78	76	75	73	70	68	67	66	66	65	65	64	100

REFERENCES

[1] WESTON, L.W., TODD. J.H., Nucl. Sci. Eng., 61 (Nov. 1976) 356-365.

[2] GAYTER, D.B., THOMAS, B.W., Measurement of the neutron capture and fission cross-section of ^{241}Am, in: Nejtronnaya fizika [Neutron Physics] (Proc. 4th All-Union Conf. on Neutron Physics, Kiev, 18-22 April 1977), Part 3, TsNIIatominform, Moscow (1977) 3-15.

[3] WISSHAK, K., KÄPPELER, F., Nucl. Sci. Eng., 76 (Nov. 1980) 148-162.

[4] VANPRAET, G., et al., Proc. International Conference on Nuclear Data for Basic and Applied Science, Santa Fe, New Mexico, 13-17 May 1985, v.1, 493-497.

[5] MUGHABGHAB, S.F., Neutron Cross Sections, Vol. 1, Neutron resonance parameters and thermal cross sections, Part B, Z = 61-100, BNL, Upton, N.Y., USA (1984) 55-100.

[6] ZOLOTAREV, K.I., Cross section data for dosimetry reaction ^{241}Am(n,f) and ^{243}Am(n,f). The WGRD-VVER Workshop on RPV Neutron Dosimetry, 29 September - 5 October 1997, Sandanski, Bulgaria.

[7] EXFOR Library, ENTRY = 20785, SUBENT = 002.

[8] JENDL-3.2 Library, MAT 9437, eval. M. Kawai et al., NAIG, rev. 2, February 1993.

[9] CONDE, H., Editor, Nuclear Data Standards for Nuclear Measurements, Report NEANDC-311U, OECD, Paris (1992).

[10] ENDF/B-VI Library, MAT-325, eval. G.M. Hale, P.G. Young, LANL, April 1989.

[11] ENDF/B-IV Library, MAT-1261, eval. L. Stewart et al., LASL, AI, March 1974.

[12] ENDF/B-VI Library, MAT-, eval. L.W. Weston et al., ORNL, LANL, April 1989.

[13] ENDF/B-VI Library, MAT-525, eval. G.M. Hale, P.G. Young, LANL, Nov. 1989.

[14] ENDF/B-VI Library, MAT-7925, eval. P.G. Young et al., LANL, April 1990.

[15] YOUNG, P.G., ARTHUR, E.D., GNASH; A Preequilibrium Statistical Nuclear Model Code for Calculation of Cross Section and Emission Spectra, Report LA-6947, Los Alamos (1977).

[16] DIETRICH, S.S., BERMAN, B.L., Atomic Data and Nuclear Data Tables 38 (1988) 199.

[17] Mc DANIELS, D.K., Nucl. Phys., A384 (1982) 88.

[18] IGNATYUK, A.V., Private communication, IPPE, Obninsk (1997).

[19] BADIKOV, S.A., ZOLOTAREV, K.I., PASHCHENKO, A.B., Evaluation of the cross-section for the reaction ^{93}Nb(n,n')^{93}Nb^{m} from the threshold to 20 MeV. Preprint FEhI-2252, Obninsk (1992) [in Russian].

[20] BADIKOV, S., ZOLOTAREV, K., RABOTNOV, N., Proc. NEANSC Specialist's Meeting on Evaluation and Processing of Covariance Data, Oak Ridge National Laboratory, USA, 7-9 October 1992, OECD, Paris (1993) 105.

[21] BADIKOV, S., et al., The PADE-2 rational approximation program. Preprint FEhI-1686, Obninsk (1985) [in Russian].

[22] MASLOV, V.M., et al., Evaluation of neutron data for americium-241. Report INDC(BLR)-005 (Distr. G.), IAEA, Vienna, October 1996.

[23] NAKAGAVA, T., Report JAERI-M 88-008 (1988).

[24] ENDF/B-VI Library, Mat-9543, eval. P.G. Young et al., LANL-CNDC, Rev. 2, August 1994.

98-10984 (76)
Translated from Russian

UDC 539.172

SERIYA: YADERNYE KONSTANTY, Vypusk 3-4, 1997, s. 94
(Series: Nuclear Constants, Issue No. 3-4 1997, p. 94)

NEUTRON RADIATIVE CAPTURE GAMMA SPECTRA STRUCTURE

O.T. Grudzevich
Institute of Atomic Energy, Obninsk

ABSTRACT

NEUTRON RADIATIVE CAPTURE GAMMA SPECTRA STRUCTURE. The structure of gamma spectra observed in neutron capture reactions is described by modelling of discrete levels. The tendency of structure to decrease as neutron energy increases is reproduced in calculations. Modification of E1 strength functions according to observed maximum values at low transition energy is proposed and tested on gamma spectra. It is shown that E1 and M1 strengths have the same values at energy ≤ 2 MeV. The energy dependence of the E3-transition strength function is derived from experimental data.

The energy distributions of gamma quanta, occurring during neutron radiative capture are of particular interest from the point of view of nuclear theory and the theory of nuclear reactions, since they provide information on the structure of the nucleus and its de-excitation processes. Another interesting aspect of gamma spectra has to do with research on the isomer population in various reactions, including neutron and photonuclear reactions, since information on the spectra makes it possible to refine the parameters and functionals of the level density models, giant resonances and evaporation cascades, etc. The applied aspects of the research on gamma spectra are also quite broad, ranging from reactor shielding and nuclear pumped of lasers to astrophysics and medicine.

Repeated analysis of the experimental energy distributions of photons shows three basic features of the spectra: structure with thermal neutron capture, pygmy resonances for E_n = 0.01-1 MeV and finally, non-statistical effects for neutron energies E_n = 14 MeV.

The objective of this work is to seek methods of reproducing the structure of the spectra of the reaction (n,γ) in theoretical calculations for thermal and non-resonance neutrons using the latest data on reduced radiative strength functions and the density of nuclear levels, and to investigate the energy dependencies of the radiative strength functions in the low energy range.

1. BASIC EXPRESSIONS

In the statistical model of nuclear reactions, the gamma emission spectra from the reaction (n,γ) may be calculated using the Hauser -Feshbach formalism:

$$S_0(E_\gamma) = \pi\lambda^2 \sum_{lJ} g_J \frac{T_{lj}^{J^\pi}(E_n) \sum T_{XL}(E_\gamma)}{N(E, J^\pi)} \rho(E - E_\gamma, J^\pi), \tag{1}$$

$$\begin{aligned} N(E, J^\pi) = & \sum_{J'^{\pi'}} \int_0^{E-B_n} dE_n T_{nlj}(E_n) \rho_n(E - B_n - E_n, J'^{\pi'}) + \\ & + \sum_{J'^{\pi'}} \sum_{XL} \int_0^{E} dE_\gamma T_{\gamma XL}(E_\gamma) \left[1 + \alpha_{XL}(E_\gamma)\right] \rho(E - E_\gamma, J'^{\pi'}), \end{aligned} \tag{2}$$

where E is the excitation energy of the compound nucleus, E_n, E_γ are the neutron and gamma energies, ρ(U,J) is the level density of the nucleus with excitation energy U and total momentum J, and α is the internal conversion coefficient. The main quantities determining the spectral shape according to Eq. (1) are the level density of the nucleus ρ(U,J) and the coefficients $T_{\gamma XL}$. Just like any other spectra, gamma spectra depend most strongly on these two quantities. Cascade transitions occurring due to the absence of energy binding the photon with the nucleus are an additional feature.

The gamma ray transfer coefficients of the nucleus $T_{\gamma XL}$ are related to the reduced radiative strength functions f_{XL} and energy E_γ by the expression:

$$T_{\gamma XL}(E_\gamma) = 2\pi f_{XL} E_\gamma^{2L+1}. \tag{3}$$

Spectra obtained using formulae (1)-(3) are primary gamma spectra and only have structure in the hard part which is the result of the transitions of the highly-excited nucleus to discrete energy levels. In order to obtain the observed spectra, it is necessary to take into account the possibility of cascade chains of sequential gamma emissions. For this purpose, the cascade-evaporation model [1] is used which, taking into account the conservation laws for total momentum and parity, results in a system of equations with populations of a certain level after a specific number of transitions **n** (n ≥ 1):

$$W_n(E', J'^{\pi'}) = \rho(E', J'^{\pi'}) \sum_{J^\pi} \int_{E'}^{E} W_{n-1}(E, J^\pi) \frac{\Gamma_\gamma(E, J^\pi; E', J'^{\pi'})}{\Gamma(E, J^\pi)}, \tag{4}$$

where the ratio of the partial transition width to the total decay width - the branching ratio - is calculated as follows:

$$R = \frac{\sum_{XL} T_{\gamma XL}(E - E')}{N(E, J^\pi)}. \tag{5}$$

The initial condition for calculating populations is:

$$W_0\left(E', J'^{\pi'}\right) = S_0\left(E_\gamma\right), \tag{6}$$

and the gamma sum spectrum is calculated as the sum of the populations in all cascades:

$$S\left(E_\gamma\right) = \sum_n W_n\left(E', J'^{\pi'}\right) + S_0\left(E_\lambda\right). \tag{7}$$

The multiplicity of gamma quanta - the number of gamma quanta with a given energy emitted during the capture of one neutron - is calculated as the ratio:

$$\mu\left(E_\gamma\right) = \frac{S\left(E_\gamma\right)}{\sigma_{n,\gamma}\left(E_n\right)}. \tag{8}$$

The excitation energy integrals in formulae (1), (2) and (4) are replaced by the summation for the range of discrete levels. In particular, for calculations of populations using cascade transitions, the ratio of the widths in Eq. (4) is replaced by the branching ratios for the discrete energy levels R_{ij}, which are the probabilities of transition from a given level i to various final levels j. Usually, experimental values of R are used in calculation but it often happens that such data are incomplete or unavailable, in which case the calculated values from Ref. [2] may be used:

$$R_{ij} = \frac{\sum_{XL} T_{\gamma XL}\left(E_i - E_j\right)}{\sum_j \sum_{XL} T_{\gamma XL}\left(E_i - E_j\right)}. \tag{9}$$

This method of calculating the branching ratios has been successfully applied in the analysis of the isomeric cross-sections and isomeric ratios of the reactions (n,2n), (n,p), (n,α), (n,γ) and others [2].

When analysing the spectra, the level density was calculated according to the phenomenological variant of the superfluid model of the nuclear [3], and its parameters [4] were not varied.

The reduced radiative strength functions are most often calculated using the Lorentzian dependence:

$$f_{XL}\left(E_\gamma\right) = const\left[\frac{\sigma_0 E_\gamma^2 \Gamma_0^2}{\left(E_\gamma^2 - E_0^2\right) + E_\gamma^2 \Gamma_0^2}\right] E_\gamma^{-(2L-1)}. \tag{10}$$

For calculations of the radiative strength functions of quadrupole electric transitions, the approach in Ref. [5] was used with an additional temperature dependence (hereinafter

referred to as the KMF[1] method). The main difference between this method and the Lorentzian dependence is that at low gamma energies the value of f_{E1} tends towards the finite limit, determined by the giant resonance parameters E_0, Γ_0, and σ_0 and the temperature of the nucleus T in the final state:

$$f_{E1} = const\left[E_\gamma \frac{E_\gamma \Gamma\left(E_\gamma\right)}{\left(E_\gamma^2 - E_0^2\right) + E_\gamma^2 \Gamma\left(E_\gamma\right)^2} + \frac{0.7 \cdot \Gamma_0 4\pi T^2}{E_0^5} \right] \sigma_0 \Gamma_0 , \tag{11}$$

$$\Gamma\left(E_\gamma\right) = \Gamma_0 \frac{E_\gamma^2 + 4\pi^2 T^2}{E_0^2} . \tag{12}$$

The KMF dependence (11)-(12) has been confirmed experimentally [6] at energies of 0.2-2 MeV, i.e. precisely in the range E_γ where the differences between the KMF method and Lorentzian dependence are the greatest. Verification of the applicability of formulae (11)-(12) according to other data, carried out with respect to the spectra and cross-sections of the reaction (n,γ) [7, 9] and according to the description of the isomeric cross-sections of neutron reactions [2], has shown that the KMF approach is preferable for a wide range of nuclei. In this work, GDR parameters from Ref. [8] or their systematics [9] have been used.

2. MODELLING OF THE LEVEL SCHEMES

Ample data exist on neutron radiative capture spectra where structure is observed. For example, in the measurements [10-14] the multiplicities of gamma quanta of the radiative capture of thermal neutron by many target nuclei were obtained with a large energy resolution. For the purposes of comparison with the results of calculations, in this work, the author artificially decreased the experimental resolution by summing experimental values over 100 keV intervals, since it was with this resolution that the spectra for higher incident neutron energies [15] were obtained. These so treated data are shown in Figs 1-4, together with the results of the calculations performed with the cascade-evaporation model. The sloping straight line in the histograms in Figs 1-4 indicates the absence of data in the corresponding energy range.

A feature of all experimental dependencies $\mu(E_\gamma)$ is the presence of structure in the whole spectrum, despite the summation carried out for all energies. In the calculated spectra such structure over the entire spectrum is to be found only for the ^{23}Na nucleus, while in the remaining spectra it only occurs with soft and hard gamma rays. The reason for such behaviour of the calculated spectra may be understood from the data in Fig. 5, where information is given on the discrete energy levels of decaying nuclei.

It seems obvious that the structure of the spectra in Figs 1-4 is caused by E1-transitions to discrete energy levels. At the same time, the information on these levels is

[1] Translator's Note: These are the initials of the names of the authors of Ref. [5].

considered to be incomplete for excitations U ≥ 2-3 MeV, in particular for odd-odd nuclei, due to the suspected large number of missing levels. For the calculations, the usual procedure was followed of limiting the scheme used to the maximum energy at the point where the curve of the cumulative sum of levels deviates (Fig. 5). The discrete energy levels included in the calculation also cause structure in the soft and hard part of the spectra, so that, whereas the structure in the hard part is caused by primary transitions (with level $U \approx B_n$), the structure in the soft part of the spectrum is caused by cascade transitions which remove the initial population of discrete energy levels. This means that, if the observed spectrum has structure in the middle part, this is the manifestation of separate discrete energy levels having energies up to $U_{lim} \approx B_n/2$. In fact, from Fig. 5 it follows that the discrete levels of ^{24}Na may be given up to U ≈ 4 MeV, completely covering the spectrum range, while for ^{90}Y and ^{179}Hf nuclei the missing levels begin as early as U ≈ 1 MeV. Thus, in order to obtain structure in the calculated spectra, it is necessary to model the discrete energy levels up to energies of the order of $B_n/2$ for those nuclei in the experimental schemes for which the missing levels begin much earlier.

The modelling of discrete energy levels has already been used [17, 18] in the calculation of isomeric cross-sections. The difference between the proposed method and those used previously consists in the application of another level density model and another scheme for obtaining the branching ratios of transitions between discrete energy levels which involves the use of the superfluid model of the nucleus [3], the branching ratios, calculated according to the method in Ref. [2], and the spin distributions, fitted to the experimental data in Ref. [19].

Another reason for the modelling is the need to ensure a smooth transition, for all characteristics (not just the total number of levels), from the discrete to the continuous level scheme of the decaying nucleus.

Beginning with the energy of the last, given experimental discrete energy level, the total level density was calculated with parameters fitted to the description of the neutron resonance density and to the value $N_0(U_0)_{exp}$ [4]. After this, in the excitation energy range ΔU we introduced $\rho(U_0 + \Delta U/2)$ of the equidistant levels whose spins were calculated with the distribution parameter derived from experimental data [19]. This ensured a smooth transition to the continuous part of the excitation spectrum for the numbers of levels with a determined spin, i.e. in this part the level density was calculated with the same expressions used for the modelled part of the spectrum.

From Fig. 5, it can be seen that the number of levels populated by dipole electric transitions and modelled in the transitional part of the spectrum fits well with the discrete part for ^{179}Hf, where the relevant data exist. Thus, the use of the spin distribution parameter derived from the observed level schemes enables the behaviour of the dependence ρ(U,J) to be extrapolated satisfactorily into the higher excitation energy range. Of course, it should not be expected that the modelled levels will reproduce sufficiently well the actual order of sequence of the spin levels, but this is not required for gamma spectrum calculations - the important thing is to ensure that in a specific excitation energy section there is a specific number of levels with spins in a fixed range. Nuclei, which are formed in the reactions shown in Figs 1-4, have considerable differences in the absolute value of the level density. In order to obtain the structure in the spectrum of Fig. 2, it is sufficient to provide an additional 350 levels, whereas for ^{176}Lu and ^{179}Hf this number of levels is insufficient. Despite the strong fluctuations in the numbers of photons as a function of energy existing in the experimental data with specially

"worsened" resolution, it can be seen that, in many cases, it has been possible to reproduce in sufficient detail the structure of the spectra. Thus we have satisfactory reproduction of the structure of the spectrum from the reaction $^{89}Y(n,\gamma)$ in Fig. 2, where detailed agreement of the position of the peaks is obtained in many cases. In the reaction $^{175}Lu(n,\gamma)$ (Fig. 4), although 350 levels were not sufficient to cover the entire spectrum range, two broad peaks were obtained in the hard part of the spectrum without fitting. A certain similarity of the observed structure appeared for $^{178}Hf(n,\gamma)$ (Fig. 3) in the range E_γ = 4-5 MeV. The considerable (higher than an order) deviation from the experimental data for E_γ = 1.5-3 MeV is a flaw in the calculated spectra obtained for the last two reactions. Possibly this is due to special features of the collective E2-transition which lead to a large increase in the strength functions at energies $\leq$ 1.5-2 MeV (Fig. 15), or to the nature of the population of the isomeric levels existing in ^{176}Lu and ^{179}Hf nuclei at the corresponding excitation energies.

When the energy in the entrance channel of the reaction (n,γ) increases, the contribution of the neutrons with orbital angular momenta $l > 0$ also increases, and this results in an expansion of the populations of the states of the compound nucleus over the entire angular momenta, and consequently the structure of the photon spectra must gradually become larger and finally disappear. By way of example, we shall present data on the spectra of the reaction (n,γ) for neutrons with energies of 0.5 MeV (Figs 6-8).

The method of modelling the discrete level schemes applied for thermal neutrons may be verified for E_n = 0.5 MeV. The basic parameter when modelling is the value of the range ΔU, within the limits of which the equidistant level spectrum is given. For all the spectra shown in Figs 2, 4, 6-8 the value ΔU = 1 MeV is used, which results in the appearance of structure in the dependence N(U) (Fig. 5). Figure 6 shows a clear repetition of the two broad peaks at energies $E_\gamma \approx$ 4.5 and 6 MeV. This is also true of the data in Fig. 7 where the three broad peaks obtained in the hard part of the spectrum are slightly displaced with respect to energy. The situation is interesting for ^{209}Bi, where the number of calculated peaks is much higher than the observed peaks, which is most likely caused by incorrect selection of the value of ΔU during modelling, i.e. the special features of the gamma-transitions between levels of a different nature were not taken into account in the calculations, and no attempts were made to perform individual fitting of the spectra.

The further development of the method of modelling discrete energy levels by fitting the calculated spectra and obtaining closer agreement with the observed structures may be coupled with the introduction into the energy dependence of the level density of the quasi-particle excitation structure of the superfluid model of the nucleus having the same “step” order for the excitation energy [3]. The data in Fig. 8 again indicate that the slope of the calculated spectrum differs greatly from the general trend of the experimental data. At first glance, this may point to the need to correct the energy dependence of the level density. However, changing the level density parameters obtained from the neutron resonance density is hardly justified, since these parameters need to be changed too much to describe the slope of the spectrum.

3. RADIATIVE STRENGTH FUNCTIONS

The second important functional in the calculation of the gamma spectra of the reaction (n,γ) consists of the reduced radiative strength functions, determined from the experimental data on neutron resonances as:

$$f_{XL}\left(E_\gamma\right) = \frac{\Gamma_\gamma}{E_\gamma^{2L+1} D}, \tag{13}$$

where Γ_γ is the average radiation width and D is the average distance between the decaying levels.

As a rule, photon absorption cross-sections, where the function $f_{XL}(E_\gamma)$ may be refined in the limits 7-20 MeV, serve as a source of information about the energy dependence of radiative strength functions. In calculating the spectra, this dependence needs to be extrapolated to the lower energy range. In so doing, it is important to test the values obtained since they will determine the spectral shape. For this purpose one can use data on radiative transitions between discrete energy levels and derive the reduced radiative strength function from their characteristics:

$$f_{XL}\left(E_\gamma\right) = \frac{\hbar \ln 2}{T_{1/2}(1+\alpha)\left(1+\delta^2\right) E_\gamma^{2L+1} MeV}, \tag{14}$$

where $T_{½}$ is the half-life of the excited discrete energy level, α is the conversion coefficient, and δ is the mixing ratio with competing transitions of anothermultipolarity.

Of course, for such transitions, the scale of the fluctuation in the values of f_{XL} is very large, but we are interested in the strongest transitions, because they are the ones appearing in the spectra. In other words, it is necessary to establish an upper limit for the experimental values, and to correct the parameters of the calculated strength functions according to these data. A similar procedure was used in Ref. [20] for the systematics of the strength functions.

DIPOLE GAMMA TRANSITIONS

Figure 9 contains data on the strength functions of electric dipole transitions of nuclei with A = 160-185, obtained from data in the ENSDF file [16] using the formula (14). As was to be expected, the scatter of the values is very high, but the peak values over the entire range exhibit an unexpected trend: weak dependence on the gamma transition energy and on the energy of the final level. It is clear that these data cannot be described via the normal approach (10), and that the KMF dependence must be used. Furthermore, for transitions to the ground state when the formula (11) is close to the Lorentzian dependence, it is necessary to introduce an effective minimal temperature (fitted parameter) T_{min} = 0.1 MeV, so that the calculated strength function will coincide with the peak experimental values.

The results of the calculations of spectra with a fitted strength function are compared with experimental data [15] in Fig. 10. The use of the proposed parameterization results in a

significant improvement in agreement at neutron energy 0.5 MeV: the calculated curves practically pass through the points of the experimental spectra. A feature of the spectra at these energies of bombarding neutrons is the presence of small peaks, often interpreted as resonances in the reduced radiative strength functions - pygmy resonances [21]. There are two basic arguments in favour of the existence of these resonances in the dependence f_{E1}, and not in the level density: 1) The constant position of the resonance peak in the spectrum with variation in the energy of the bombarding neutrons, and 2) The increase in the resonance energy with increasing mass number of the target nucleus. The first argument may be partially refuted by Fig. 11 which presents the results of calculations of spectra without the use of pygmy resonance but with a modified strength function, and also data from Ref. [21] for different neutron energies. Sufficiently good agreement for all three neutron energies is obtained without any fitting. A certain structure remains at $E_\gamma \approx 2.5$ MeV. However, on the one hand, the deviation from the calculations does not exceed 30% and, on the other hand, one can use the conclusions of Ref. [22] on the presence of intermediate levels precisely at excitation energy 2.5 MeV resulting in resonances in the cross-section for the isomeric level population in the reaction (γ,γ').

The behaviour of the radiative strength functions of the dipole transitions is, to a large extent, typical for a wide range of mass numbers. Thus, for the range A = 50-140, f_{E1} (Fig. 12) and also f_{M1} (Fig. 13) behave in a similar way. Figures 12 and 13 show that both the electric and magnetic reduced strength functions at low transition energies can be described more readily by the KMF method than by the Lorentzian dependence. However, it should be noted that in Weisskopf's model [23] using the single particle approximation, the data contained in Fig. 13 are well predicted, at least as regards energy dependence.

At low energies E_γ, the limiting value of f_{M1} differs little in magnitude from f_{E1}, as distinct from the region of giant resonance, although, considering the limited information on magnetic dipole resonances [9], confirmation of the weak energy dependence of f_{M1} is premature. It might also be useful to extrapolate this dependence to the high energy region according to formulae (11)-(12), using the data in Figs 12 and 13. The use in calculations of the isomeric cross-sections and gamma spectra of the reduced magnetic radiative strength functions fitted according to Fig. 13 can evidently increase the sensitivity of the results to the distribution of the level density according to parity in the region of the continuous excitation spectrum.

GAMMA TRANSITIONS WITH L ≥ 2

Usually, not enough attention is paid to radiation with multipolarities L = 2, 3 in the calculation of spectra and nuclear reaction cross-sections. It is assumed that these transitions have a probability much lower than E1 and M1 and, even if they cannot be totally disregarded, their influence on the results of the calculations does not have to be taken into account too strictly. A more important reason is the considerably lower volume of experimental data on resonances, which means that it is not possible to establish reliable systematics for their parameters or to investigate energy dependencies. In this connection, the data on transitions between discrete energy levels are of particular interest. In order to illustrate the importance of E2-transitions, let us compare their average radiation widths with the same values for E1-

radiation. With the well-known characteristics of the transition, the average radiation width may be obtained as:

$$\overline{\Gamma}_\gamma = \frac{1}{N}\sum \frac{\hbar \ln 2}{T_{1/2}(1+\alpha)(1+\delta)}, \tag{15}$$

where the summation is carried out for all N transitions of this type in a certain energy interval of a specific nucleus.

The average radiation widths of E1 and E2-transitions with $E_\gamma \leq 2$ MeV for nuclei with A = 150-200, derived from experimental data [16] using formula (15), are shown in Fig. 14. It is noteworthy that, despite the strong fluctuations, particularly of the values of $\overline{\Gamma}_\gamma^{E1}$, a clear trend is observed - the widths of E2 are two to three orders greater than the widths of E1. These differences are most likely caused by collective transitions between members of the rotational bands, which is partially confirmed by the data in Fig. 15 showing a substantial increase in the strength functions at energies ≤ 1.5 MeV in comparison with single-particle evaluations.

The radiative strength functions of electric quadrupole transitions shown in Fig. 15 vary in wide limits because the data are not assigned to transitions between levels of a different nature. Such an analysis, which would be quite difficult and laborious, may provide valuable information on transitions between levels of uniform nature, and eliminate the disagreement existing with the extrapolation of the giant resonance into the low gamma energy region. It can also be seen that the lower limit of the value of f_{E2} agrees satisfactorily with the single-particle evaluation, and that the values of f_{M2} are consistent with Weisskopf's evaluation.

The data on the strength functions of radiation with L = 3 (Fig. 16) are not as numerous as the data for quadrupolar transitions. However, this information enables a conclusion to be drawn on the energy dependence $f_{E3}(E_\gamma)$ - an increase in the strength function at energies $E_\gamma \geq 0.1$ MeV is clearly observed. This trend conflicts with Eq. (10), since in the low energy region this equation gives an opposite dependence $f_{E3}(E_\gamma) \approx C/E_\gamma^3$. The difference in masses of this region, can also not cause the increase occurring in f_{E3} since according to the single-particle evaluation, the strength functions can only differ by a factor of less than 10 due to the differences in A. The observed trend may be described by the empirical formula:

$$f_{E3}(E_\gamma) = a\frac{E_\gamma^2 b^2}{\left(c^2 - E_\gamma^2\right)^2 + E_\gamma^2 b^2} + d\ , \tag{16}$$

where the coefficients $a = 10^{14}$, b = 1.5 MeV, c = 1.5 MeV and $d = 10^{-17}$ MeV^{-7} were selected from the data in Fig. 16.

4. TESTING THE METHOD

When calculating the gamma spectra on the basis of the statistical model, the level density and radiative strength functions always go into the relations as a product and therefore, when choosing or fitting one of the quantities, it should not be forgotten that an obvious simplification is being made when another value is fixed. In this work, the methods of calculating the level density and the strength functions are tested on various characteristics and features occurring at different neutron energies. For example, the spectrum structure during thermal neutron capture may be caused not only by the features of the level schemes, but also by resonances in the strength functions. In the latter case (E_n = 0.5 MeV), correcting the strength functions seems more justified than changing the level density which, on the one hand, is fixed in precisely this excitation energy range, and on the other hand, would require too big changes in order to describe the observed spectra.

The logical question arises: is it impossible to find data by means of which the proposed changes in the method of calculation can be additionally verified? The required data are isomeric ratios for isomers, whose spins differ greatly from the spins of the target nucleus and the basic state of the residual nucleus. Furthermore, the distributions of the angular orbital momenta of the bombarding particle must be sufficiently narrow. In Ref. [24] it is shown that, in such a case, the calculated isomeric ratios may differ from the experimental values by several orders. Thus, the value $r_{exp}(m2) = 5.4 \times 10^{-10}$ [25] for $^{178}Hf^{m2}(16^+)$ excited in the reaction $^{177}Hf(n,\gamma)$ with thermal neutrons, but the calculated value is six orders lower $r_{calc} = 6.2 \times 10^{-16}$. It was not possible to eliminate such a large difference by altering the spin distributions of the level density - the main fitted quantity in such cases. The use of the method proposed in this work for correcting the radiative strength function leads to the reasonable result $r_{calc} = 9.6 \times 10^{-10}$.

The search for data in which the features of f_{E1} appear at low or zero temperatures of the final states of transitions may continue, guided by the obvious criterion that the value of the isomeric ratio must be low, let us say $r \leq 10^{-3}$.

In addition to the thermal radiative capture reaction, the required conditions for the population of isomeric levels may be achieved by some target nuclei, including isomeric nuclei in photonuclear reactions [26]. As an example of this let us consider the data on the excitation of isomers in the reactions $^{167}Er(\gamma,\gamma')$, $^{167}Er^m$ and $^{179}Hf(\gamma,\gamma')$, $^{179}Hf^m$ (Figs 17 and 18). The results of the calculations show the unexpectedly good agreement of the isomeric cross-sections (Fig. 17), and an analysis of the reasons for the discrepancy in the second reaction (Fig. 18) is required. Nevertheless, considering the very low values of the observed cross-sections on the one hand, and the complexity and multi-parameter theoretical dependence on the other, the agreement may be considered to be satisfactory.

In this work, the basic characteristics of the statistical model of nuclear reactions influencing the neutron radiative capture gamma spectrum were investigated. It was shown that the observed structure of these spectra may be reproduced in theoretical calculations by statistical modelling of the discrete energy level schemes. The spin dependencies of the level density obtained with such modelling agree satisfactorily with the data on discrete energy levels. Information was obtained on the energy dependence of reduced radiative strength functions with multipolarities $L \leq 3$ from the experimental data on the characteristics of transitions at low energies. It was shown that the functions f_{ML} have a weak energy dependence while the data obtained on the function f_{E1} for transitions to the ground state

contradict the theoretical dependencies used for calculating them. Modification of the formulae and the parameterization of the function $f_{E3}(E_\gamma)$ were proposed in accordance with the energy dependence that was established.

For nuclei with $160 \leq A \leq 185$ it was possible to describe the observed spectra, not by including an additional resonance in the radiative strength function but by correcting its energy dependence for low energies. For standardization the author proposed using the upper limit derived from the experimental data on transitions between discrete energy levels.

The changes in the strength functions used to described the observed spectra were verified according to the isomeric ratios of neutron radiative capture, and it was possible to eliminate the previous discrepancy with experimental data amounting to six orders. It was shown that the method used for calculating spectra based on statistical and modified cascade models may be used for the gamma inelastic scattering reaction leading to the formation of isomers.

The author wishes to thank Dr. A.A. Goverdovskij for the discussions which stimulated this work.

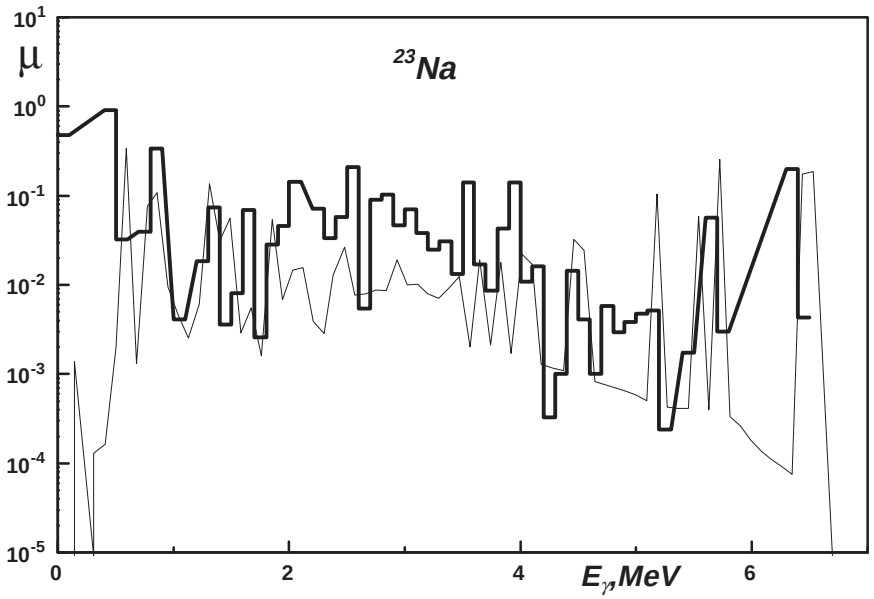

Fig. 1. Gamma multiplicities from thermal radiative capture by a ^{23}Na nucleus. The experimental data [10] summed in the ranges $\Delta E_\gamma = 0.1$ MeV are shown by the histogram. The curve shows the calculation results.

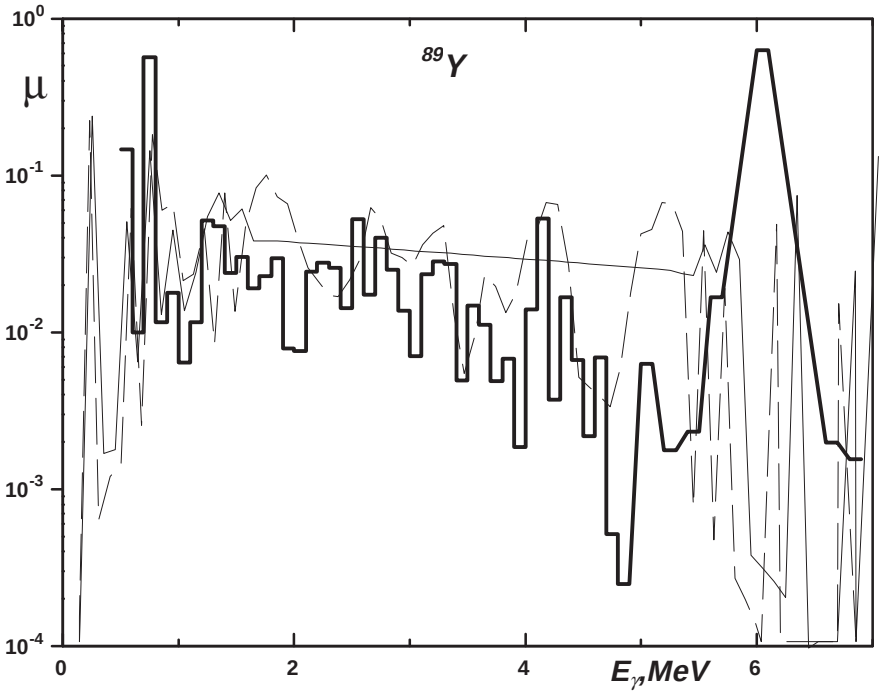

Fig. 2. Gamma multiplicities from thermal radiative capture by a ^{89}Y nucleus. The experimental data [11] summed in the ranges $\Delta E_\gamma = 0.1$ MeV are shown by the histogram; the solid curve represents the customary calculation and the broken curve the calculation with modelled discrete energy levels.

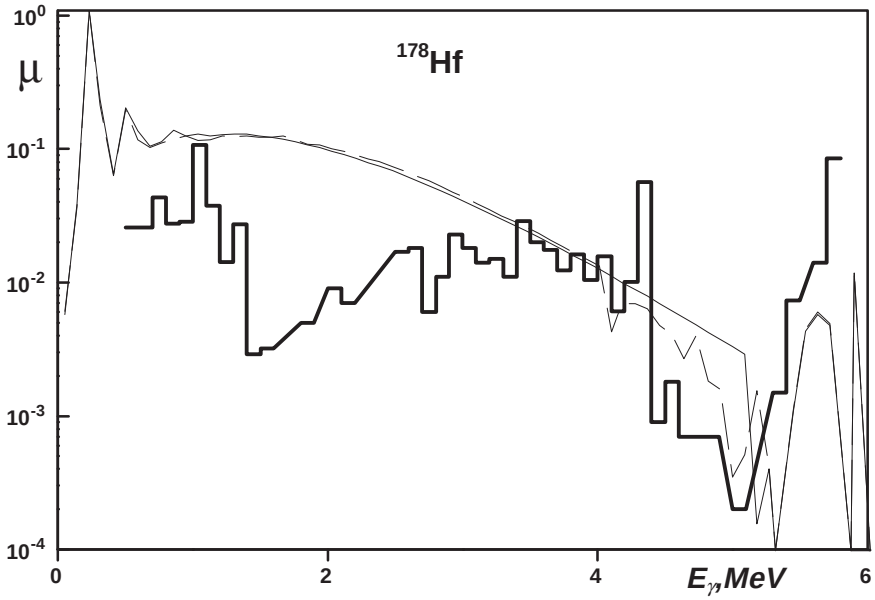

Fig. 3. Same as Fig. 2 but with ^{178}Hf target nucleus. Experimental data from Ref. [12].

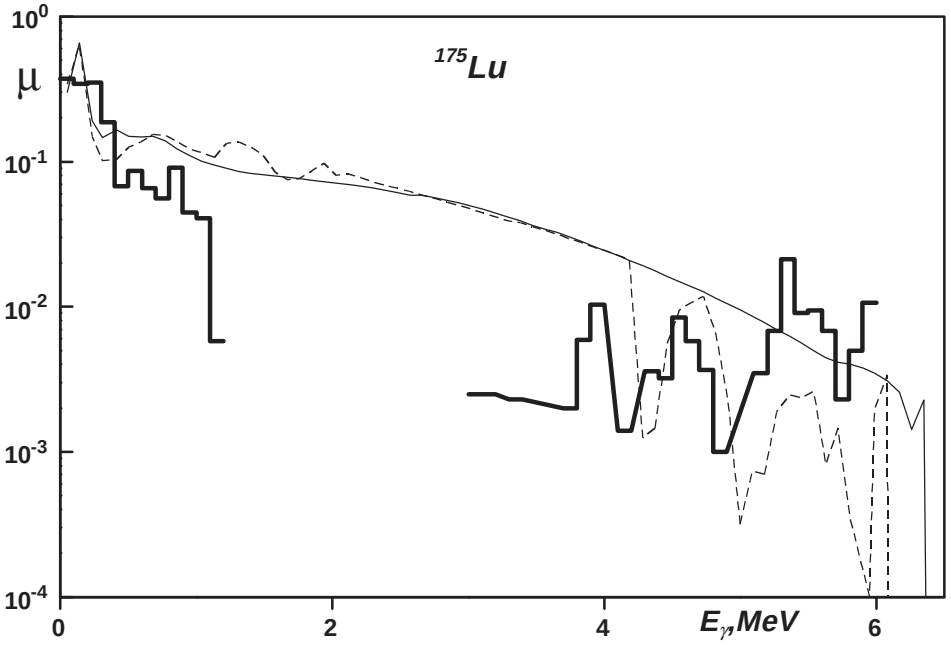

Fig. 4. Same as Fig. 2 but for the reaction ^{175}Lu(n,γ). Experimental data from Refs [13, 14].

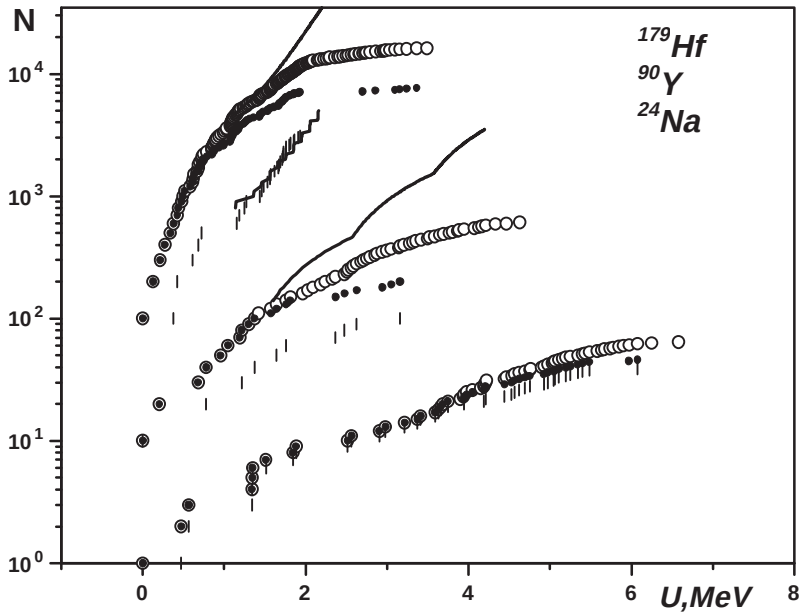

Fig. 5. Data on the discrete energy levels of the nuclei ^{179}Hf, ^{90}Y and ^{24}Na [16]. The light circles show all the identified levels, the dark circles show the levels with known spins, and the dashes show the levels populated by E1-transitions. Themodelling results are shown by the curves. All the data for ^{179}Hf have been multiplied by 100, and those for ^{90}Y by 10.

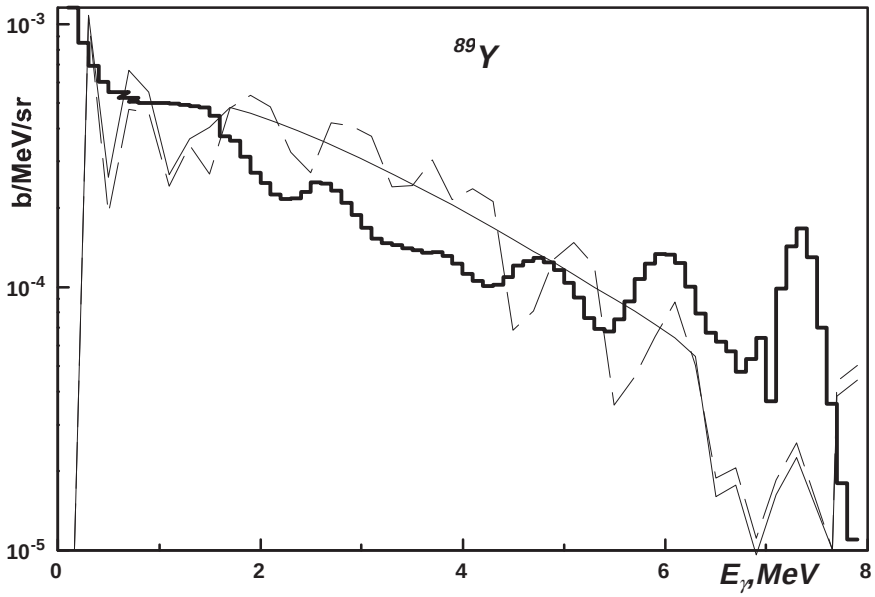

Fig. 6. Gamma spectra for the reaction ^{89}Y(n,γ) at E_n = 0.5 MeV. Experimental data (histogram) from Ref. [15], the curve notation is the same as in Fig. 2.

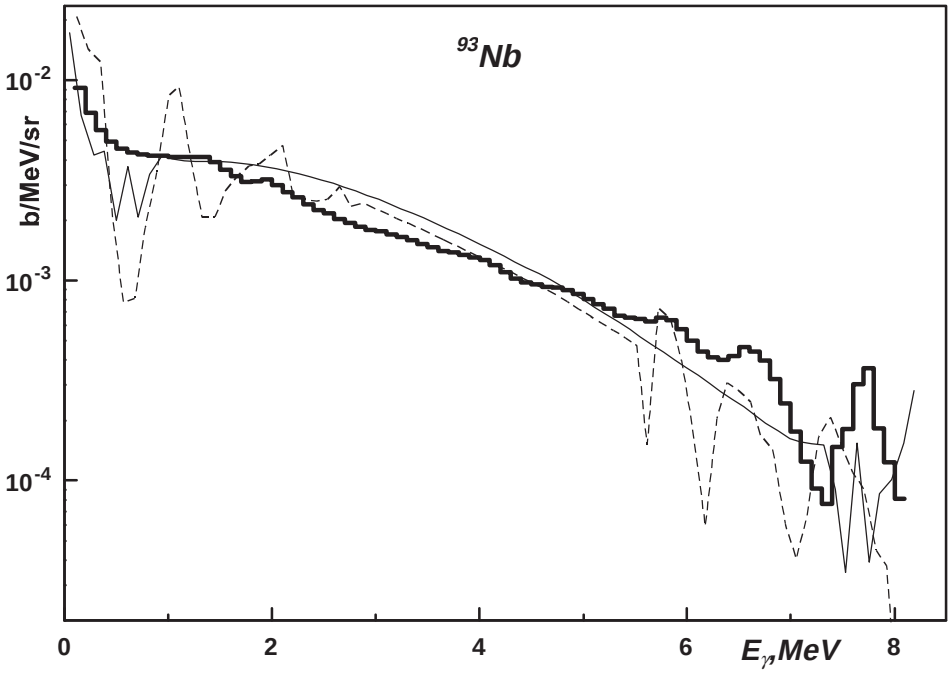

Fig. 7. Same as Fig. 6 but for the reaction ^{93}Nb(n,γ).

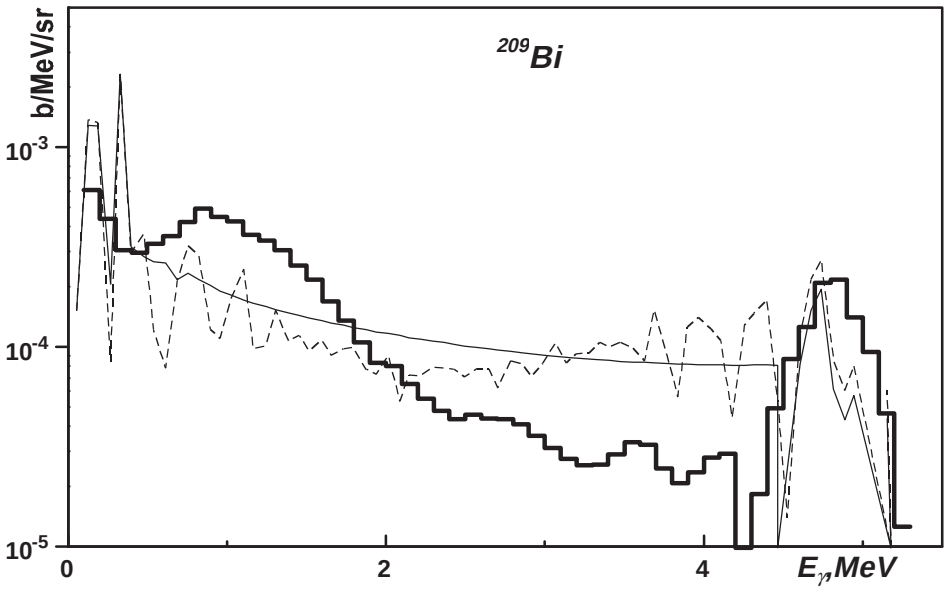

Fig. 8. Same as Fig. 6 but for the reaction ^{209}Bi(n,γ).

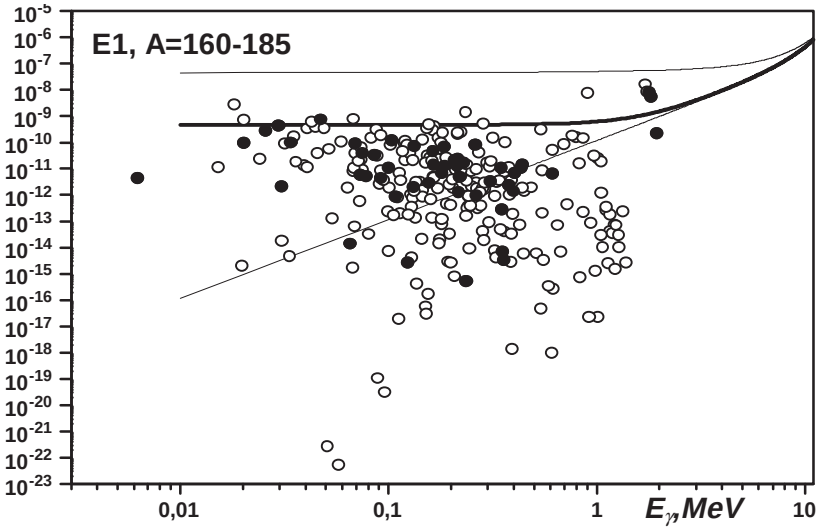

Fig. 9. Reduced strength functions (MeV^{-3}) of E1-transitions for nuclei with A = 160-185. The points are experimental data obtained using formula (14); the closed circles correspond to transitions to the ground state. The curves are the results of calculations with formula (11) for a nucleus with A = 170 at different values of parameter T: upper curve = 1 MeV, middle = 0.1 MeV and lower = 0.

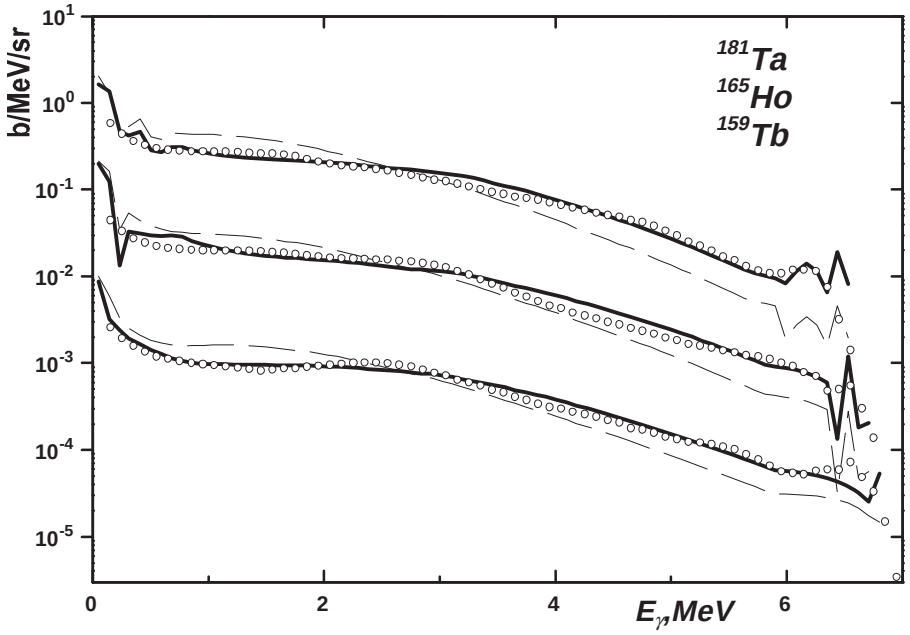

Fig. 10. Gamma spectra from the reaction (n,γ) on ^{181}Ta (top), ^{165}Ho and ^{159}Tb (bottom). The points represent experimental data [15]. The curves represent calculations: the broken curves show the unadjusted strength function E1, the solid curves show f_{E1} corrected according to the data of Fig. 9. The data for ^{181}Ta have been multiplied by 20 and those for ^{159}Tb divided by 20.

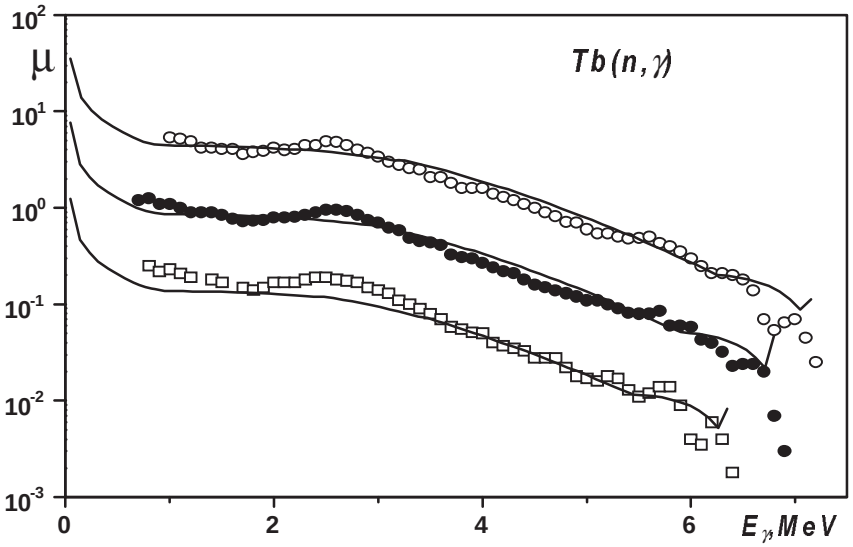

Fig. 11. Gamma multiplicities (MeV^{1}) from the reaction Tb(n,γ) at E_n = 0.8 MeV (top), 0.4 MeV and 0.01 MeV (bottom). The points represent experimental data [21], the curves calculations with fitted f_{E1}. The data for 0.8 MeV have been multiplied by 5, and those for 0.01 MeV divided by 5.

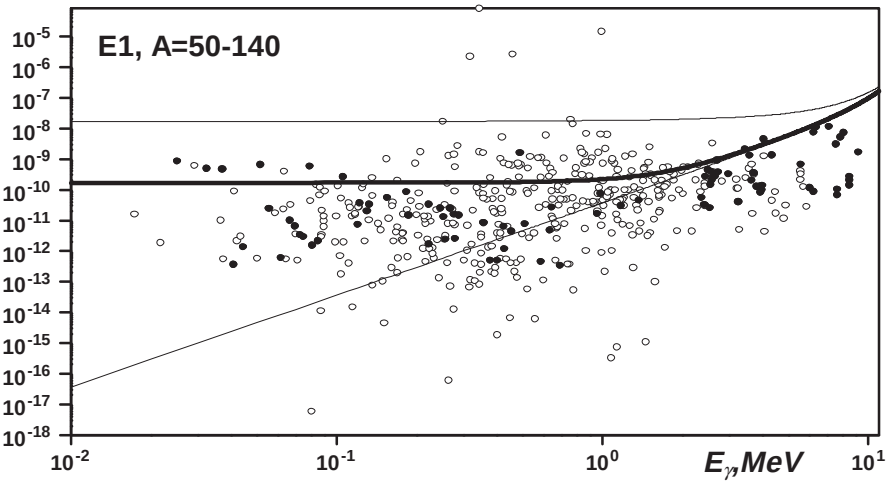

Fig. 12. Reduced strength functions (MeV^{-3}) of E1-transitions for nuclei with A = 50-140. The points represent experimental data obtained using formula (14): the closed circles correspond to transitions to the ground state. The curves show the results of calculations (11) for a nucleus with A = 120 at different values of the parameter T: the upper curve is for 1 MeV, the middle one 0.1 MeV and the bottom one 0.

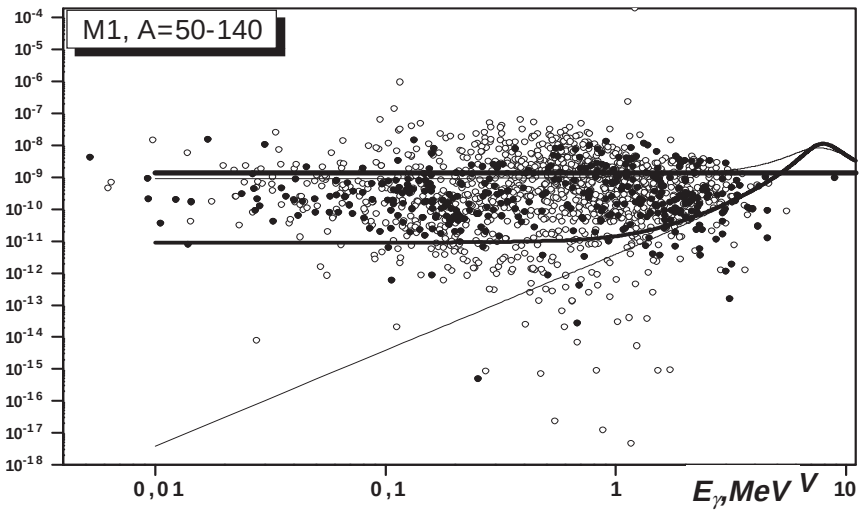

Fig. 13. Reduced strength functions (MeV^{-3}) of M1-transitions. Same representation as Fig. 12 with the addition of the single particle evaluation shown by the horizontal curve.

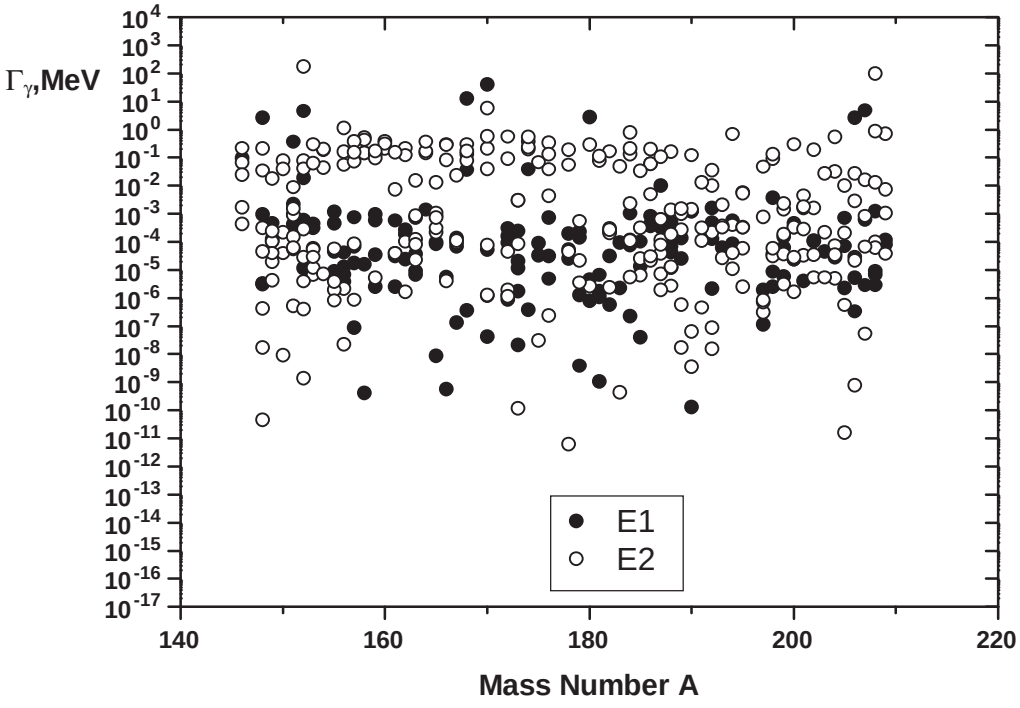

Fig. 14. Average radiation widths for E1 and E2 gamma-transitions in nuclei with A= 150-210 derived from data on the de-excitation of discrete energy levels with U ≤ 2 MeV.

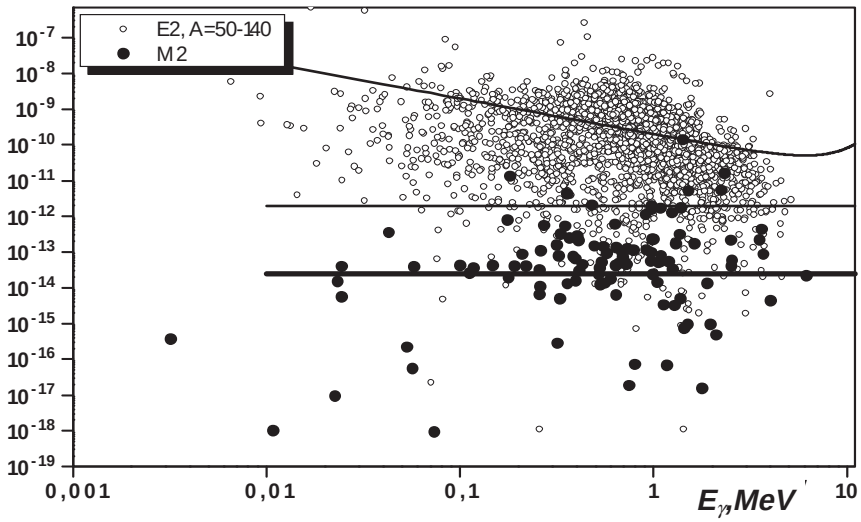

Fig. 15. Reduced strength functions (MeV^{-5}) of E2 and M2-transitions for nuclei with A = 50-140 obtained using formula (13). The horizontal curves denote the single-particle evaluations, and the upper curve calculations using theLorentzian dependence (15).

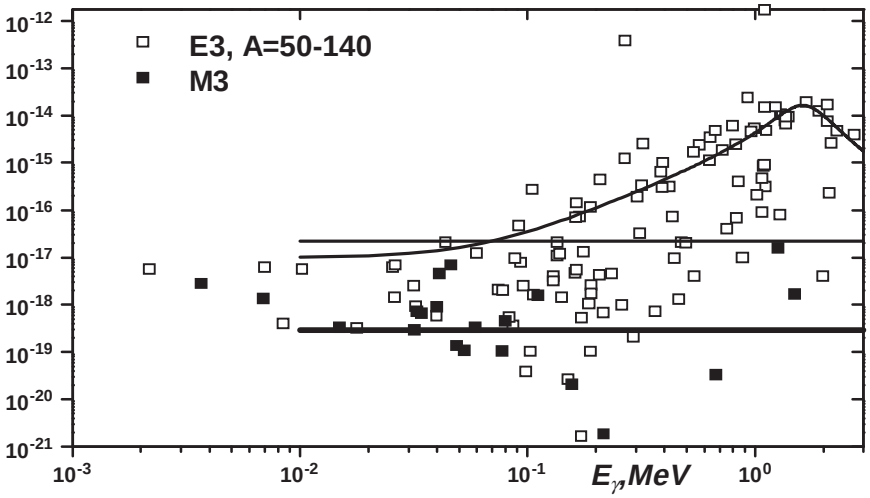

Fig. 16. Reduced strength functions (MeV^{-7}) of E3 and M3-transitions for nuclei with A = 50-140 obtained using formula (14). The horizontal curves denote the single-particle evaluations, and the upper curve denotes calculations using formula (16).

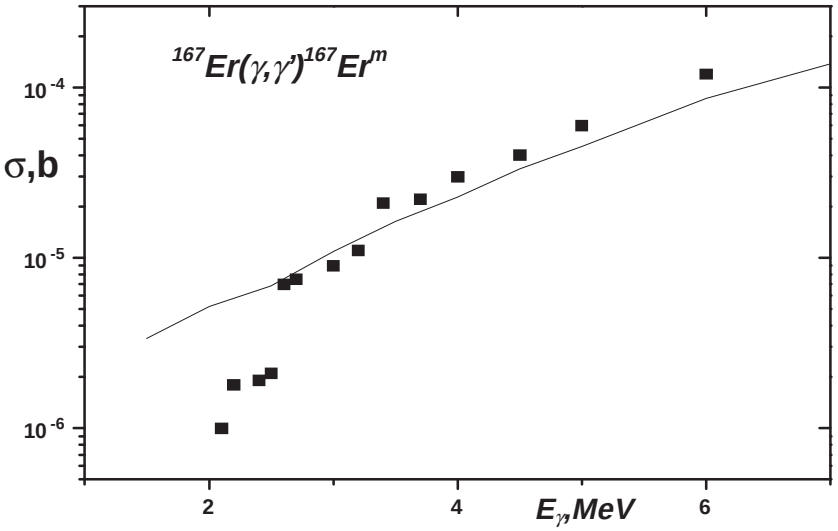

Fig. 17. Excitation cross-section of the isomer in the reaction ^{167}Er(γ,γ')^{167}Er induced by bremsstrahlung. The points represent experimental data [22], and the curve calculated values.

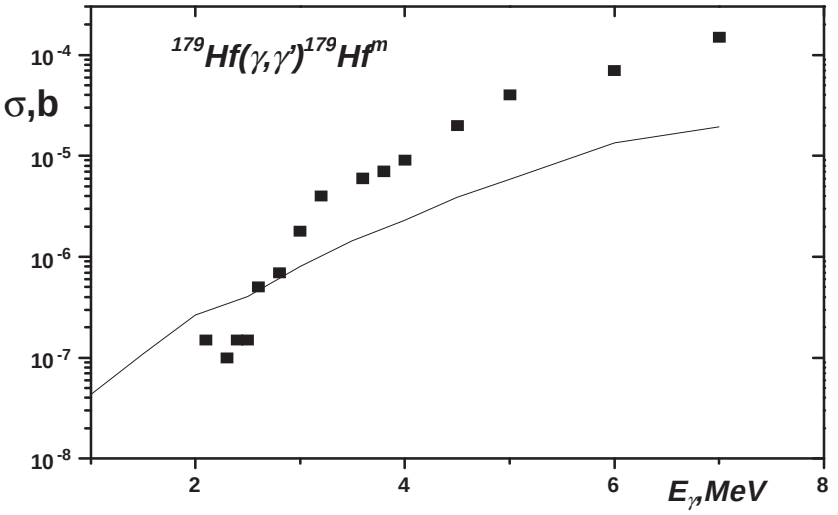

Fig. 18. Same as Fig. 17 but for the reaction ^{179}Hf(γ,γ').

REFERENCES

[1] TROUBETZKOY, E.S., Statistical theory of gamma-ray spectra following nuclear reactions, Physical Review, 122 1 (1961) 212.

[2] GRUDZEVICH, O.T., ZELENETSKIJ, A.V., IGNATYUK, A.V., PASHCHENKO, A.B., Method of harmonized description of isomer yields in neutron reactions, Yadernaya Fizika, 57 B.8 (1994) 1428 [in Russian].

[3] IGNATYUK, A.V., Statistical characteristics of excited atomic nuclei, Moscow, Ehnergoatomizdat (1983) [in Russian].

[4] GRUDZEVICH, O.T., IGNATYUK, A.V., ZELENETSKY, A.V., "Consistent systematics of level densities", Proc. Int. Conf. on Nuclear Data for Science and Technology, Mito, Japan (1988) 1221.

[5] KADMENSKIJ, S.G., MARKUSHEV, V.P., FURMAN, V.I., Radiation widths of neutron resonances and giant dipole resonances, Yadernaya Fizika, 37 2 (1983) 277 [in Russian].

[6] POPOV, Yu.P., "Decay of highly excited states by α-particle emission", Physics and Applications (Proc. Europhysics Topical Conference, Smolenice, 1982) vol. 10, Bratislava (1982) 121.

[7] DZHILAVYAN, L.Z., KAUTS, V.L., FURMAN, V.I., CHUPRIKOV, A.Yu., Some problems of isomeric states population, Yadernaya Fizika, 51 2 (1990) 336 [in Russian].

[8] DIETRICH, S.S., BERMAN, B.L., Atlas of photoneutron cross-sections obtained with monoenergetic photons, Atomic Data and Nuclear Data Tables, 38 (1988) 199-388.

[9] KOPECKY, J., UHL, M., Test of gamma-ray strength functions in nuclear reaction model calculations, Physical Review, C41 5 (1990) 1941.

[10] TIELENS, T.A.A., KOPECKY, J., ABRAHAMS, K., ENDT, P.M., The reaction Na-23(n,γ) Na-24 studied with unpolarized and polarized thermal neutrons, Nuclear Physics, A403 1 (1983) 13.

[11] MICHAELSEN, S., HARKER A., LIEB, K.P. et al., Complete spectroscopy of Y-90 via the Y-89(n,γ) and Y-89(d,p) reactions, Nuclear Physics, A552 (1993) 232.

[12] ALENIUS, G., ARNELL, S.E., SCHALE C., WALLANDER, E., Thermal-neutron capture investigation of the N = 107 isotopes of Yb-177 and Hf-179, Nuclear Physics, A186 (1972) 209.

[13] FUBINI, A., PROSPERI, D., TERRASI, F., VATA, I., The Lu-175 (n,γ) reaction and level structure of Lu-176, Nuovo Cimento, A8 (1972) 748.

[14] KLAY, N., KAEPPELER, F., BEER, H., et al., Nuclear structure of Lu-176 and its astrophysical consequences, Physical Review, C44 6 (1991) 2801.

[15] VOIGNIER, J., JOLY, S., GREINIER, G., Capture cross-sections and gamma-ray spectra from interaction of 0.5 to 3.0 neutron with nuclei in the mass range A = 63 to 209, Nucl. Sci. Eng., 93 (1986) 43.

[16] ENSDF - a computer file of evaluated nuclear structure data maintained by National Nuclear Data Center, BNL (file as of Nov. 1989).

[17] GARDNER, M.A., GARDNER, D.G., Evaluation of neutron-induced reaction cross-sections of the neutron-deficient isotopes of europium and gadolinium, Preprint of LLNL, UCRL-JC-110650, USA (1992).

[18] CHADWICK, M.B., YOUNG, P.G., Calculations of the production cross-sections of high-spin isomeric states in hafnium,Nucl. Sci. Eng., 108 (1991) 117-125.

[19] GRUDZEVICH, O.T., Systematics of parameters of the spin dependence of the level density, Yadernaya Fizika, 58 10 (1995) 1758 [in Russian].

[20] ENDT, P.M., Strengths of gamma-ray transitions in A = 91-150, Atomic Data and Nuclear Data Tables, 26 (1981) 47-91.

[21] IGASHIRA, M., KITAZAWA, H., SHIMIZU, M., et al., Systematics of the pygmy resonance in keV neutron capture γ-ray spectra of nuclei with N = 82-126, Nuclear Physics, A457 (1986) 301.

[22] COLLINS, C.B., CARROLL, J.J., TAYLOR, K.N., et al., Common thresholds and the role of deformations in the photoexcitation of isomers, Physical Review, C46 3 (1992) 952.

[23] BLATT, J., WEISSKOPF, V.F., Theoretical nuclear physics, Moscow, Inostr. Lit. (1954) [in Russian].

[24] GRUDZEVICH, O.T., Isomeric ratios of neutron radiative capture, Yadernaya Fizika, 61 1 (1998) [in Russian].

[25] BELANOVA, T.S., IGNATYUK, A.V., PASHCHENKO, A.B., PLYASKIN, V.I., Neutron radiative capture, Moscow, Ehnergoatomizdat (1986) [in Russian].

[26] KARAMIAN, S.A., DE BOER, J., OGANESSIAN, Yu.Ts., et al., Observation of photonuclear reactions on isomeric targets: $^{178}Hf^{m2}(\gamma,n)^{177}Hf^{m2}$, $^{180}Ta^{m}(\gamma,2n)^{178}Ta^{m,g}$ and $^{180}Ta^{m}(\gamma,p)^{179}Hf^{m2}$, Zeitschrift für Physik, A356 (1996) 23.

98-10983 (73)
Translated from Russian

UDC. 539.172.013

SERIYA: YADERNYE KONSTANTY, Vypusk 1 1998, s. 9
(Series: Nuclear Constants, Issue No. 1 1998, p. 9)

INVESTIGATION OF THE RESONANCE STRUCTURE OF NEUTRON CROSS-SECTIONS FOR THORIUM-232 AND NEPTUNIUM-237 IN THE 2 eV-100 keV ENERGY RANGE

Yu.V. Grigor'ev, V.V. Sinitsa
Russian Federation State Science Centre
A.I. Lejpunsk Institute of Physics and Power Engineering,Obninsk

G.N. Gundorin, Yu.P. Popov, Kh. Fajkov-Stanchik
Joint Institute for Nuclear Research, Dubna

INVESTIGATION OF THE RESONANCE STRUCTURE OF NEUTRON CROSS-SECTIONS FOR THORIUM-232 AND NEPTUNIUM-237 IN THE 2 eV-100 keV ENERGY RANGE. Experimental results of transmissions for three sample-filters of thorium-232 with thickness 0.01303 at/b, 0.02655 at/b and 0.0517 at/b and for three samples of neptunium-237 with thickness 0.002074 at/b, 0.00417 at/b, 0.01253 at/b are presented in this work. Thorium samples are metal discs with 45 mm diameter in aluminium containers. Samples were made of NpO_2 powder placed in cylindrical aluminium hermetic containers with 56 and 43 mm inside diameters. Measurement was carried on the pulsed neutron booster IBR-30 of JINR in Dubna on the 123 m flight path with boron counters SNM-13 as detector. Point-wise and group cross-sections were extracted from transmission data. Analogous values were calculated by GRUCON code on the basis of the evaluated data from ENDF/B-VI and JENDL-3 libraries.

The basic fuel and source materials used in nuclear power today are uranium-235 and uranium-238, which explains, to a large extent the greater quantity of nuclear data on these isotopes in comparison with the data on the fuel and source materials uranium-233 and thorium-232. Interest in the uranium-thorium cycle in the nuclear power industry is currently increasing, which is stimulating research work on refining the neutron constants of these above-mentioned isotopes. This interest is linked to the search for ways of solving the problem of transmutation and reducing the build-up of long-lived radioactive fission products and transuranium isotopes.

As we know, the build-up of neptunium-237 in power reactors is becoming a serious problem owing to its high radioactivity maintained over a long period of time. As a result of this, research is now being carried out on different neutron constants required for the

development of optimum variants for the burnup of this isotope in reactors or in other facilities.

Until now, little research has been carried out on neutron cross-sections of neptunium-237, particularly fission cross-sections in the low energy range where the cross-section reported by different authors differ by several orders of magnitude. It is now important to perform measurements to refine the total and partial cross-sections and the effects of resonance shielding in the resonance energy range for both neptunium-237 and other minor actinides including thorium. In order to determine the resonance self-shielding factors for total and partial cross-sections, it is necessary, in addition to measuring the self-indication functions, to measure total transmissions in the sample filters over a wide range of thicknesses. We measured total transmissions with three sample filters of thorium-232 and with three samples of neptunium-237.

Experiment

The measurements were performed on the IBR-30 pulsed-neutron source of the Joint Institute of Nuclear Research (JINR) (W = 10 kW, F_{burst} = 100 Hz, τ_{burst} = 4 μs) using a battery of three boron counters SNM-13 on a 123 m flight path. In order to increase the efficiency of the neutron registration and to obtain a constant efficiency values over a wide energy range, the counters were placed in a polythene disc 100 mm in diameter and 15 mm thick. Total transmissions were measured on three sample filters of ^{232}Th with thicknesses of 0.01303, 0.02655 and 0.0517 at/b, and on three sample filters of ^{237}Np with thicknesses of 0.002074, 0.00417 and 0.01253 at/b. The thorium-232 samples were metal discs 45 mm in diameter of various thickness in aluminium containers, while the neptunium samples were prepared from neptunium-237 oxide (NpO_2) powder, which was poured into hermetic aluminium containers in the shape of discs with an inside diameter of 56 mm (two thin samples) and 43 mm (one thick sample). The sample filter with a thickness of 0.00417 at/b was made up of two thin samples. The general scheme of the experiment is shown in Fig. 1.

A liquid gamma-ray detector was used for testing the method of measuring the self-indication functions in theradiative capture of thorium-232.

The time spectra with and without a sample in the neutron beam were stored in the measuring module with a PC in the energy range from 1 eV to 100 keV with energy resolutions of 0.1% and 30% respectively. The width of the time channel was equal to 2 μs. The background components in the spectra were measured with In, Mn and Al resonance filters at 1.45 eV, 337 eV, 2.4 and 35 keV. The indium and boron resonance filters were permanently located in the neutron beam to remove background recycled neutrons and to monitor the operating stability of the detector apparatus on background level at energy 1.45 eV. The power level of the neutron source was monitored by means of two monitors (boron counters, type SNM-12). The error of the measured monitoring coefficient did not exceed 0.5%.

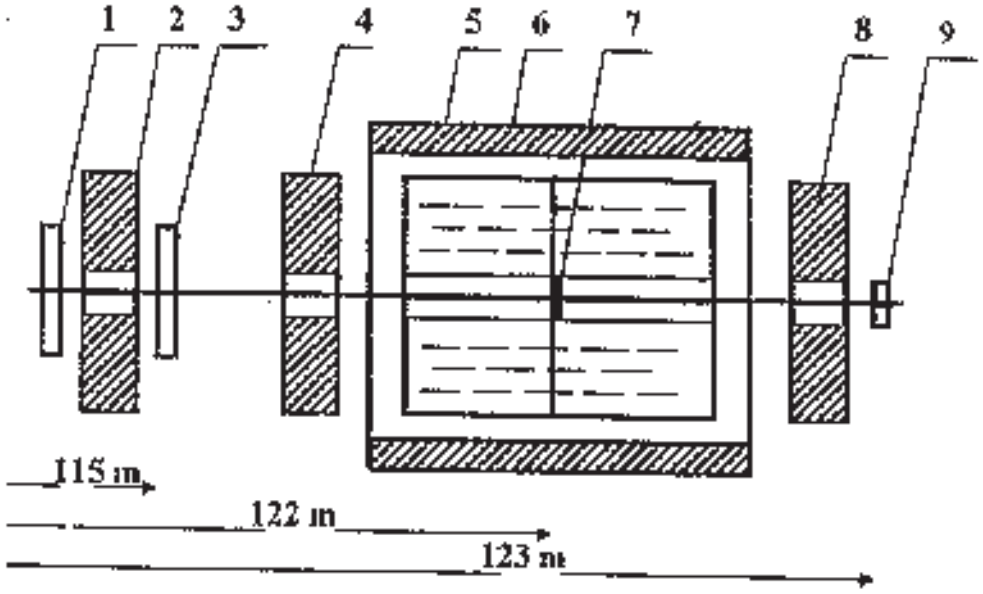

Fig.1. General scheme of the experiment
1 - monitor; 2, 4, 8 - collimators; 3 - sample filter; 5 - lead shield of the (*n*,γ) detector; 6 - 16-section liquid (*n*,γ) detector; 7 - sample radiator; 9 - neutron detector.

Results and discussion

Measurements of the total transmissions for thin samples have to be made with great accuracy when neutron beam attenuation is between 3% and 10%. In order to attain a statistical error in the energy groups of the ABBN constant system [1] of approximately 0.2-0.5%, it is necessary to measure the neutron spectra with and without a sample in the neutron beam for hundreds of hours. The typical measured time spectra without deduction of the background are shown in Figs 2 and 3. In order to facilitate comparison, the spectra in each series were normalized to the monitoring coefficient but without correction for oxygen in the NpO_2 sample. However, even with such high statistical accuracy, methodological errors may significantly affect the accuracy of determination of the group cross-sections and should therefore be looked at carefully. Uncertainties in the isotope composition and the thickness of the sample are negligible. Impurities in the thorium samples comprise 0.5%, while the impurities in the neptunium sample were removed by chemical purification up to a level of 10^{-6} in terms of the quantity of atoms, with the exception of oxygen. The uncertainty in the thickness of the sample does not exceed 0.1%. The correction for oxygen also introduces an error of 0.1%. The main contributory factors to the error in transmissions and consequently in the cross-sections are the uncertainty of the monitoring coefficient, the instability of the apparatus, and the background components in the spectra. Corrections for the monitoring coefficient, instability of the apparatus, background components and oxygen are in fact independent of energy in the range 1 eV-100 keV. The shape of the spectrum of the neutron beam passing through the sample is entirely determined by the resonance structure of the total cross-section of ^{232}Th and ^{237}Np. This makes it possible to correct the total cross-sections in the resonance region on the basis of well-known cross-sections in the inter-resonance region.

The group transmissions and observed cross-sections were determined using the following formulae:

$$T_t(n,\Theta,E)=\frac{\Delta E\int\varphi(E)\varepsilon(E)e^{-\sigma_t(E,\Theta)n}dE}{\Delta E\int\varphi(E)\varepsilon(E)dE}=\frac{N_{samp}-F_{samp}}{N_{o/n}F_{o/n}}K/T_{tk}\,, \tag{1}$$

$$\sigma_t=(-\ln T_t)/n, \tag{2}$$

where $\varphi(E)$ is the neutron beam spectrum, $\varepsilon(E)$ is the detector efficiency, σ_t is the total cross-section, n is the thickness of the sample filter, E is the neutron energy, Θ is the temperature of the sample filter, N_{samp}, $N_{o/n}$ is the detector count with and without a sample, F_{samp}, $F_{o/n}$ is the detector background count with and without a sample, K is the monitoring coefficient, T_{tk} is the transmission due to the presence of oxygen. The transmission due to the presence of oxygen is determined by calculation.

Tables 1 and 2 show the experimental transmissions and observed total group cross-sections in barns for thorium-232 and neptunium-237 respectively.

The last two columns of tables 1 and 2 contain the calculated observed total cross-sections σ_t^{calc} for the thickest sample filters of thorium-232 and neptunium-237.

The calculated values of the total transmissions and cross-sections were obtained using the group constant programme (GRUKON) [2] on the basis of evaluated data from the ENDF/B-VI [3] and JENDL-3 [4] libraries in the investigated energy range.

The group transmissions and cross-sections were averaged over the Fermi spectrum. Experimental transmission errors amount to 0.2-0.5%, and errors in the total observed cross-sections to 2-10%.

The total transmissions are usually measured at $n\sigma_t$ = 0.2-0.4, which leads to values of the mean group cross-section 20-40% too low in the unresolved resonance region if no correction is made for the resonance shielding of the averaged cross-sections. As the thickness of the sample filter is reduced, the effects of resonance shielding decrease. Thus, when $n\sigma_t$ = 0.01 the observed cross-section is 2% less than the mean group total cross-section, and when $n\sigma_t$ = 1 the observed cross-section is half the total cross-section for zero thickness of the sample filter.

As shown in Tables 1 and 2, the calculated total cross-sections σ_t^{calc} obtained on the basis of evaluated data from both libraries, agree with the experimental observed group cross-sections $\sigma_t^{\exp}$ in the energy range from 2.15 eV to 100 keV for the thickest sample filters with thicknesses of 0.0517 at/b for ^{232}Th, and 0.01253 at /b for ^{237}Np.

In thin sample filters of thorium-232 and neptunium-237, the observed total cross-sections of the experiment increase significantly in comparison to the cross-sections for thick samples and are systematically greater than the calculated values in the energy range 2.15 eV-100 keV, which can be seen in Tables 1 and 2 and Figs 4, 5, 6 and 7. This shows that the resonance structure of the neutron cross-sections of thorium-232 and

neptunium-237 is significant up to 100 keV, and that resonance shielding had not previously been sufficiently allowed for, which resulted in underestimation of the evaluated cross-sections in the unresolved resonance region.

The mean group total cross-sections were obtained by extrapolating the experimental observed cross-sections to the cross-section at zero thickness of the sample filter, i.e. by multiplying the observed cross-sections by the calculated shielding coefficients K_{sh}:

$$\left\langle \sigma_t^{\exp} \right\rangle = K_{sh}\sigma_t^{\exp}, K_{sh} = \left\langle \sigma_t^{calc} \right\rangle / \sigma_t^{calc}, \quad (3)$$

where $\sigma_t^{\exp}$ and σ_t^{calc} are the experimental and calculated observed total cross-sections, and $\left\langle \sigma_t^{\exp} \right\rangle$ and $\left\langle \sigma_t^{calc} \right\rangle$ are the experimental and calculated mean group total cross-sections.

The calculated resonance shielding coefficients in individual energy groups differ from one another for various libraries, and therefore averaged values were used for determining the group cross-sections.

For ^{237}Np, the experimental mean group total cross-sections in the energy range 2.15 keV-100 keV were obtained by averaging the observed cross-sections with sample filter thicknesses of 0.002074 and 0.00417 at/b, since in the ENDF/B-VI and JENDL-3 libraries, the resonance structure of the cross-sections is less apparent in this energy range.

Table 3 shows the experimental and calculated average group total cross-sections for thorium-232 and neptunium-237 in the energy range from 2.15 eV to 100 keV. In the majority of energy groups, the experimental values of the total cross-sections are 5-30% greater than the calculated ones.

In addition to the group averaged values the point-wise values of the total transmissions and cross-sections were also determined. The method of processing the initial time spectra was the same as that described above, but it was done by channels (the number of time channels = 4096). Figures 8 and 9 show the experimentally observed point-wise total cross-sections without corrections for energy resolution and the Doppler effect. As can be seen from these figures, individual resolved resonances are observed in this experiment up to 300 eV. Higher statistical accuracy is required in order to obtain the parameters for particularly weak resolvedresonances, and we aim to achieve this in the following stage.

In addition to measuring the total cross-sections, preliminary investigations of radiative capture were performed on a thin thorium sample with a thickness of 0.000641 at/b using a liquid 16-section gamma-ray detector. The gamma multiplicity spectra for different resonances coincide within the limits of experimental error, and have virtually identical multiplicities of approximately 2.65, pointing to the possibility of measuring the resonance parameters, cross-sections and self-indication functions in the radiative capture of thorium-232 with a gamma-ray detector.

Measurements of the total transmissions were performed, and from these the group and point-wise total cross-sections of ^{232}Th and ^{237}Np in the energy range 2 eV-100 keV were determined.

Similar integral characteristics for these isotopes were obtained by calculation with the GRUKON program on the basis of the latest evaluated data from the ENDF/B-VI, JENDL-3 libraries. In the experiment stronger resonance shielding of the total cross-sections of thorium-232 and neptunium-237 is observed than with calculation, and therefore the evaluated total cross-sections of these isotopes should be revised upwards.

In the future, it is proposed to conduct more accurate measurements of the total transmissions and self-indication functions in radiative capture on a wider set of thicknesses of ^{232}Th and ^{237}Np samples, which will make it possible to refine the values of the average resonance parameters, neutron cross-sections and their resonance shielding factors.

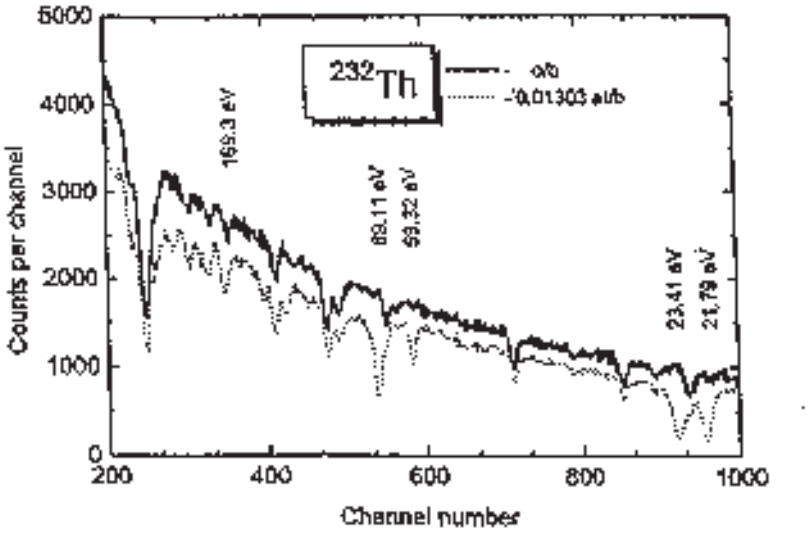

Fig. 2. Time-of-flight spectra of the open beam and with a sample of ^{232}Th. Width of the time channel 2μs.

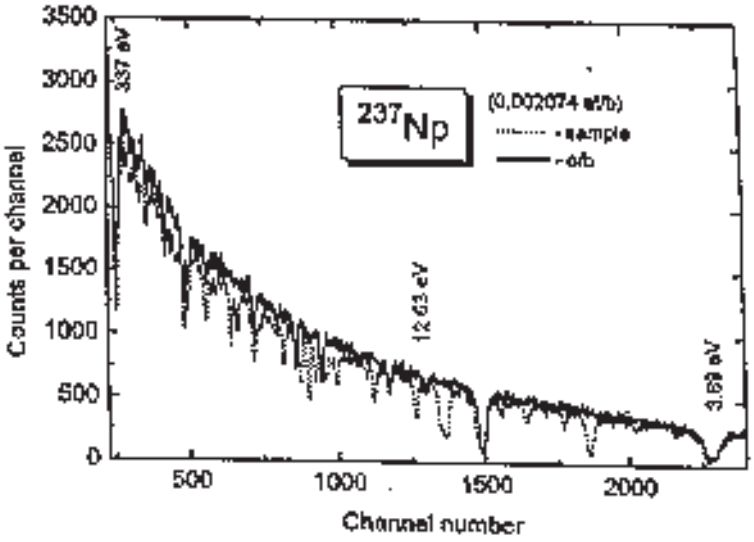

Fig. 3. Time-of-flight spectra of the open beam and with a sample of ^{237}Np. Width of the time channel 2μs.

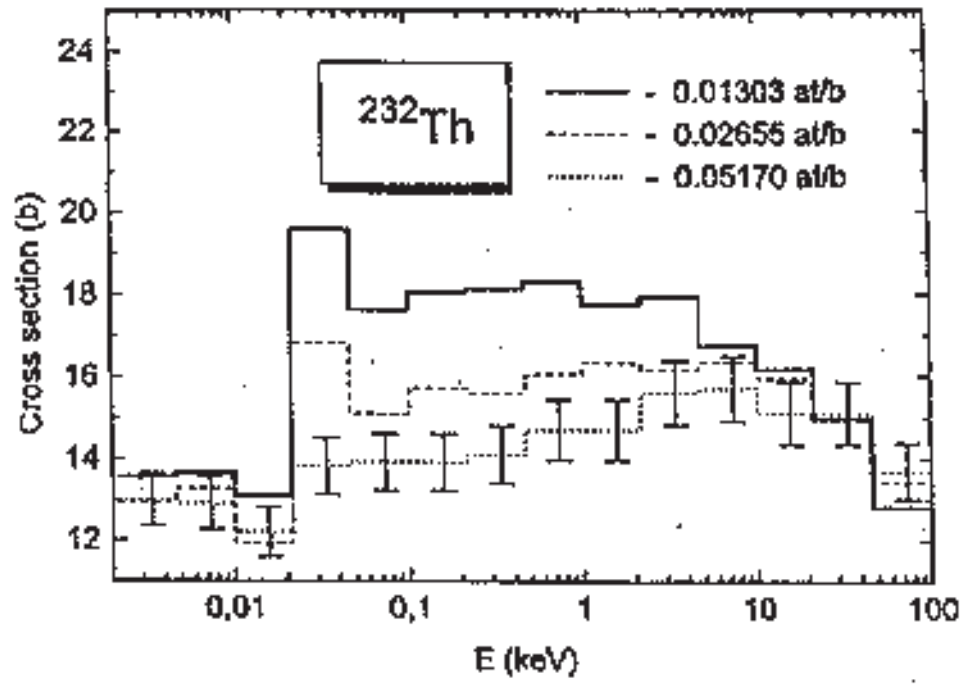

Fig. 4. Experimental observed group total cross-sections of Thorium-232.

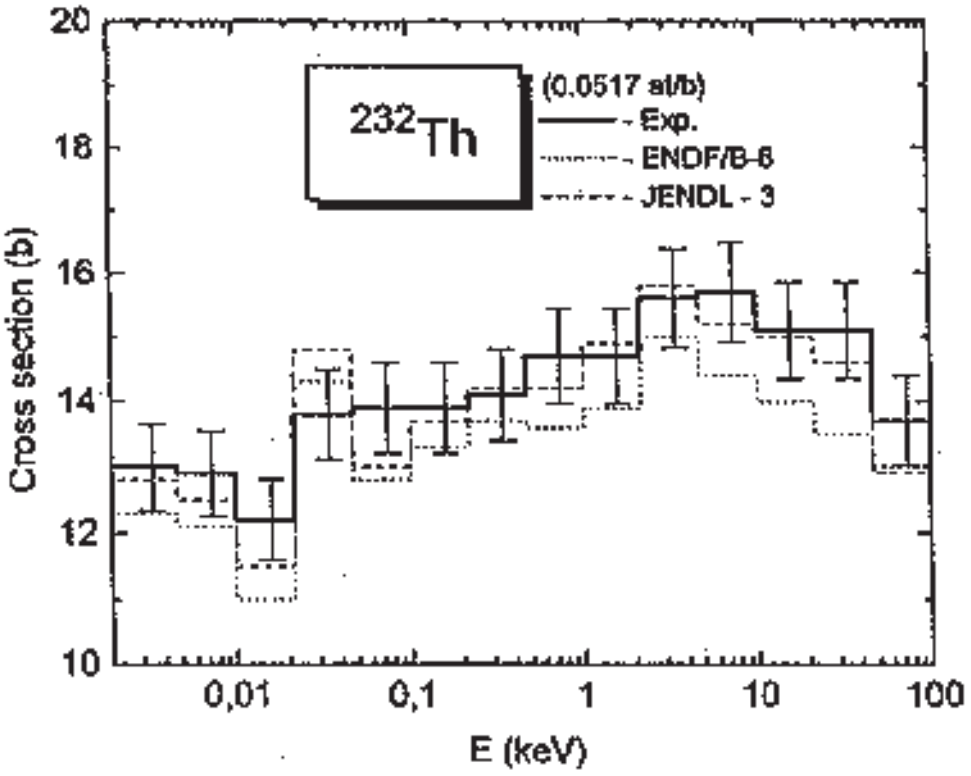

Fig. 5. Experimental and calculated observed group total cross-sections of Thorium-232.

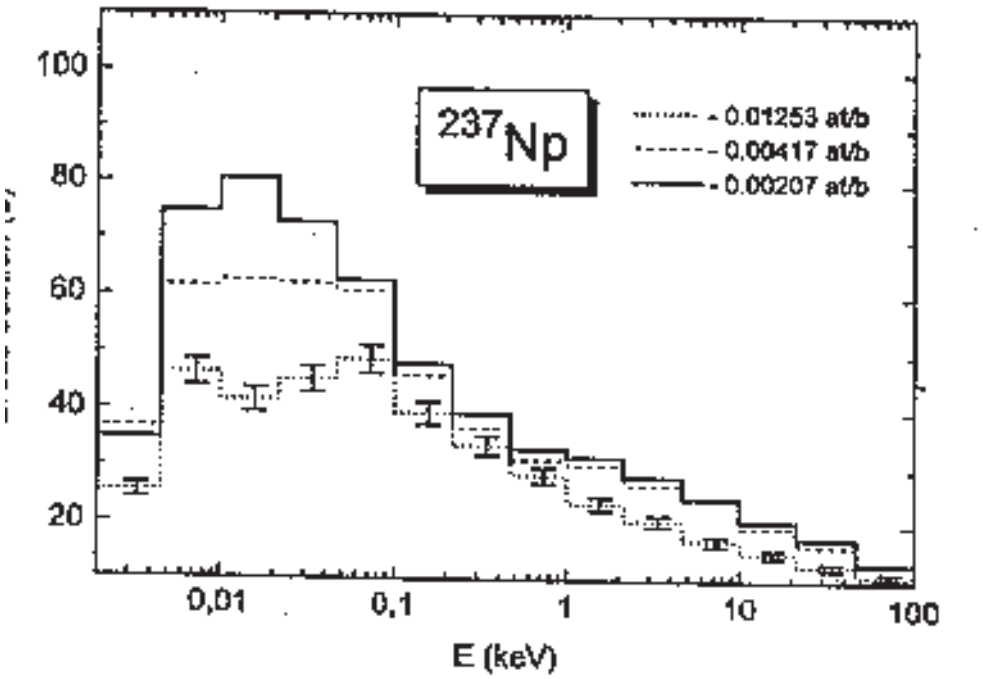

Fig. 6. Experimental observed group total cross-sections of Neptunium-237.

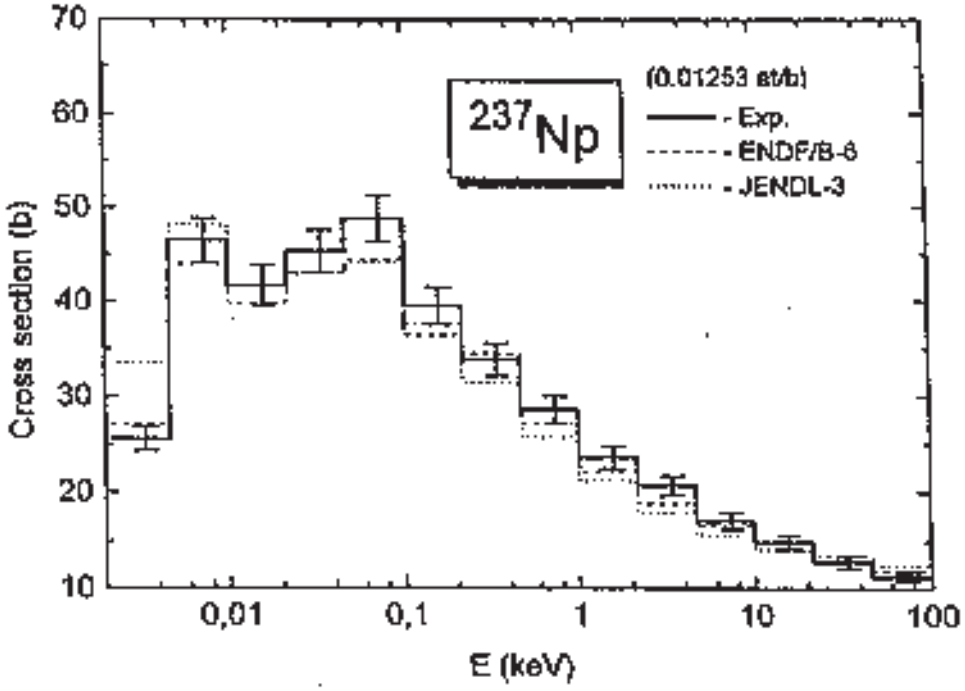

Fig. 7. Experimental and calculated observed group total cross-sections of Neptunium-237.

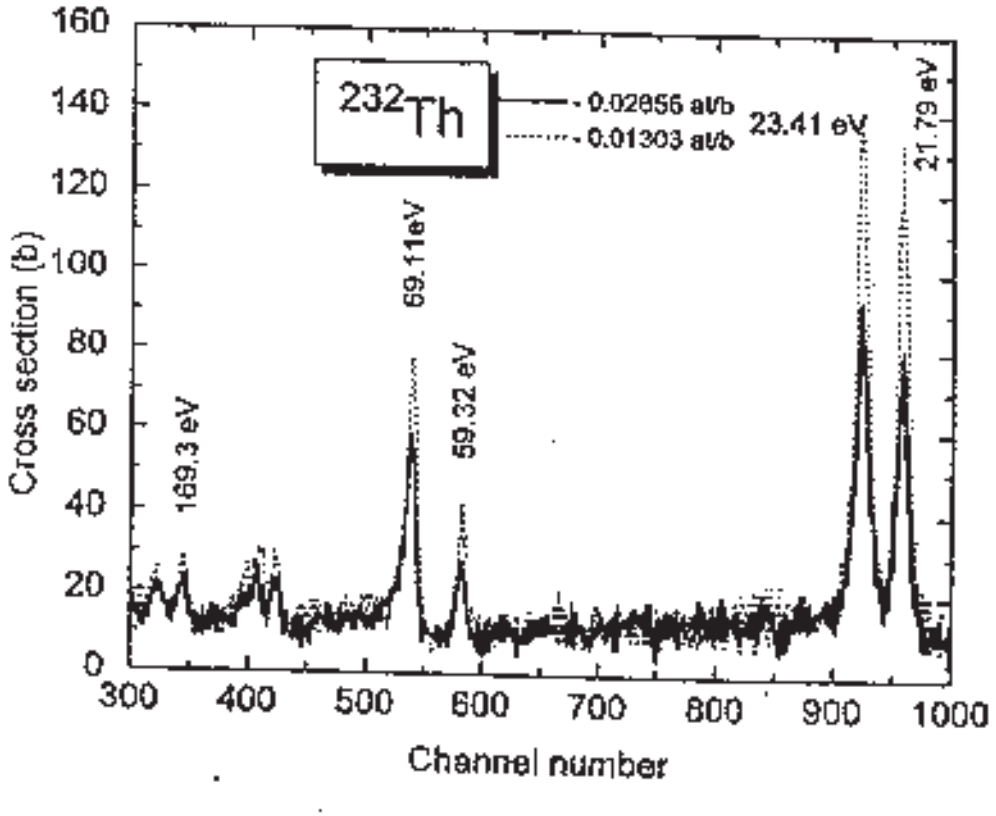

Fig. 8. Experimental observed total cross-sections of Thorium-232.

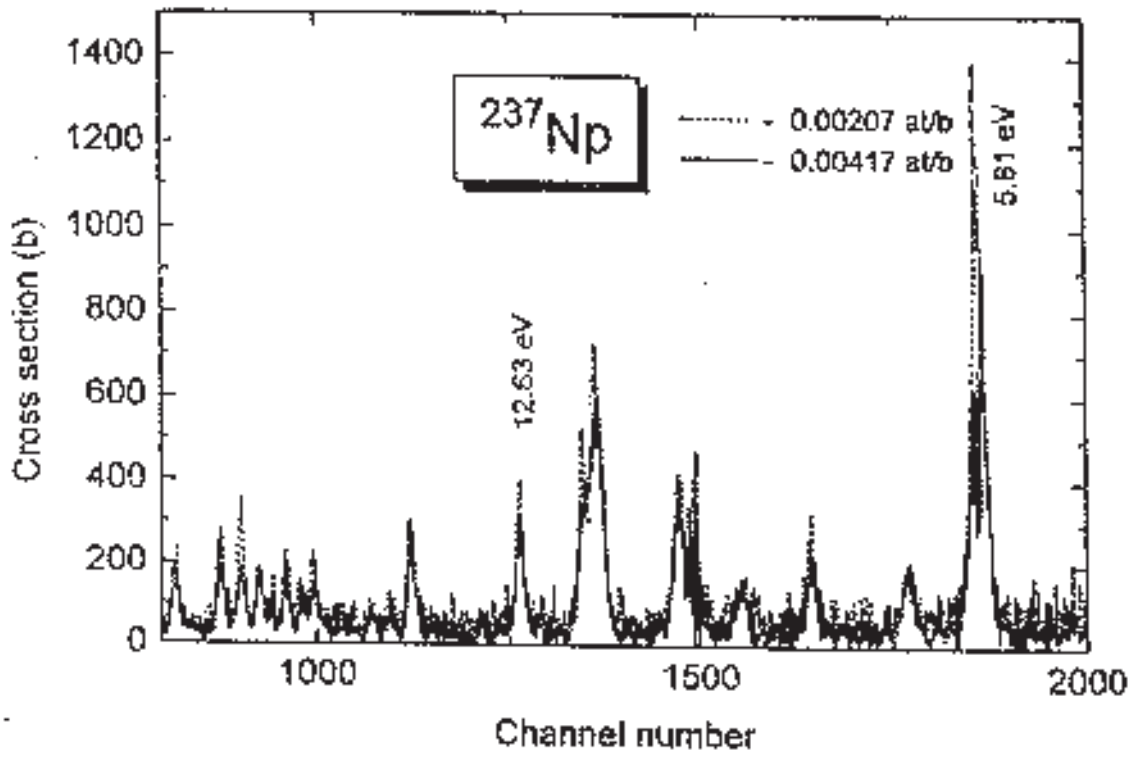

Fig. 9. Experimental observed total cross-sections of Neptunium-237.

REFERENCES

[1] Abagyan, L.P., Bazazyants, N.S., Nikolaev, M.N., Tsibulya, A.M., "Group constants for the calculation of reactors and protection", Moscow, (1981) [in Russian].

[2] Sinitsa, V.V., "Programme for calculating group constants on the basis of the library of evaluated neutron data" VANT, Seriya Yadernye Konstanty (1984) Edition 5, (59) 34 [in Russian].

[3] Rose, P.F., Dunford, C.L., eds. ENDF-102, Data Formats and Procedures for the Evaluated Nuclear Data File, ENDF, report BNL, Upton, New York (1988) 11973.

[4] Shibata, K., et al., Japanese Evaluated Nuclear Data Library, Version 3, JENDL-3, Report JAERI (1990) 1319.

Table 1

Group total transmissions and observed cross-sections of Thorium-232

		Experiment (this work)						Calculation	
Thickness (at/b)		0,01303		0,02655		0,0517		0,0517	
N_{gr}	E_{gr}(keV)	T_t^{exp}	σ_t^{exp}	T_t^{exp}	σ_t^{exp}	T_t^{exp}	σ_t^{exp}	σ_t^{calc} [3]	σ_t^{calc} [4]
9	100 -46,5	0,846	12,8	0,700	13,4	0,490	13,7	13,0	12,9
10	46,5-21,5	0,823	15,0	0,672	15,0	0,457	15,1	13,5	14,6
11	21,5-10,0	0,810	16,2	0,655	15,9	0,457	15,1	14,0	15,0
12	10,0-4,65	0,804	16,7	0,648	16,3	0,443	15,7	14,4	15,2
13	4,65-2,15	0,792	17,9	0,651	16,2	0,444	15,6	15,0	15,8
14	2,15-1,00	0,794	17,8	0,648	16,3	0,465	14,7	13,9	14,9
15	1,0-0,465	0,788	18,3	0,653	16,1	0,465	14,7	13,6	14,3
16	465-215 eV	0,790	18,1	0,661	15,6	0,481	14,1	13,7	14,2
17	215 - 100	0,791	18,1	0,659	15,7	0,485	13,9	13,3	13,7
18	100 -46,5	0,795	17,6	0,670	15,1	0,487	13,9	12,8	13,0
19	46,5-21,5	0,775	19,6	0,640	16,8	0,489	13,8	14,3	14,8
20	21,5-10,0	0,843	13,1	0,729	11,9	0,532	12,2	11,0	11,5
21	10,0-4,65	0,837	13,7	0,703	13,3	0,511	12,9	12,1	12,5
22	4,65-2,15	0,838	13,6	0,709	13,0			12,6	13,2

Table 2

Group total transmissions and observed cross-sections of Neptunium-237

		Experiment (this work)						Calculation	
Thickness (at/b)		0,002074		0,00417		0,01253		0,01253	
N_{gr}	E_{gr}(keV)	T_t^{exp}	σ_t^{exp}	T_t^{exp}	σ_t^{exp}	T_t^{exp}	σ_t^{exp}	σ_t^{calc} [3]	σ_t^{calc} [4]
9	100 -46,5	0,973	13,2	0,957	10,5	0,869	11,2	11,9	12,4
10	46,5-21,5	0,964	17,7	0,934	16,3	0,852	12,8	13,5	12,8
11	21,5-10,0	0,958	20,7	0,922	19,5	0,830	14,9	14,8	14,1
12	10,0-4,65	0,950	24,7	0,903	24,5	0,808	17,1	16,6	15,7
13	4,65-2,15	0,943	28,5	0,894	27,0	0,771	20,7	18,9	18,0
14	2,15-1,00	0,936	31,9	0,880	30,5	0,743	23,7	22,2	21,3
15	1,0-0,465	0,933	33,4	0,877	31,4	0,698	28,7	27,2	25,8
16	465-215 eV	0,921	39,5	0,857	36,9	0,654	33,9	34,5	31,5
17	215 - 100	0,905	48,1	0,825	46,1	0,610	39,5	36,4	37,7
18	100 -46,5	0,878	62,7	0,776	60,8	0,543	48,8	44,5	44,1
19	46,5-21,5	0,860	72,7	0,772	62,1	0,567	45,3	43,1	42,9
20	21,5-10,0	0,846	80,6	0,770	62,7	0,593	41,7	39,8	41,8
21	10,0-4,65	0,857	74,4	0,773	61,7	0,558	46,5	44,0	48,1
22	4,65-2,15	0,930	35,0	0,859	37,0	0,725	25,6	27,1	33,6

Table 3

Mean group total cross-sections of ^{232}Th and ^{237}Np

Isotope		Thorium-232			Neptunium-237		
N_{gr}	E_{gr}(keV)	$<\sigma_t^{exp}>$	σ_t^{calc} [3]	σ_t^{calc} [4]	$<\sigma_t^{exp}>$	σ_t^{calc} [3]	σ_t^{calc} [4]
9	100 -46,5	13,3±0,6	13,0	12,9	11,9±1,3	12,3	12,5
10	46,5-21,5	15,0±0,7	13,9	14,3	17,0±1,7	13,5	13,1
11	21,5-10,0	16,1±0,7	14,9	15,5	20,1±2,2	14,8	14,1
12	10,0-4,65	17,7±0,8	16,4	17,3	24,6±2,5	16,6	15,7
13	4,65-2,15	19,6±0,9	19,0	19,9	27,8±2,8	18,9	18,0
14	2,15-1,00	21,9±0,9	20,7	21,4	31,3±2,7	22,3	21,5
15	1,0-0,465	24,9±1,1	23,9	22,1	32,7±3,0	27,2	26,6
16	465-215 eV	33,5±1,3	32,9	32,2	39,1±3,3	34,6	34,2
17	215-100	45,3±1,5	41,8	43,6	49,5±4,0	43,3	45,2
18	100-46,5	71,8±3,0	65,5	65,3	76,7±4,5	74,3	72,3
19	46,5-21,5	74,6±4,0	71,9	73,2	98,8±5,0	96,5	93,3
20	21,5-10,0	12,4±0,6	11,1	11,5	107,5±5,0	103,8	101,7
21	10,0-4,65	13,3±0,7	12,1	12,5	104,5±6,0	103,1	105,5
22	4,65-2,15	13,3±0,7	12,7	13,2	57,3±3,5	60,7	67,55

Nuclear Data Section
International Atomic Energy Agency
Vienna International Centre, P.O. Box 100
A-1400 Vienna
Austria

e-mail: services@iaeand.iaea.org
fax: (43-1) 26007
telephone: (43-1) 2600-21710
Web: http://www-nds.iaea.org